VYSOKÉ UČENÍ TECHNICKÉ V BRNĚ
BRNO UNIVERSITY OF TECHNOLOGY

FAKULTA STROJNÍHO INŽENÝRSTVÍ
ÚSTAV MECHANIKY TĚLES, MECHATRONIKY A BIOMECHANIKY

FACULTY OF MECHANICAL ENGINEERING
INSTITUTE OF SOLID MECHANICS, MECHATRONICS AND BIOMECHANICS

OPTIMIZATION OF A PARALLEL MECHANISM DESIGN WITH RESPECT TO A STEWART PLATFORM CONTROL DESIGN

OPTIMALIZACE NÁVRHU PARALELNÍHO MECHANISMU VZHLEDEM K ŘÍZENÍ STEWARTOVY PLATFORMY

DOKTORSKÁ PRÁCE

DOCTORAL THESIS

AUTOR PRÁCE — Ing. LUKÁŠ BŘEZINA
AUTHOR

VEDOUCÍ PRÁCE — prof. Ing. EDUARD MALENOVSKÝ, DrSc.
SUPERVISOR

BRNO 2010

Bibliographic citation

Březina, L.: *Optimization of a parallel mechanism design with respect to a Stewart platform control design.* Brno: Brno University of Technology, Faculty of Mechanical Enginnering, 2010. 78 p. Supervisor: prof. Ing. Eduard Malenovský, DrSc.

Announcement

I announce that I created this work by myself with use of the presented references.

Abstrakt

Předkládaná práce se zabývá návrhem modelu dynamiky paralelního manipulátoru optimálního pro účely návrhu řízení. Zvolený přístup je založen na modelování dynamiky systému v simulačním prostředí Matlab SimMechanics následovaném linearizací modelu. Výsledný stavový lineární model mimo jiné umožňuje snadné posouzení řiditelnosti a pozorovatelnosti modelu. Díky své relativní jednoduchosti je model také výpočetně nenáročný. Přístup je demonstrován na návrhu dvouvrstvého řízení SimMechanics modelu Stewartovy platformy, na kterém bylo následně navržené řízení úspěšně testováno.

Podstatná část práce obsahuje přístup k modelování neurčitých parametrů dynamického modelu Stewartovy platformy a stejnosměrného motoru Maxon RE 35 a jeho výsledky. Předložený přístup je založen na modelování parametrické neurčitosti způsobem, kdy je neurčitost definována individuálně pro jednotlivé prvky stavových matic modelu. Samotná neurčitost je potom určena rozdílem mezi jednotlivými parametry příslušných matic nominálního modelu a modelu se stanovenou maximální neurčitostí parametrů. Výsledný neurčitostní model je vzhledem ke své stavové reprezentaci vhodný pro návrh regulátoru založeném na metodách návrhu robustního řízení, například minimalizaci normy H-nekonečno.

Popsaná metoda byla použita pro kompenzaci posunu mezi pracovními body, okolo kterých je prováděna linearizace a pro kompenzaci nepřesnosti modelování vybraných parametrů modelů Stewartovy platformy a stejnosměrného motoru.

Získané modely (v prostředí SimMechanics a neurčitostní model) byly experimentálně porovnány s chováním jednoho z lineárních pohonů Stewartovy platformy. Rozdíl v datech obdržených ze simulace v prostředí SimMechanics a naměřených na reálném stroji byl téměř kompletně pokryt neurčitostním modelem.

Prezentovaná metoda neurčitostního modelování je velice univerzální a aplikovatelná na libovolný stavový model.

Klíčová slova: Stewartova platforma, parametrická neurčitost, simulační modelování

Abstract

The proposed work is dealing with an optimal model of a parallel manipulator dynamics for a control design purposes. The approach is based on modeling of the system dynamics in Matlab Simmechanics followed by the model linearization. The obtained linear model may be simply inspected from the controllability and observability point of view. It is also computational modest thanks to its simplicity. This is demonstrated on designing of a two – layer control for a model of a Stewart platform. The control based on such a linear model was successfully tested on the original nonlinear model.

The essential part of the the work is dealing with modeling of uncertain parameters in the dynamic model of the Stewart platform and DC motor Maxon RE 35. The proposed approach is based on modeling of a parametric uncertainty where the uncertainty is defined individually for particular elements of the model state matrices. The uncertainty itself is set by the difference between parameters of corresponding matrices of the nominal linear model and model with maximally perturbed parameters. The obtained uncertain model is for its form suitable for the robust control design methods, for example via minimizing an H-infinity norm.

The method was used for a compensation of the shifting of the linearization operating points in the Stewart platform and for compensation of the modeling inaccuracy of selected parameters in the Stewart platform and the DC motor model.

The obtained models (SimMechanics and uncertain state - space) were compared with the single linear actuator of the Stewart platform. The difference between the simulated SimMechanics model and measured data was almost completely covered by the uncertain model.

The method is highly versatile and applicable on any state-space model.

Keywords: Stewart platform, parametric uncertainty, simulation modeling

Preface

Modeling and simulation of mechanic and mechatronic systems is significant part of development of a new product or improving of a current one. It allows introducing new technologies to industry, decreasing product costs, increasing a product quality and at last but not least it indirectly contributes to the environmental protection. These are just some of fundamental factors influencing the human civilization development.

There are nowadays opened new possibilities to the modeling of systems thanks to the fast growth of the computer technologies. This makes possible to simulate and model complicated systems which would be unthinkable to simulate only twenty years ago.

The proposed work presents an approach to modeling of parallel mechanisms which recently gained ground in machining applications, fast pick and place applications or in high accurate positioning applications. The approach is highly versatile thus applicable on wide spectrum of systems.

Acknowledgements

Herein, I would like to acknowledge several people who assisted me and supported me through the postgraduate studies.

First of all, I wish to express my gratitude to my supervisor, prof. Eduard Malenovský, for his professional and very encouraging approach to me. A word of thanks goes to my father associate professor Tomáš Březina for his not just parental support but for many inspiring ideas which are realized within this work. Acknowledgement also goes to associate professor Vladislav Singule for his very useful comments and to Ing. Ondřej Andrš for many practical and beneficial debates and assistance with experiments. I am also indebted to Ing. Pavel Houška, Ph.D. for providing an engineering design of presented Stewart platform which he developed, to prof Jindřich Petruška and Ing. Lubomír Houfek, Ph.D. who provided me with opportunity to work at Instute of Solid Mechanics, Mechatronis and Biomechanics.

A special word of thanks goes to professor Erno Keskinen from Tampere University of Technology in Finland for his incredibly friendly approach to me on my internship at TUT and to Ing. Vladimír Dospěl who offered me to participate on this internship.

I am also very thankful to my present and former colleagues from labs 716 and 713 – Ing. Jiří Kovář, Ing. Tomáš Hejč, Ing. Zdeněk Hadaš, Ph.D, Ing. Jan Vetiška, Ing. Milan Turek, Ing. Miroslav Světlík and Bc. Lukáš Ertl – for numerous not just scientific debates and creating very friendly atmosphere.

Finally, I wish to express my gratefulness to my family for their endless encouragement and to my beloved girlfriend Veronika for her patience and love.

Contents

1.

Introduction

Design of complex systems is an iterative process which is often cross-disciplinary. The goal is to create a system with given parameters, thus all of simulation based methods require initial model of the system with predictable properties. Simulations as close to reality as possible are then used for experiments with the system properties and for achieving of desired information about the system.

The problem is that there is no universal design process. Known approaches are more often characterized as methodical instructions.

The fundamental approach to the design of the complex systems is for example described in [38]. The core of the system is typically made of the basic system which might be mechanical, electrical or other physical principle. It is connected through sensors and actuators to elements processing the information. Let's note that it is also possible to realize sensors, measuring the state values, in form of observers, i.e. in a software way. The measured data then defines actions influencing the system states in the desired way. The actions are linked to the system via actuators.

The aim of the design of the model based system is compact prognosis and optimization of the system behavior. The advantage of the model based design is then in possibility of testing of the control software with controllers before a prototype is manufactured.

It is also necessary to test the functionality of the system in the designing phase because it is often impossible to suppress the design errors in its later phases.

Nowadays the model is often used for design of a control system which is then able to predicate the system behavior. This might be used for dynamical compensation of unwanted behavior. The use of a model is suitable for [54]:

- kinematic compensation,
- processing of signals from additive state sensors,
- dynamic compensation,
- thermal compensation,
- prediction of error by detection of the deviation from the standard behavior,
- suppression of critical states (vibrations) by prediction of critical areas from the model.

The model based control is very interesting possibility not even for robotics but also for other technical disciplines. Obtaining of high accuracy control is nowadays often solved by implementing of the model to the control system. Model of the system built into the control system monitors data obtained from the sensors and actuators. Implementation of such controllers is nowadays possible thanks to the computational power of modern computers [24].

The models are differentiated according to the structure and prediction quality. Basic concepts are mainly [54]:

- simplified models, mainly linear,
- fenomenologic equation,
- neural networks,
- decision trees,
- look- up tables.

From the presented point of view arise following requirements on the optimal model of the system and on the optimization of the design with the model support:

- evaluation in the shortest possible time,
- possibility of the processing of the deviations from the reality,
- (simple) investigation of the system controllability
- (simple) investigation if it is possible to use the model for estimation of selected parameters (especially in cases of parameters which is difficult or impossible to measure)

The proposed work is then focused on such an optimal modeling of a parallel robot generally known as Stewart platform.

The construction of general parallel robot basically stands on a closed kinematic chain. Therefore a load carried by the end-effector is divided between particular kinematic chains linking the effector to the base. Such a construction of a manipulator leads to very high stiffness of the device and high load/robot mass ratio, possibility of lighter construction, thus better dynamics. Other advantages may be higher positioning accuracy, using same parts for all links or possibility of mounting of the actuators to the base of the device. These are some of advantages when comparing parallel manipulators with serial ones (open kinematic chain). The main disadvantage of a parallel manipulator construction is then quite small volume of the workspace limited by singular areas and usually quite complicated kinematics and dynamics.

The history of the first industrially used parallel manipulators started in a year 1955 when Gough [30] constructed the first prototype of a six degrees of freedom parallel manipulator for tire wear testing (used in Dunlop Tires till year 2000). The machine consisted of a platform (end-effector) and six extendable links which connected the platform to the base frame. The very similar construction was used approximately 10 years later by Cappel and also by Stewart for a flight simulator construction. From then parallel manipulators have been used in many other sectors of industry where their advantages as high stiffness, precise

positioning, high load/robot mass ratio, may be used. Let's name for all fast pick and place applications (ABB FlexPicker, Fanuc M-1iA), machining robots (Metrom P-800), positioning of heavy antennas, microscopes (usually hexapods in general), spot welding (Fanuc F-200iB), etc.

The parallel robots are in general suitable for applications where high positioning accuracy is more important than volume of the workspace, for applications where manipulation with heavy loads in small workspace (simulators, antenna manipulation, …) is needed or fast pick and place applications.

The presented work is based on needs of projects MSM0021630518 "Simulation modeling of mechatronic systems" and MŠMT KONTAKT 1P05ME789 "Simulation of mechanical function of selected elements of human body" which had been solved at BUT recently. One of aims of named projects was to construct a Stewart platform. The device is planned to use for biomechanical experiments such as joints endoprosthesis (hip, knee) wear testing or for spinal elements testing. Such an usage leads to specific requirements in construction and control. Hence it was necessary to build a model of the system dynamics and kinematics according to the engineering design at first. The model was built in such a way to satisfy requirements for a control design and for testing of the designed control as well as for testing of the device behavior. In other words the model had to be sufficiently precise in the system description but on the other hand it had to be modest in computational time consumption.

Building a model which is suitable for simulation and optimal for a control design at the same time might be quite complicated task – especially in case of dynamic model containing high number of interacting bodies within a spatial closed kinematics chain with six degrees of freedom of the end-effector.

The proposed approach is based on modeling of dynamics within a modern simulation tools with possibility of linearization. The modeling inaccuracies are compensated by defining of uncertain parameters in the model. The obtained structure of the model is in a state-space form which is suitable either for simulations or for a control design.

Let's note that proposed approach demonstrated on the Stewart platform is highly versatile and easily applicable to wide range of systems and processes. The method reflects actual industry needs leading to increase of a product quality, preciseness, production capacity, dependability, system economy and decrease of the environment damage. The simulation and control of the system significantly influences all of these needs.

2.

State of the art

2.1 Kinematics of parallel manipulators

Modeling of a parallel mechanism kinematics may be solved as direct and inverse task. The inverse kinematics is characteristic with known position and orientation of the end-effector and joint coordinates are solved. Solving the inverse kinematics is necessary for the position control of a manipulator. There are generally two approaches to the solving of the inverse kinematics – analytical based on work with transformation matrices [29], [48] and geometrical [50].

The opposite is the direct kinematics where the joint coordinates are known and position and orientation of the end-effector is solved [2], [20]. Solving of the direct kinematics is much more complicated than inverse in case of parallel manipulators. This is in opposite with kinematics of serial manipulators. The method is usually based on a numerical iterative principle [51], [48], use of genetic algorithm [4] or for example using of extra sensors [37]. Very interesting method based on solving the determinant of Sylvester's matrix suitable for a real –time use was proposed in [43].

2.2 Dynamics of parallel manipulators

The model of system dynamics is usually needed for a control of devices which move fast or heavily loaded devices, i.e. of devices where their dynamics effects strongly affect the system behavior. The one of problems of dynamics modeling is that not all of the parameters are known precisely even with use of on-line estimation methods. The other problem is the computational time intensity.

There are often used common methods for dynamics of machines modeling in case of parallel manipulators. These are Newton-Euler principle [14], [18], [19], [21], principle of virtual works [13], [17], [28], [30], [45], Lagrange's equations [15], [63] and the Hamilton principle [52]. There are sometimes used combinations of methods, e.g. combination of Lagrange's equations and Newton-Euler principle in [49].

Description of a parallel manipulator full dynamics via one of these methods is usually quite complicated and numerical solution of the obtained model is too much time consuming. Such a dynamics model is inappropriate for a control design. Therefore simplifying suggestions shortening the computational time are often made.

One of such simplifications might be neglecting of inertia moments of the robot links and at the same time assuming their masses at their ends [17], [56]. This approach was successfully applied on Delta robot (the robot structure is using for example ABB in their FlexPicker). Although the approach was successfully implemented with Delta robot, neglecting of links inertia moments in case of Stewart platform leads to insufficient positioning accuracy of the controller [27]. Another approach is presented in [42] where the simplification is based on small workspace of the Stewart platform. The configuration-dependent coefficient matrices of the dynamic equations are approximated to be constant. The introduced modeling error is compensated by the H-infinity controller. Other publications dealing with the simplification of a model dynamics are for instance [16], [25], [47], [57], [62], [64].

Very interesting possibilities of dynamics modeling are nowadays offered by numerous simulation softwares – Adams, Matlab – SimMechanics, Chrono R3D, Inventor, SolidWorks, etc. The advantage is that such environments allow user to work with the model in much more complex way (build a model, design a controller, connecting of models, etc.). This might be very efficient tool for "rapid prototyping" or classical mechatronic approach where it is taken into account that different phases of a product design are mutually connected and strongly influencing each other. Very inspiring example from the point of view of parallel manipulators is used in Matlab demos where a simple model of a Stewart platform was built, linearized and consequently a PID controller was designed [61]. However the model is in its simplest form and contains no uncertainties.

2.3 Notes to the control of parallel manipulators

Control of parallel manipulators might be quite complicated especially in cases where the dynamics model is needed. Most common is the position control [41], [42], [59] but in some cases also a torque control is used [66]. Possibilities of simplified dynamics models are studied recently (see above). Interesting possibility of H-infinity controller application for compensation of inaccuracies caused by a model simplification was studied in [42]. Nonlinear adaptive control applied on a 6 DOF manipulator describes [35]. The possibilities of parallel manipulators control are also described in [5], [12], [22], [23], [46], [47], [62], [64], [65].

2.4 Notes to modeling of systems with uncertainties

The most of models describing dynamics of systems are more or less inaccurate. It may be mostly caused by mentioned simplifications, neglecting of some factors influencing the dynamics or general modeling inaccuracy. It is possible to describe these inaccuracies by defining an uncertainty of the whole model or of the chosen parameters. The model containing the uncertainty description is then applicable for design of a robust controller. Such a controller is then able to control all systems within a given uncertainty range.

The uncertain modeling is very versatile and easily applicable on wide spectrum of human activity. The standard approach to modeling of uncertain mechanical systems for a robust control purposes is described in [32] or [33].

2.5 Summary and the problem description

The inverse kinematics of the parallel manipulators has been intensively studied for several decades and its solution is no more a problem. On the other hand the direct kinematics is for its strong nonlinearity still quite challenging task especially in cases where a real-time application is considered. Very promising solution of a Stewart platform real-time direct kinematics was proposed in [43].

The modeling of dynamics of parallel manipulators is mostly solved by classical methods of dynamics but often also by a simulation modeling. The problem is typically insufficient computational efficiency for a real-time use. This is often treated by simplifying suggestions where some of the system parameters are neglected or the model is simplified [42].

The problem of simplifications or approximations of the dynamic models introduced in order to increase the computational efficiency is following. It has to be very carefully considered for every individual type of a mechanism which simplifications it is possible to make. Some of simplifications can be made for some type of a mechanism but for other not – the method is not versatile.

The other problem is that a model of dynamics usually contains many inaccuracies. The problem is getting worse by introducing of mentioned simplifications and approximations.

Modeling of systems with uncertainties is nowadays used in many even nontechnical applications [34], [44], [60] for description of a model inaccuracy. But in case of modeling of parallel robots it is very rare.

3.

Goals of the work

The main goal of the work is to propose and verify a methodology for design of dynamic models of parallel manipulators optimal for a control design. Such an optimal model must satisfy following conditions:

- evaluation in the shortest possible time,
- possibility of the processing of the deviations from the reality,
- (simple) investigation of the system controllability
- (simple) investigation if it is possible to use the model for estimation of selected parameters (especially in cases of parameters which is difficult or impossible to measure)

Let's note that actual needs of the modern industry are taken into account, thus it is expected use of more advanced controllers than just a simple PID and use of modern control techniques.

The method should be also universal and applicable on other mechatronic systems such as machining tools, robotics in general, engines and other.

Building of such an optimal model satisfying the above requirements will be illustrated on the Stewart platform developed at BUT which has intended use in biomechanical applications [10], [11].

Thus the model will be optimized for investigation of possibility of control design techniques application, description of modeling inaccuracies and for computational modesty.

Sectional goals are following:

- Analyze present methods of modeling of parallel mechanism
- Design an appropriate method for a parallel robot modeling
- Build a model describing kinematics and dynamics of the Stewart platform
- Optimize the model for the control design purposes
- Verify the model with the real device
- Formulation of conclusions

4.

Background theory

4.1 Linear vs. nonlinear systems

The linear system must satisfy conditions of superposition $f(x+y)=f(x)+f(y)$ and homogeneity $f(kx)=kf(x)$ for inputs *x*, *y* and any real number *k*. Any other system is considered as nonlinear.

Hence a linear system may be divided into several parts which are then solved separately. There is a wide background theory of working with linear systems but the most of engineering problems are mostly nonlinear.

Nonlinear systems are typical with many possible equilibrium points, system stability depending on initial conditions, possible chaotic behavior, etc. It is then often proceeded to linearization of the nonlinear models because of its complicated possibilities of study. Obtained linear model has behavior very close to the nonlinear model but only for a small area around the linearization point.

Typical sources of nonlinearities in mechanical systems are for example Coulomb friction or a backlash.

The nonlinear system is generally not suitable for a control design purposes. While the linear representation of the system offers standardized tools for inspection of controllability and observability, as well as other linear control theory methods [55]. Let's just briefly walk through some of these methods.

Let's consider a linear continuous state – space system

$$\begin{aligned} \dot{x} &= Ax + Bu \\ y &= Cx + Du \end{aligned} \quad . \tag{4.1}$$

The system is stable if all eigenvalues of matrix *A* have negative real parts, i.e. if $\mathrm{Re}(\lambda_i)<0$.

The controllability condition is satisfied for $A \in R^{n\times n}$, $B \in R^{n\times m}$ and $R_r = \begin{bmatrix} A^0B^1 & A^1B^1 & A^2B^1 & \dots & A^{n-1}B^1 \end{bmatrix}$ if

$$rank(R_r) = n. \tag{4.2}$$

The controllability in general says if it is possible to change a state of the system by an input.

The observability then guarantees the possibility to observe all of the system states, i.e. possibility of reconstruction of the system states based on knowledge of input. This is profitable especially in cases of the system states which is difficult or impossible to measure by standard techniques. The observabiliy condition is satisfied for $A \in R^{n \times n}$, $C \in R^{n \times n}$ and $R_o = \left[\left(C^T\right)^0 A^T \quad \left(C^T\right)^1 A^T \quad \left(C^T\right)^2 A^T \quad \ldots \quad \left(C^T\right)^{n-1} A^T \right]$ if

$$rank\left(R_o\right) = n. \tag{4.3}$$

The typical methods utilizing a linear state – space model for a controller design are for example pole placement method [40] or linear quadratic regulator design [32].

4.2 Modeling of uncertain systems

The precise description of a model is not always possible even with use of advanced modeling tools. The modeling inaccuracy is typically caused by unmodeled dynamics, neglected nonlinearities, reduced order of the system, parameter variations or inaccurate description in general. The model is an approximation of the real system. However this might be a problem when designing a control of the system – the precise model is needed for proper design of a controller.

The approach dealing with this problem is based on modeling of the real system as a set of linear time-invariant models built around a nominal one, i.e. the model is built as uncertain within known boundaries. The benefit of such a representation of a model is the possibility of designing a robust controller stabilizing a closed loop system even with uncertainties. The most degraded model within defined uncertainty is then called “the worst case scenario”. The ideal goal is to design a controller capable of stabilizing even the “the worst case scenario”. Such a controller then also guarantees stabilizing all of realizations of the model within the given uncertainty boundaries.

There are two most general ways of representing the uncertainty [33] – the unstructured and structured uncertainty.

4.2.1 The unstructured uncertainty

The unstructured uncertainty is “a global” uncertainty of the system where individual contributions to the uncertainty are described by a single perturbation. This kind of uncertainty is typical for instance for unmodeled dynamics or neglected nonlinearities. It is mostly used for high-frequency dynamics description.

The most common representations of the unstructured uncertainty are for the nominal system $\bar{G}$, perturbed system G_p and perturbation block Δ following [33]:

- Additive perturbation $G_p = \bar{G} + \Delta$
- Multiplicative perturbation $G_p = \bar{G}(I + \Delta)$
- Inverse additive perturbation $G_p^{-1} = \bar{G}^{-1} + \Delta$
- Inverse multiplicative perturbation $G_p^{-1} = \bar{G}^{-1}(I + \Delta)$

It is characteristic for the unstructured uncertainty that block Δ may be unknown transfer function matrix, in general it is a full matrix.

4.2.2 The structured uncertainty

The other uncertainty representation – the structured uncertainty – is describing all of the uncertainty contributions individually. It is typical especially for description of variations of the system parameters (parametric uncertainty) or shifting of operating points, i.e. for low-frequency dynamics description.

The standard form of the structured uncertainty representation is for the augmented system *M* presented in Fig. 4.1 It is standard configuration called M - Δ describing relation between inputs and outputs of the system and their affection by uncertainties.

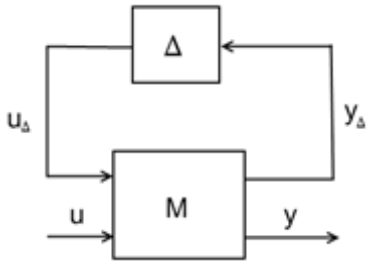

Fig. 4.1 M - Δ configuration of a model with uncertainty

It is typical for the structured uncertainty that the perturbation matrix **Δ** is diagonal, i.e. it has certain structure $\mathbf{\Delta} = \mathrm{diag}\{\Delta_1, ..., \Delta_m\}$. The augmented system *M* is obtained from the nominal system $\bar{G}$ with its nominal parameters and their variations $\Delta_1, ..., \Delta_m$ by upper linear fractional transformation.

Let's note that the standard M – Δ configuration is also applicable on the unstructured uncertainty as well but with a full Δ matrix.

4.2.3 Upper linear fractional transformation

Upper linear fractional transformation was for the first time in connection with a robust control described in [58]. From then it is widely used for uncertainty modeling. The general principle is following.

M is an interconnection transfer function matrix according to

$$\mathbf{M} = \begin{bmatrix} \mathbf{M}_{11} & \mathbf{M}_{12} \\ \mathbf{M}_{21} & \mathbf{M}_{22} \end{bmatrix} \tag{4.4}$$

and

Δ is the perturbation matrix with dimensions conformed to $\mathbf{M}_{11}$.

$\mathbf{M}_{11}$, …, $\mathbf{M}_{22}$ are obtained according to

$$\mathbf{F}_u(\mathbf{M}, \boldsymbol{\Delta}) = \mathbf{M}_{22} + \mathbf{M}_{21}\boldsymbol{\Delta}(\mathbf{I} - \mathbf{M}_{11}\boldsymbol{\Delta})^{-1}\mathbf{M}_{12}, \tag{4.5}$$

where $\mathbf{F}_u(\mathbf{M}, \boldsymbol{\Delta})$ is called upper linear fractional transformation of **M** and **Δ**.

The unstructured uncertainty may be then defined with interconnection matrices **M** according to [33] as:

additive perturbation $\mathbf{M} = \begin{bmatrix} 0 & I \\ I & \bar{G} \end{bmatrix}$, multiplicative perturbation $\mathbf{M} = \begin{bmatrix} 0 & I \\ \bar{G} & \bar{G} \end{bmatrix}$, inverse additive perturbation $\mathbf{M} = \begin{bmatrix} -\bar{G} & \bar{G} \\ -\bar{G} & \bar{G} \end{bmatrix}$ and inverse multiplicative perturbation $\mathbf{M} = \begin{bmatrix} -I & I \\ -\bar{G} & \bar{G} \end{bmatrix}$.

4.2.4 Robust stability for unstructured uncertainty

A system is robust when it remains stable for a bounded set of perturbations according to [32]. Thus it is necessary to find a stabilizing controller of a closed loop containing a controller and a nominal system under a defined perturbation that stabilizes the closed-loop for all possible perturbations of the system. Such a controller is then of course stabilizing even the nominal plant.

The following Fig. 4.2 presents a closed – loop system containing a controller *K* and a nominal system $\bar{G}$ with given additive perturbation **Δ** which is a full matrix.

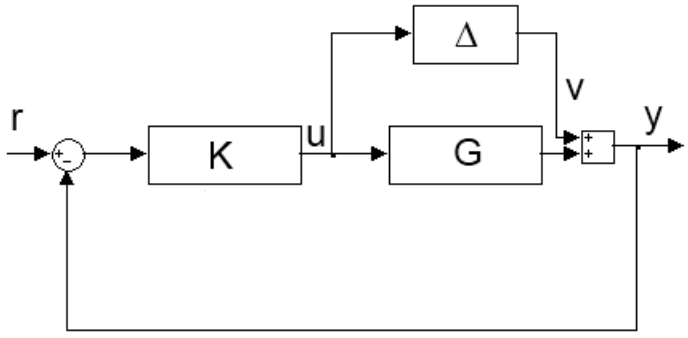

Fig. 4.2 Closed loop system with additive uncertainty

The transfer function of the *v* to *u* is then $T_{uv} = -K\left(I + \bar{G}K\right)^{-1}$. It is obtained by applying the Small – Gain theorem [53] that a closed loop is robustly stable if *K* stabilizes the nominal system and

$$\left\|\Delta K\left(I + \bar{G}K\right)^{-1}\right\|_\infty < 1 \text{ and } \left\|K\left(I + \bar{G}K\right)^{-1}\Delta\right\|_\infty < 1 \tag{4.6}$$

or

$$\left\|K\left(I + \bar{G}K\right)^{-1}\right\|_\infty < \frac{1}{\|\Delta\|_\infty}. \tag{4.7}$$

The control design problem is then formulated as finding an optimal stabilizing controller *K* that minimizes the norm (4.7).

Conditions of the robust stability may be similarly expressed for other forms of representation of the unstructured uncertainty [33]:

multiplicative perturbation $\left\|K\bar{G}\left(I + \bar{G}K\right)^{-1}\right\|_\infty < \frac{1}{\|\Delta\|_\infty}$, inverse additive perturbation $\left\|\bar{G}\left(I + \bar{G}K\right)^{-1}\right\|_\infty < \frac{1}{\|\Delta\|_\infty}$ and inverse multiplicative perturbation $\left\|\left(I + \bar{G}K\right)^{-1}\right\|_\infty < \frac{1}{\|\Delta\|_\infty}$.

4.2.5 Robust stability for structured uncertainty

The general robust stability conditions may be also written in form $\det\left[I - M(j\omega)\Delta(j\omega)\right] \neq 0$, $\forall\omega \in R, \forall\Delta$, where *M* is the nominal closed loop system which is assumed to be stable, [53].

The structured uncertainty is characterized by diagonal perturbation matrix $\Delta = \text{diag}\{\Delta_1, ..., \Delta_m\}$. Δ_i may be in general any transfer matrix satisfying $\bar{\sigma}(\Delta_i) \leq 1, \forall\omega$.

Then may be defined so called structured singular value $\mu_\Delta(M)$ which analyzes the smallest possible uncertainty that makes $\det\left[I - M(j\omega)\Delta(j\omega)\right] \neq 0$. It is then

$$\mu_\Delta(M) \equiv \frac{1}{\min_\Delta\left\{\bar{\sigma}(\Delta)\middle|\det(I - M\Delta) = 0 \text{ for some structured } \Delta\right\}}, \tag{4.8}$$

if there is no Δ satisfying $\det(I - M\Delta) = 0$, then $\mu_\Delta(M) \equiv 0$, [26].

The robust stability condition for the system with a structured uncertainty is then

$$\mu_\Delta(M) < 1, \forall\omega. \tag{4.9}$$

4.2.6 Notes to the robust performance

Sometimes it is not sufficient to design a controller which is only stabilizing but also other properties are desired. The given properties depend on the minimized norm. An overview of minimized norms and corresponding properties is following [33]: good tracking $\left\|\left(I+\bar{G}K\right)^{-1}\right\|_{\infty}$, disturbance attenuation $\left\|\left(I+\bar{G}K\right)^{-1}\right\|_{\infty}$, noise suppression $\left\|-\left(I+\bar{G}K\right)^{-1}\bar{G}K\right\|_{\infty}$ and control energy minimization $\left\|K\left(I+\bar{G}K\right)^{-1}\right\|_{\infty}$.

Combination of norms leads to solving a mixed sensitivity optimization problem. Mixed sensitivity norm may be for example described as $\left\|\begin{matrix}\left(I+\bar{G}K\right)^{-1}\\ K\left(I+\bar{G}K\right)^{-1}\end{matrix}\right\|_{\infty}$. A controller K minimizing the norm then offers good tracking with minimal possible control energy.

The proposed work utilizes mainly described upper linear fractional transformation. The robust stability and performance was not solved because it exceeds the scope of the work.

5.

Proposed approach

The proposed approach is based on mentioned advantages of the linear model representation.

The model itself utilizes advantages of Matlab SimMechanics simulation environment which offers many tools for modeling of kinematics and dynamics of mechanisms as well as the possibility of linearization. The simulation environment is for its good connectivity with Simulink suitable for simulations of a control and for the model and data manipulation.

There are also derived standard equations of the inverse kinematics for the simulation and control purposes.

The linear model obtained from SimMechanics guarantees simplicity, computational efficiency and wide spectrum of methods for the manipulation with the model and for a model based controller design.

Inaccuracies of the model caused by the linearization, neglected dynamics or improperly defined parameters are then described by definition of uncertainties for the individual model parameters.

The uncertain modeling is used for describing of inaccuracies caused by shifting of the linearization operating points of the Stewart platform and by modeling inaccuracy of selected parameters of the Stewart platform and the DC motor model.

The method for modeling of uncertainties of the DC motor is based on the standard parametric uncertainty definition. It is then proposed a method for defining of individual parameters of the model state matrices as uncertain. This is profitable especially in cases of higher order models. The method is used in case of the Stewart platform uncertainty modeling.

The uncertain model may be with advantage used for a “worst case scenario” analysis and for a robust control design. The uncertain model is linear thus keeping all advantages of the linear representation.

6.

The device description

6.1 The linear actuator with gearings

The Stewart platform consists of six linear actuators (links) which manipulate with top plate of the platform. The change of the actuator length leads to the change of the platform position and orientation. The links lengths needed to obtain desired position and orientation of the platform are then easily evaluated with the knowledge of the inverse kinematics.

The choice of joints within the linear actuator itself is subjected to the overall movement of the platform which has to be fully three dimensional, i.e. with six degrees of freedom. Thus the upper joint connecting the actuator to the platform is spherical (three rotational degrees of freedom) and the lower joint connecting the actuator to the base is universal (two rotational degrees of freedom). With the middle translational joint (ball screw in our case) connecting together upper and lower part of the linear actuator.

6.1.1 Mechanical parts of the linear actuator

Let's note at first that the linear actuator is the most complicated part of the whole Stewart platform because of the number of its mechanical parts. The actuator parts may be in general divided into two groups. The first group would be joints and the second group would be bodies (this will be very useful for later SimMechanics modeling). The joints group (Fig. 6.1) contains the spherical joint 1, a ball screw (screw joint) 2, the ball screw guidance 3, plate for attachment of a DC motor 4, a screw nut 5, gearings (a spur gearing and a planetary gearbox) 6 and finally the universal joint 7. The bodies group (Fig. 6.2) basically contains the upper part of the actuator (the ball screw 1a with its nut 2a) and the lower part of the actuator 3a which is connected to the DC motor 4a by the plate 4. These are main parts having influence on kinematics and dynamics of the machine.

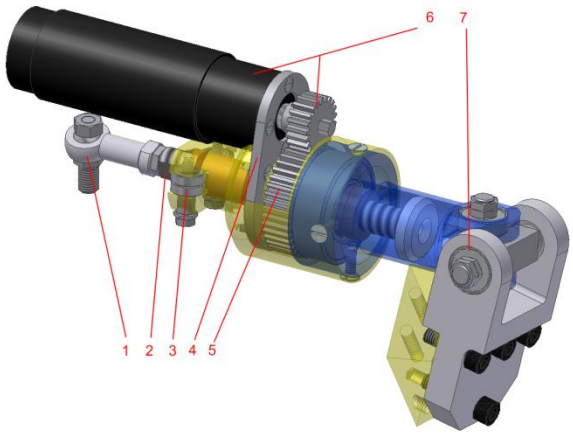

Fig.6.1 Joints of the linear actuator (by Houška, P.)
1 spherical joint, 2 ball screw, 3 ball screw guidance, 4 motor attachment plate, 5 screw nut, 6 gearings, 7 universal joint

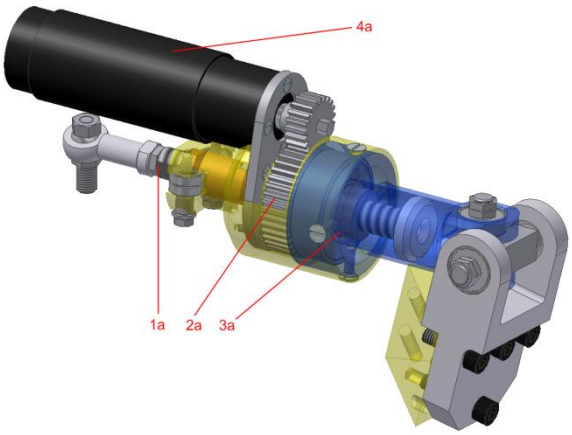

Fig.6.2 Bodies of the linear actuator (by Houška, P.)
1a ball screw, 2a screw nut, 3a lower part of the link, 4a DC motor

Technical parameters are following. The used DC motor is Maxon RE 35 (90 W), single stage planetary gearbox Maxon GP 32 C with gear ratio 4.8:1, the gear ratio of the spur gearing is 41:21, the screw-thread is 4 mm. The maximal length of the single linear actuator is 188 mm, the minimal length is 159 mm.

6.2 The Stewart platform

The basic geometry of the device (Fig. 6.3, 6.4) is defined by position of the base and platform connection points for linear actuators attachment, Fig 6.5, 6.6. The basic geometry of the Stewart platform is amongst others described in [50].

6.2.1 Basic geometry of the Stewart platform and its inverse kinematics

The Stewart platform geometry may be in the simplest form described as follows: The circular movable platform is defined by coordinates of points $\mathbf{p_i} = [p_{i\_x} \quad p_{i\_y} \quad p_{i\_z}]^T$. There are six links (linear actuators) $\mathbf{b_i p_i}$ connecting the platform to the base circular body which is defined by points $\mathbf{b_i} = [b_{i\_x} \quad b_{i\_y} \quad b_{i\_z}]^T$, $i = 1, ..., 6$. The platform and base are parallel and axially aligned in the steady state. The points of the platform and the base are $\frac{1}{3}\pi$ mutually shifted.

The inverse kinematics describes relation between actuated joints coordinates and given end-effector configuration. The actuated joints are prismatic in case of the Stewart platform, thus the joint coordinates are defined as lengths of the links.

Let's note that establishing of the inverse kinematics equations is the fundamental step to the position control design. The inverse kinematic equations might be according to [3], [8],[36] also used for determination of the system Jacobians and consequently to analyze the singular states of the machine.

Fig. 6.3 The designed Stewart platform – 3D model (by Houška, P.)

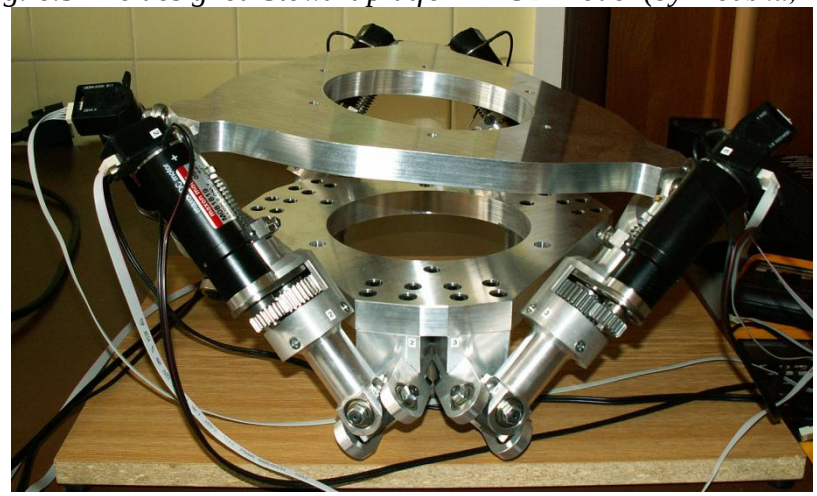

Fig. 6.4 The designed Stewart platform – reality (by Houška, P.)

There are defined two main coordinate systems on the Stewart platform, Fig. 6.5, 6.6. It is the coordinate system of the base (CSb) which at the same time corresponds with the global coordinate system and local coordinate system of the platform (CSp). Both systems are in the steady state of the platform axially aligned along the z-axis.

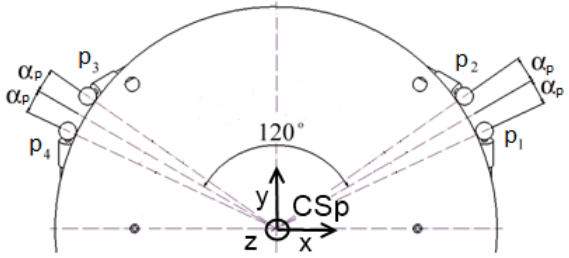

Fig. 6.5 Platform angles

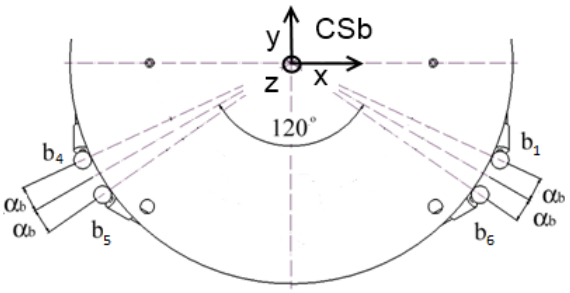

Fig. 6.6 Base angles

The position of the base connection points $\mathbf{b_i}$ is defined in CSb (Appendix B) as

$$\mathbf{b_{2i-1}} = r_b \begin{bmatrix} \cos\beta_{mb\_i} \\ \sin\beta_{mb\_i} \\ 0 \end{bmatrix}, \quad \mathbf{b_{2i}} = r_b \begin{bmatrix} \cos\beta_{pb\_i} \\ \sin\beta_{pb\_i} \\ 0 \end{bmatrix} \tag{6.1}$$

for $\beta_{mb\_i} = \frac{2}{3}\pi(i-1) + \alpha_b - \frac{1}{6}\pi, \quad \beta_{pb\_i} = \frac{2}{3}\pi(i-1) - \alpha_b + \frac{1}{2}\pi$ and $i = 1, ..., 3$.

The meaning of terms is following: $\alpha_b = 10,84°$ is the offset angle on the base according to Fig. 2.6 and $r_b = 175,02mm$ is the base radius. The same process was used for obtaining coordinates of the platform connection points.

The position of the platform points $\mathbf{p_i}$ is defined in CSp (Appendix B) as

$$\mathbf{p_{2i-1}} = r_p \begin{bmatrix} \cos\beta_{mp\_i} \\ \sin\beta_{mp\_i} \\ 0 \end{bmatrix}, \quad \mathbf{p_{2i}} = r_p \begin{bmatrix} \cos\beta_{pp\_i} \\ \sin\beta_{pp\_i} \\ 0 \end{bmatrix}, \tag{6.2}$$

for $\beta_{mp\_i} = \frac{2}{3}\pi(i-1) - \alpha_p + \frac{1}{6}\pi, \quad \beta_{pp\_i} = \frac{2}{3}\pi(i-1) + \alpha_p + \frac{1}{6}\pi$ and $i = 1, ..., 3$.

$\alpha_p = 6,47°$ is the offset angle on the platform (Fig. 6.5), $r_p = 190mm$ is the platform radius.

It is necessary to transform the platform points to the coordinate system of the base (global coordinate system) for obtaining the general position of the platform points in a 3D space:

$$\mathbf{p_{T_i}} = \mathbf{T} + \mathbf{p_i}\mathbf{R}, \tag{6.3}$$

for $\mathbf{p_{T_i}} = \begin{bmatrix} p_{T_{i\_x}} & p_{T_{i\_y}} & p_{T_{i\_z}} \end{bmatrix}^T$ and $i = 1, ..., 6.$

$\mathbf{T} = \begin{bmatrix} t_x & t_y & t_z \end{bmatrix}^T$ is the translation vector and $\mathbf{R}$ is the matrix of rotations

$$\mathbf{R} = \begin{bmatrix} \cos\psi\cos\phi - \sin\psi\cos\theta\sin\phi & \cos\psi\sin\phi + \sin\psi\cos\theta\cos\phi & \sin\psi\sin\theta \\ -\sin\psi\cos\phi - \cos\psi\cos\theta\sin\phi & -\sin\psi\sin\phi + \cos\psi\cos\theta\cos\phi & \cos\psi\sin\theta \\ \sin\theta\sin\phi & -\sin\theta\cos\phi & \cos\theta \end{bmatrix}$$ with Euler angles ϕ, ψ, θ.

The lengths of the links are then defined as

$$\left|\mathbf{p_{T_i}}\mathbf{b_i}\right| = \sqrt{\left(p_{T_{i\_x}} - b_{i\_x}\right)^2 + \left(p_{T_{i\_y}} - b_{i\_y}\right)^2 + \left(p_{T_{i\_z}} - b_{i\_z}\right)^2}, \tag{6.4}$$

for $i = 1, ..., 6$.

The link lengths might be then easily evaluated for the desired position of the platform gravity centre (i.e. translation vector **T**) and desired orientation of the platform gravity centre

(Euler angles). This is the commonly used approach for the Stewart platform kinematics description.

However the construction of the proposed Stewart platform is slightly different [11]. The main difference is in the universal joint construction. The standard construction has the universal joint with axes of its revolute joints intersecting at the base connection point $\mathbf{b_i}$. The used universal joint has axes of its revolute joints orthogonal but shifted between each other by c_i, Fig. 6.7, 6.8. It is because of simpler manufacturability. This results into a bit more complicated kinematics described in [9].

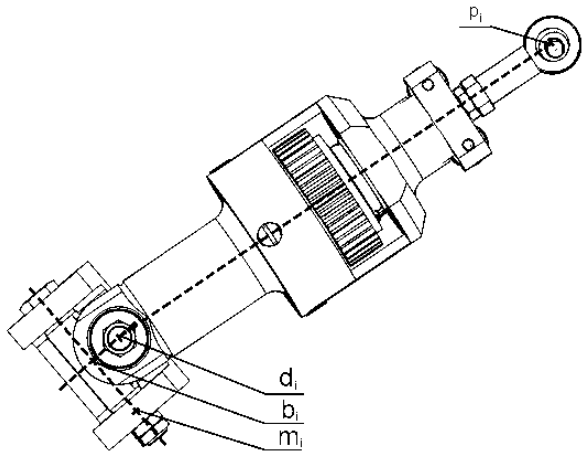

Fig. 6.7 The latest construction of the link (by Houška, P.)

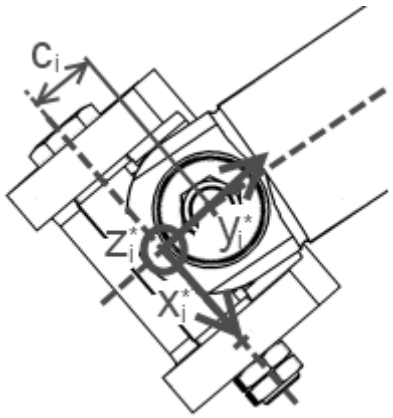

Fig. 6.8 Geometry of the u-joint (by Houška, P.)

The connection points on the base $\mathbf{b_i}$ and on the platform $\mathbf{p_i}$ are already known. Also approach for obtaining coordinates of $\mathbf{p}_{T_i}$ remains unchanged. The global coordinates of the new points $\mathbf{d_i}$ representing connection points of the shifted revolute joints and the links have to be determined. The new lengths of the links are then $\mathbf{p}_{T_i}\mathbf{d_i}$.

There were determined auxiliary points $\mathbf{m_i}$ (Appendix B) which represent the central points of bearings. Their global coordinates are known from the construction design. The solution for i-th link is following.

New local coordinates are defined according to

$$\mathbf{x}_i^* = \mathbf{m_i} - \mathbf{b_i},$$
$$\mathbf{w}_{z_i} = \mathbf{p}_{T_i} - \mathbf{b_i}, \mathbf{z}_i^* = \mathbf{x}_i^* \times \mathbf{w}_{z_i}, \tag{6.5}$$
$$\mathbf{y}_i^* = \mathbf{z}_i^* \times \mathbf{x}_i^*.$$

The coordinates of $\mathbf{d_i}$ transformed into a global coordinate system are

$$\mathbf{d_{T_i}} = \mathbf{d_i R_i} + \mathbf{T}, \tag{6.6}$$

where $\mathbf{T}$ represents the translation of $\mathbf{b_i}$ with respect to the origin of the global coordinate system and $\mathbf{R_i}$ is the rotation matrix

$$\mathbf{R_i} = \begin{bmatrix} \frac{x^*_{xi}}{|\mathbf{x}^*_i|} & \frac{y^*_{xi}}{|\mathbf{y}^*_i|} & \frac{z^*_{xi}}{|\mathbf{z}^*_i|} \\ \frac{x^*_{yi}}{|\mathbf{x}^*_i|} & \frac{y^*_{yi}}{|\mathbf{y}^*_i|} & \frac{z^*_{yi}}{|\mathbf{z}^*_i|} \\ \frac{x^*_{zi}}{|\mathbf{x}^*_i|} & \frac{y^*_{zi}}{|\mathbf{y}^*_i|} & \frac{z^*_{zi}}{|\mathbf{z}^*_i|} \end{bmatrix}. \tag{6.7}$$

The link lengths are then

$$|\mathbf{p_i d_{T_i}}| = \sqrt{(p_{i\_x} - d_{T_{i\_x}})^2 + (p_{i\_y} - d_{T_{i\_y}})^2 + (p_{i\_z} - d_{T_{i\_z}})^2}\,. \tag{6.8}$$

7.

SimMechanics modeling of the device

7.1 Stewart platform and the linear actuator modeling

The joints and bodies groups of the linear actuator are already known from the engineering design [10], [11] as well as the geometry information. The geometry information in this case means the information about location of connection points between bodies and centre of gravity on the particular body. These are then defined as vectors related to global or local coordinate system. The information about body inertia moments and body masses may be easily obtained from the software where the engineering design was projected (Inventor).

The model of the linear actuator is then built with use of SimMechanics joints and bodies libraries, Fig. 7.1.

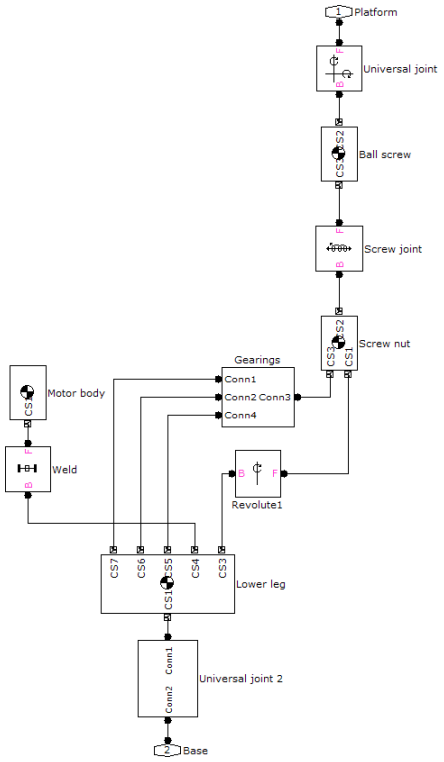

Fig. 7.1 SimMechanics model of the Stewart platform linear actuator

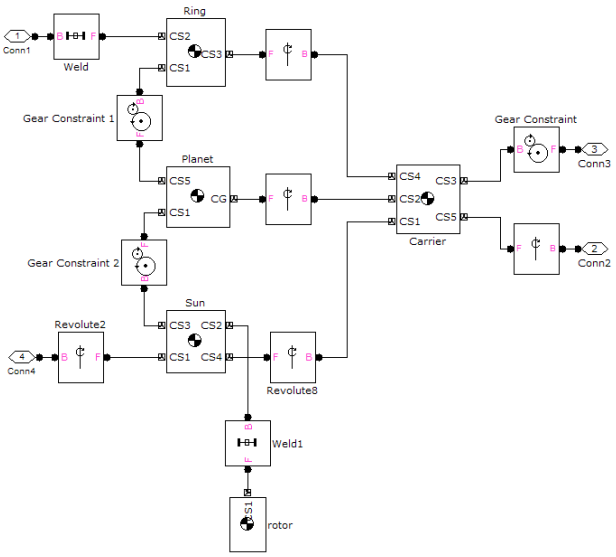

Fig. 7.2 SimMechanics model of gearings (planetary gearbox and spur gearing)

Gearings (the spur gearing and the planetary gearbox) are modeled as a system of massless bodies with "Gear constraints" blocks, Fig.7.2. These blocks defines the gear ratio between movements of bodies which create the gearings system and guarantee transfer of kinematic and force effects between constrained bodies.

The Stewart platform model is then built from six linear actuators subsystems and the platform body [6], Fig. 7.3.

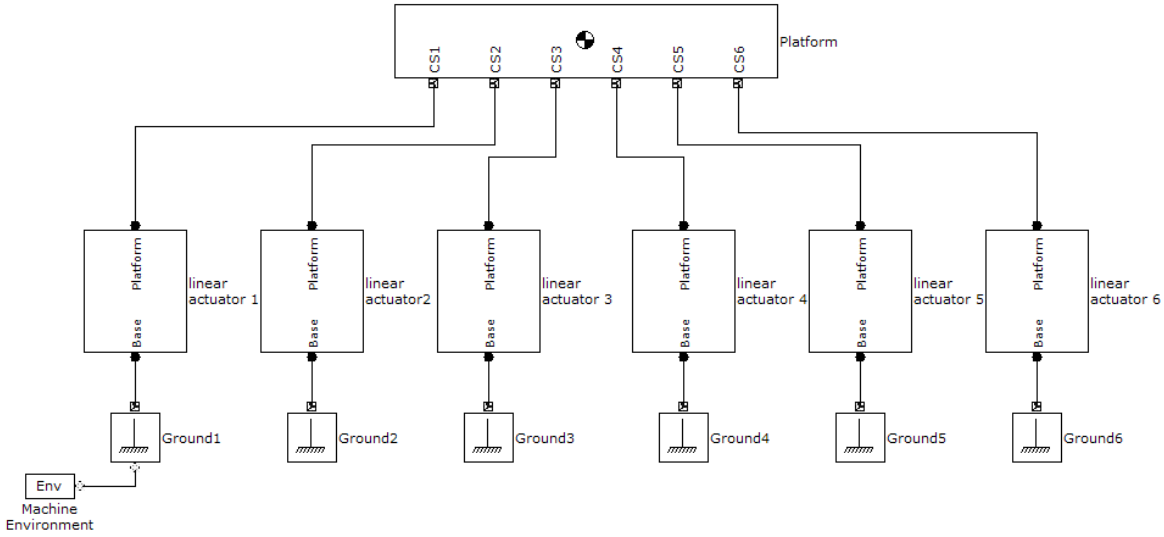

Fig. 7.3 SimMechanics model of the Stewart platform with linear actuator subsystems. Platform connection points correspond with CS1,..., CS6 and the base points with Ground1,..., Ground6

See Appendix A for the information about particular values of the body and joint parameters, position vectors of body coordinate systems origins and gearbox modeling of the linear actuator and Appendix B for the further information about the particular values of the body parameters of the Stewart platform.

7.1.1 Notes to the SimMechanics modeling of the linear actuator

It is very profitable to define within each body a local system which is the reference system for the other systems located on the body. What is also important for the modeling simplicity, such a system should have its axes aligned along axes of the body.

The global coordinate system of the Stewart platform is defined according to Fig. 6.6 The orientation of the local coordinate systems axes (valid for bodies lower link, screw nut, ball screw and motor body) may be defined via unit vectors, Fig. 7.4.

The vectors of the i^{th}-link are:

$$\mathbf{w}_i = \mathbf{p}_{T_i} - \mathbf{d}_i, \tag{7.1}$$

for $i = 1,...,6.$

The unit vectors are described as

$$\hat{\mathbf{K}}_i = \frac{\mathbf{w}_i}{|\mathbf{w}_i|},\ \hat{\mathbf{I}}_i = \hat{\mathbf{K}}_i \times \begin{bmatrix} 0 \\ 0 \\ -1^i \end{bmatrix} \text{ and } \hat{\mathbf{J}}_i = -\hat{\mathbf{I}}_i \times \hat{\mathbf{K}}_i, \tag{7.2}$$

for $i = 1,...,6$.

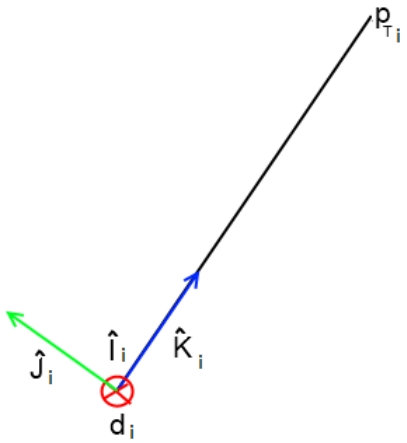

Fig. 7.4 Example of a local coordinate system axis orientation

7.1.2 Inputs/Outputs analysis

Inputs and outputs of the Stewart platform SimMechanics model are given by supposed control requirements. The basic idea is to control the position and orientation of the platform by DC motors shaft torques which are produced by the motors input voltage. The position and orientation of the platform is given by the links lengths which are described by the inverse kinematics. The changes of the links lengths are then given by rotation of the screw nut which moves the ball screw.

The inputs/outputs of the Stewart platform mechanical model are on the most basic layer following: the inputs are torques $\mathbf{m} = (M_1,\ldots,M_6)^T$ produced by DC motors and outputs are angular displacements of the screw nuts $\mathbf{q} = (\varphi_1,\ldots,\varphi_6)$ and their angular velocities $\dot{\mathbf{q}} = (\dot{\varphi}_1,\ldots,\dot{\varphi}_6)$.

Adding chosen inputs and outputs to the SimMechanics model is provided by connecting blocks of sensors and actuators. The torque actuator is added to the input element of the planetary gearbox in case of the DC motor torques and the joint sensor is added to the revolute joint representing rotational movement of the screw nut, Fig. 7.5.

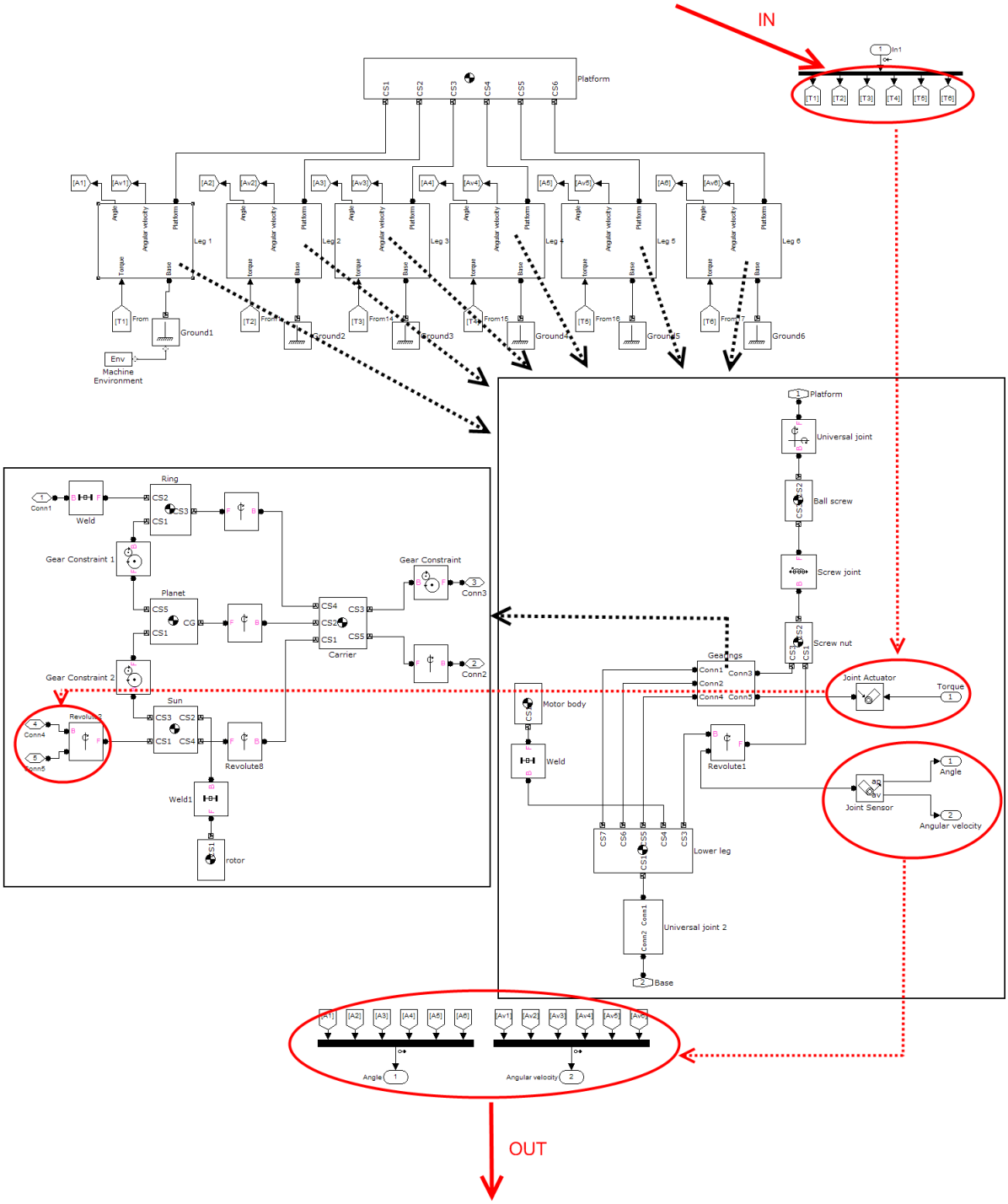

Fig. 7.5 SimMechanics model input/output routing (red arrows) within its subsystems (black arrows)

7.2 DC motor modeling

The model contained two kinds of subsystems till now. It was the linear actuator subsystem and the gearings subsystem. The new subsystem will represent the DC motor Maxon RE35.

The RE 35 (catalogue number 273754 – Appendix C) has power of 90W, its nominal torque is 0,0977Nm, nominal voltage 42V, nominal speed is 6770rpm and no load speed 7530rpm..

The unloaded DC motor model is based on well known description:

$$\begin{aligned} \frac{di}{dt} &= -\frac{R}{L}i - \frac{K_b}{L}\omega + \frac{1}{L}u \\ \frac{d\omega}{dt} &= -\frac{1}{J}K_f\omega + \frac{1}{J}K_m i \end{aligned} . \qquad (7.3)$$

The second equation is then transformed by $J\frac{d\omega}{dt} = M$ in order to obtain a shaft torque as the system output into

$$M = -K_f\omega + K_m i, \qquad (7.4)$$

where M is the motor shaft torque, K_M is the torque constant, J is the rotor inertia, K_f is the linear approximation of the viscous friction, i is the momentary value of the electrical current, ω is the momentary angular velocity of the shaft, K_b is the voltage constant, R is the terminal resistance, L is the terminal inductance and finally u is the momentary driving voltage.

The values of the terms are according to the Maxon catalogue for the RE 35 (273754) following: $R = 2,07\Omega$, $L = 0,00062H$, $K_m = 0,052\frac{Nm}{A}$, $K_b = 0,052\frac{V}{rad.s^{-1}}$, $K_f = 0,000048$, $J = 7,2.10^{-6}kg.m^2$.

The model of the motor (Fig. 7.6) was modeled as a subsystem of the Stewart platform model and the linear actuator model, Fig. 7.7. There is no need to use the SimMechanics model libraries for the DC motor modeling.

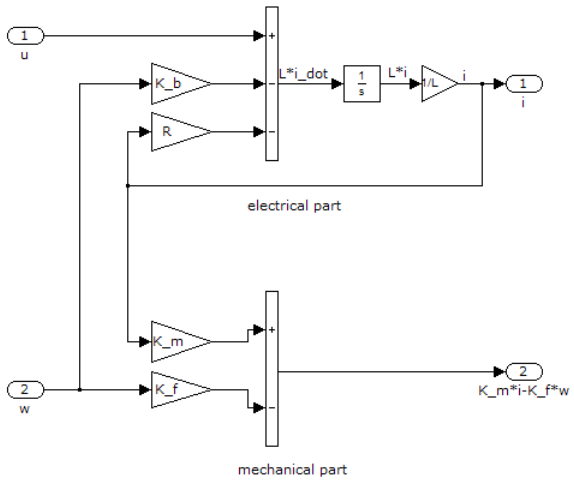

Fig. 7.6 Simulink model of the DC motor

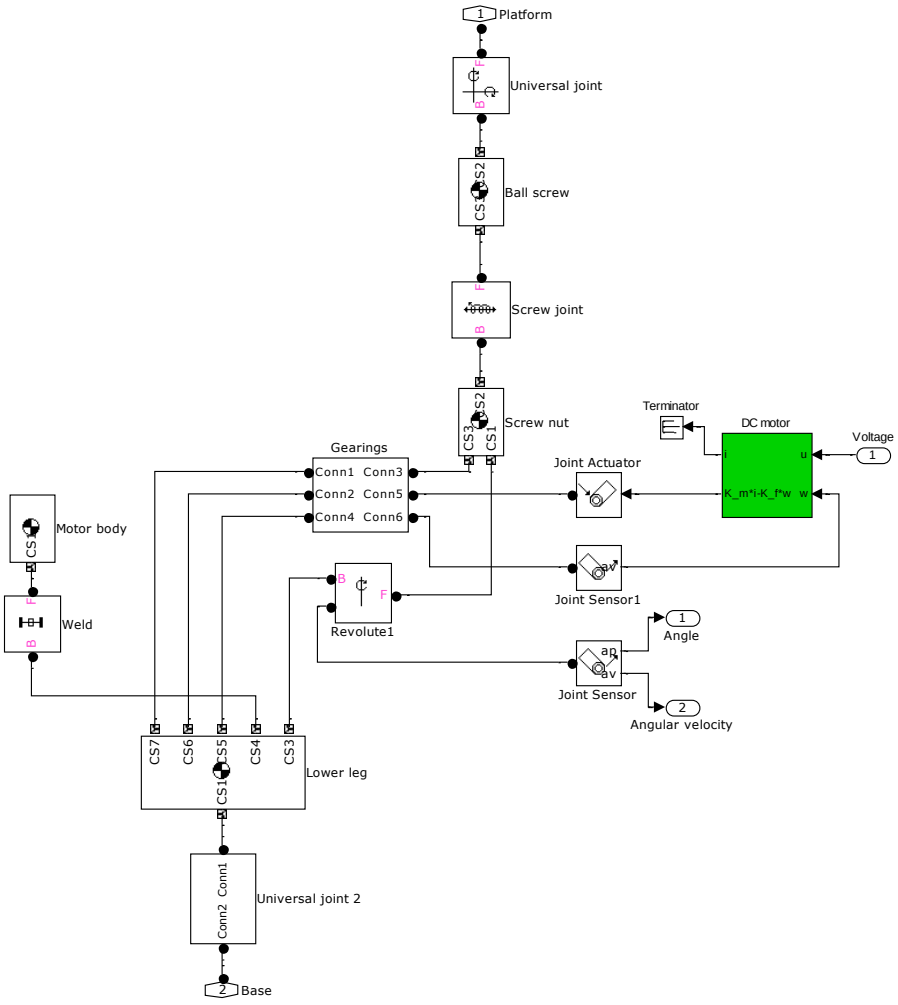

Fig. 7.7 DC motor subsystem (green) as a part of the linear actuator model

Momentary angular velocity marked at the block diagram as “w” is measured from the input element of the gearings subsystem. The output of the DC motor model corresponds with a produced torque. This signal is routed also to the input element of the gearings subsystem.

Comparison of the unloaded model of the motor in the steady state with the manufacturer data for the input of 42V proved difference in output angular velocity 1,2%. The simulated output was 779,1rad/s while the manufacturer publishes 788,5rad/s.

7.2.1 The state – space representation and investigation of the model

The basic state – space representation of the linear model of the a DC motor is

$$\frac{d}{dt}\begin{bmatrix} i \\ \omega \end{bmatrix} = \begin{bmatrix} -\frac{R}{L} & -\frac{K_b}{L} \\ \frac{K_m}{J} & -\frac{K_f}{J} \end{bmatrix}\begin{bmatrix} i \\ \omega \end{bmatrix} + \begin{bmatrix} \frac{1}{L} \\ 0 \end{bmatrix} u(t) \quad . \tag{7.5}$$

$$y(t) = \begin{bmatrix} 0 & 1 \end{bmatrix}\begin{bmatrix} i \\ \omega \end{bmatrix} + [0]u(t)$$

There were investigated controllability and observability conditions of the model (7.5) for Maxon RE 35 parameters according to (4.2) and (4.3). There were utilized Matlab functions *ctrb* and *obsv*.

The matrix of controllability is in Matlab defined as

```
co = ctrb([-R/L -K_b/L;K_m/J -K_f/J],[1/L 0]');
```

and number of uncontrollable states as

```
unco = length([-R/L -K_b/L;K_m/J -K_f/J]) - rank(co).
```

This yelds unco = 0, thus all states of the system are controllable.

The matrix of observability is in Matlab defined as

```
ob = obsv([-R/L -K_b/L;K_m/J -K_f/J],[0 1]);
```

and number of unobservable states as

```
unob = length([-R/L -K_b/L;K_m/J -K_f/J]) - rank(ob).
```

This yelds unob = 0, thus all states of the system are observable.

The investigation of controllability and observability of the model proved its suitability for a control design.

8.

Linearization

8.1Linerization in Matlab SimMechanics

There are in general two linearization algorithms in Simulink: Block-by-block analytical linearization and Numerical perturbation.

The first algorithm (block-by-block analytical) linearizes the model block by block individually and results are then combined to the linear model of the whole system. The advantage is that high amount of Simulink/SimMechanics blocs contains the analytically expressed Jacobian for the exact analytical linearization. This is very advantageous in cases that blocks contain some kind of discontinuity thus for blocks which are not suitable for the linearization by the numerical perturbation. This is the default method. Blocks which do not contain the Jacobian are automatically perturbed when using this method.

The second algorithm linearizes the whole system at once by slight changes of inputs and states. The method is quite simple and fast thus suitable for complicated systems. The disadvantage is that even blocks containing Jacobian for the exact linearization are linearized by the perturbation.

The obtained linear model is then in both of cases according to [39] described in state-space form as

$$\begin{aligned} \boldsymbol{\delta\dot{x}} &= \mathbf{A}\boldsymbol{\delta x} + \mathbf{B}\boldsymbol{\delta u} \\ \boldsymbol{\delta y} &= \mathbf{C}\boldsymbol{\delta x} + \mathbf{D}\boldsymbol{\delta u} \end{aligned}, \tag{8.1}$$

where

$$\begin{aligned} \boldsymbol{\delta x} &= \mathbf{x} - \mathbf{x}_0 \\ \boldsymbol{\delta u} &= \mathbf{u} - \mathbf{u}_0 \\ \boldsymbol{\delta y} &= \mathbf{y} - \mathbf{y}_0 \end{aligned}. \tag{8.2}$$

It is valid for the outputs at the operating point:

$$\begin{aligned} \dot{\mathbf{x}} &= \mathbf{f}\left(\mathbf{x}_0, \mathbf{u}_0\right) = \dot{\mathbf{x}}_0 \\ \mathbf{y} &= \mathbf{g}\left(\mathbf{x}_0, \mathbf{u}_0\right) = \mathbf{y}_0 \end{aligned}. \tag{8.3}$$

A, **B**, **C** and **D** are constant coefficient matrices defined as the Jacobians of the system, evaluated at the operating point

$$\mathbf{A} = \left.\frac{\partial \mathbf{f}}{\partial \mathbf{x}}\right|_{x_0,u_0} \qquad \mathbf{B} = \left.\frac{\partial \mathbf{f}}{\partial \mathbf{u}}\right|_{x_0,u_0}$$
$$\mathbf{C} = \left.\frac{\partial \mathbf{g}}{\partial \mathbf{x}}\right|_{x_0,u_0} \qquad \mathbf{D} = \left.\frac{\partial \mathbf{g}}{\partial \mathbf{u}}\right|_{x_0,u_0} . \tag{8.4}$$

8.2 Linearization of the Stewart platform model

The linearization is performed for the pure mechanical model of the Stewart platform without DC motors.

It is necessary to set the operating point at first. The operating point is given by coordinates of the platform mass center in the global coordinate system [0 0 0,1262] m. This position is approximately in the middle of the possible z-axis workspace of the platform and corresponds with the assumed initial position.

The input parameters for the linearization describing the operating point are the input torques holding the platform in the desired initial position against gravity. The torques may be easily measured from the model when zero movement to the platform joints is prescribed. The measured torque value is $0{,}8701.10^{-3}$ Nm for each linear actuator.

It may be proceed to the linearization itself when the input parameters defining the operating point are known. It is also important to mark the model inputs and outputs in the scheme according to the Fig. 7.5. There was chosen the step-by-step analytical linearization algorithm as the linearization method because of the described advantages.

A state-space model consisting of matrices **A**, **B**, **C**, **D** is obtained after the linearization. The model has 6 inputs (torques produced by DC motors) and 12 outputs (angular displacements and angular velocities of the srew nut) according to the input/output analysis. The minimal realization of the model has 12 states which are automatically chosen by SimMechanics (typically joint states).

8.2.1 Comparison between the linear model and the nonlinear SimMechanics model

The comparison between the linear and the nonlinear model was performed for the same input torque with amplitude 0,1Nm and frequency 2Hz for all of the linear actuators, Fig. 8.1. Thus the movement of the platform is just in the z-axis. The maximal z-axis distance between the centers of gravity of the base and the platform allowed by construction of the device is 0,1462m. The maximal distance reached during the simulation was 0,1407m – the platform was very close to its maximal workspace borders, Fig. 8.2.

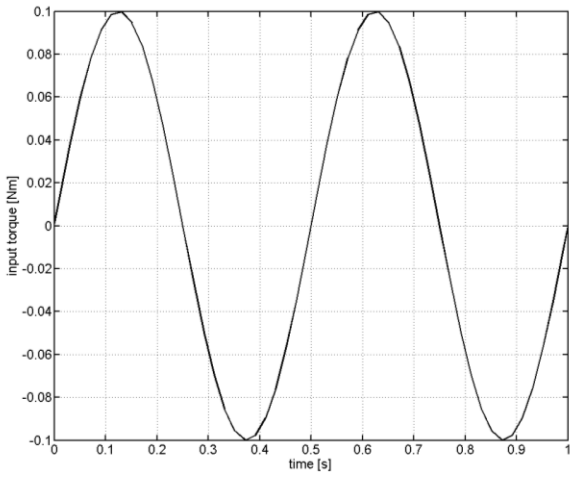

Fig. 8.1 Input torque of all linear actuators for both linear and nonlinear model

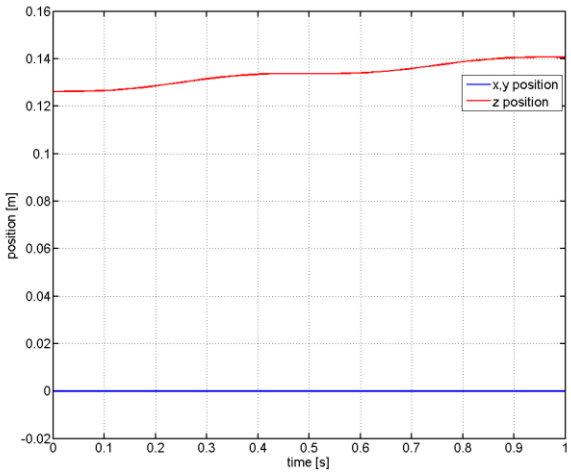

Fig. 8.2 Position of the platform during the simulation (nonlinear model)

There were compared outputs of both models (angular displacement and angular velocity of the screw nut) during the simulation, Fig. 8.3, 8.4.

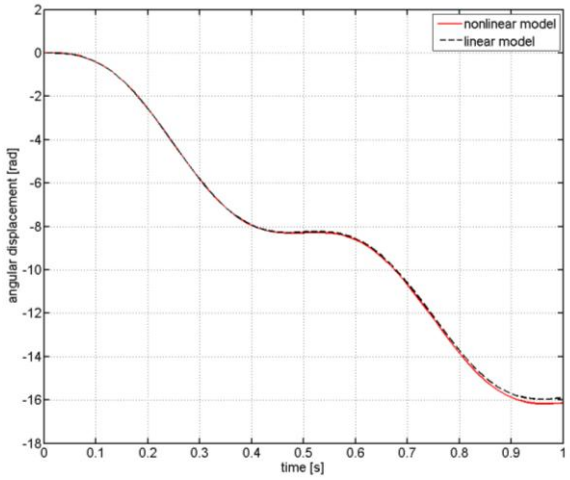

Fig. 8.3 Comparison between linear and nonlinear model – angular displacements

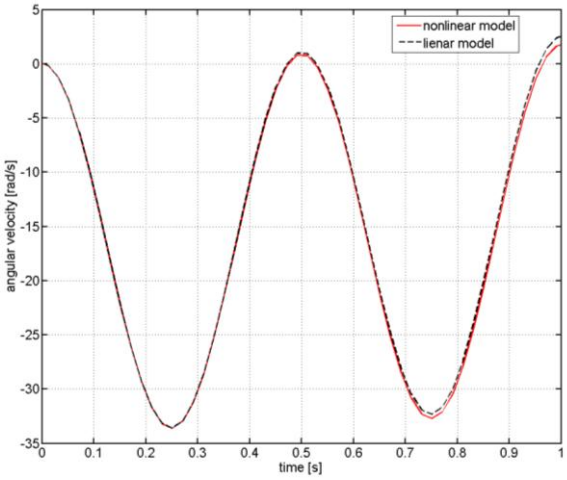

Fig. 8.4 Comparison between linear and nonlinear model – angular velocities

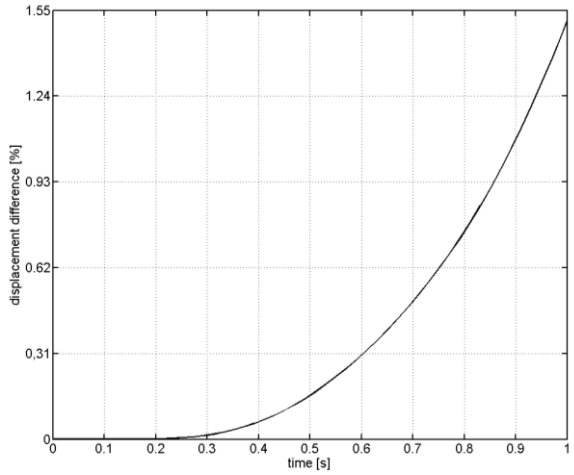

Fig. 8.5 Comparison between linear and nonlinear model – angular displacements (%)

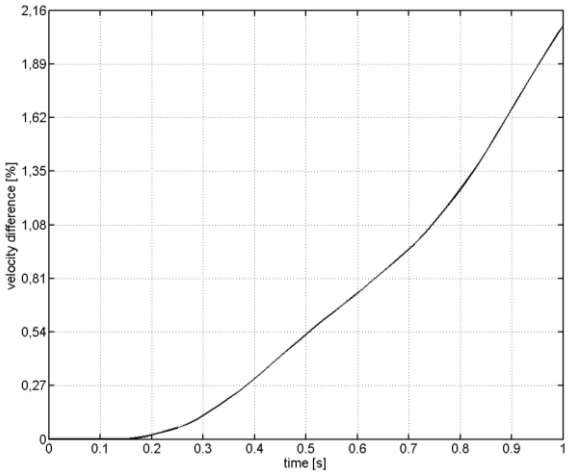

Fig. 8.6 Comparison between linear and nonlinear model – angular velocities (%)

The behavior of the linear model is obvious and expected – with increasing distance from the operating point decreases identity of both models. The difference between outputs is approximately 1,5% (angular displacement) and 2,1% (angular velocity) close to the workspace borders, Fig. 8.5, 8.6.

Advantage of such a linear model is that it is with its twelve states quite simple. Thus its simulations are very fast and model itself is for its computational modesty suitable for a control design.

8.2.2 Controllability and observability of the obtained linear model

The minimal realization of the obtained linear state – space model is defined as Matlab variable *Model_sys*. The matrix of controllability is then defined as

co = ctrb(Model_sys.A,Model_sys.B);

and number of uncontrollable states as

unco = length(Model_sys.A) - rank(co).

This yields unco = 0, thus the linear model of the Stewart platform is controllable.

The matrix of observability is defined as

ob = ctrb(Model_sys.A,Model_sys.C);

and number of unobservable states as

unob = length(Model_sys.A) - rank(ob)

This yields unob = 0, thus the system is observable.

The investigation of the controllability and observability proved that the linear state – space model of the Stewart platform is suitable for a control design.

9.

Stewart platform control design

9.1 SimMechanics model based control design

The Stewart platform linear state-space model was obtained in the previous chapter. The model was used for a control design which described in [12]. The control was successfully tested with original SimMechanics nonlinear model.

The basic idea of the control structure is to divide it into two layers – upper and lower layer. The upper layer (Fig. 9.1) is represented by a multichannel PID controller which prescribes torques produced by DC motors according to a desired position and orientation of the platform. The desired position and orientation of the platform may be easily transformed into linear actuators extensions and screw nuts angular displacements by using inverse kinematics description (6.8). The controller representing this layer is based on the Stewart platform linear state-space model.

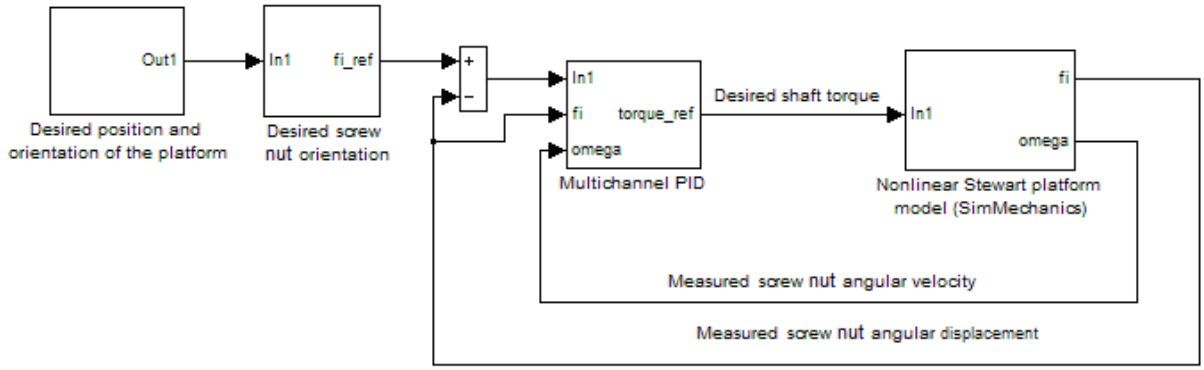

Fig. 9.1 Upper control layer [12]

The lower layer (Fig. 9.2) consists of six independent PID controllers which prescribe driving voltages for each of six DC motors according to the torques prescribed by the upper layer. The controllers in this layer are based on the state-space model of the DC motor (7.3-7.4).

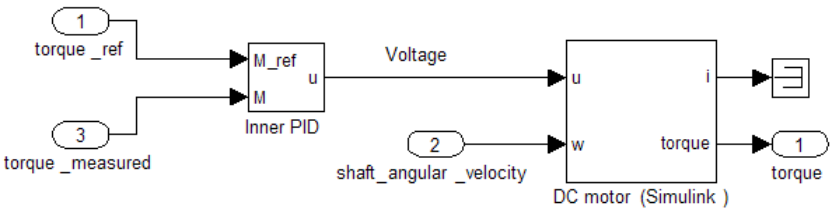

Fig. 9.2 Lower control layer [12]

9.1.1 Upper layer control design

The control law for the multichannel PID of the upper layer is according to [12] described as:

$$\mathbf{m} = \mathbf{K}_i \int_0^t \left(\mathbf{q}_{ref} - \mathbf{q} \right) d\tau - \mathbf{K}_p \mathbf{q} - \mathbf{K}_d \dot{\mathbf{q}}, \tag{9.1}$$

where **m** the vector of actuating torques $\mathbf{m} = \left(M_1, \ldots, M_6 \right)^T$, **q** is the vector of corresponding measured angular displacements of the screw nuts $\mathbf{q} = \left(\varphi_1, \ldots, \varphi_6 \right)$ and $\mathbf{q_{ref}}$ is the vector of referential angular displacements. $\mathbf{K_i}, \mathbf{K_p}, \mathbf{K_d}$ are the controller gains.

According to

$$\dddot{\mathbf{q}} + 3p\ddot{\mathbf{q}} + 3p^2\dot{\mathbf{q}} + p^3\mathbf{q} = p^3\mathbf{q}_{ref}, \tag{9.2}$$

the Stewart platform dynamics is stable on aperiodicity margin for $\mathbf{K}_p = \mathbf{D}^{-1}\left(3p^2\mathbf{I} + \mathbf{C}\right)$, $\mathbf{K}_d = \mathbf{D}^{-1}\left(3p\mathbf{I} + \mathbf{B}\right)$, $\mathbf{K}_i = p^3\mathbf{D}^{-1}$ for $p > 0$. **B**, **C**, **D** are the state matrices of the linear model of the Stewart platform.

9.1.2 Lower layer control design

The control law for the lower layer is then according to [12] following

$$u = \int_0^t \left(k_i \int_0^\tau \left(\left(M_m \right)_{ref} - M_m \right) d\upsilon - k_p M_m - k_d \dot{M}_m \right) d\tau, \tag{9.3}$$

where M_m is the torque produced by a DC motor (measured), $\left(M_m\right)_{ref}$ is then the referential torque.

Choosing $k_d = \left(3pLJ - LK_f - RJ\right)/\left(K_m J\right)$, $k_p = \left(3p^2 LJ - RK_f - K_b K_m\right)/\left(K_m J\right)$, $k_i = \left(p^3 L\right)/K_m$ leads for $p > 0$ to stable dynamics on aperiodicity margin according to

$$\dddot{M}_m + 3p\ddot{M}_m + 3p^2\dot{M}_m + p^3 M_m = p^3 \left(M_m\right)_{ref}. \tag{9.4}$$

9.1.3 Simulation results

The simulation movement of the platform may be simply described as follows. The platform gravity center moves from its initial position [0 0 0,1262]m to the position [0 0 0,1312]m at the first stage. Then (approximately at 2s of the simulation time) the movement in all of degrees of freedom continues with a sine wave. The simulation movement was chosen in such a way because of the real working cycle of the device is expected to be at least very similar.

The sine waves have following parameters: amplitudes for all of the position waves are 0,005m, amplitudes for all of the orientation waves are 0,02rad. Frequency is same for all signals 0,5Hz.

The comparison between desired and measured position and orientation of the platform gravity center is documented in Fig. 9.3, 9.4, 9.5.

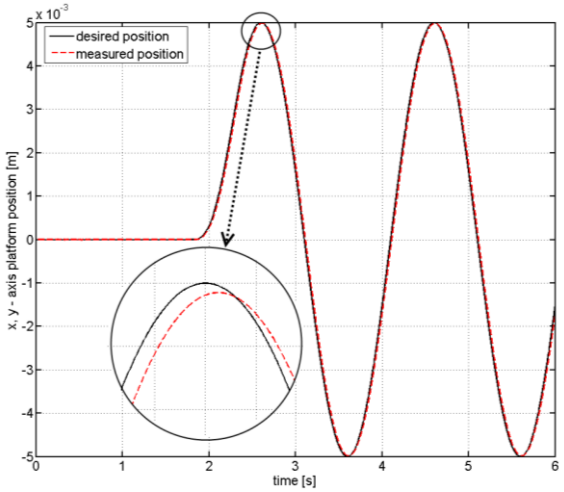

Fig. 9.3 X, Y – axis position of the platform gravity center (desired and measured)

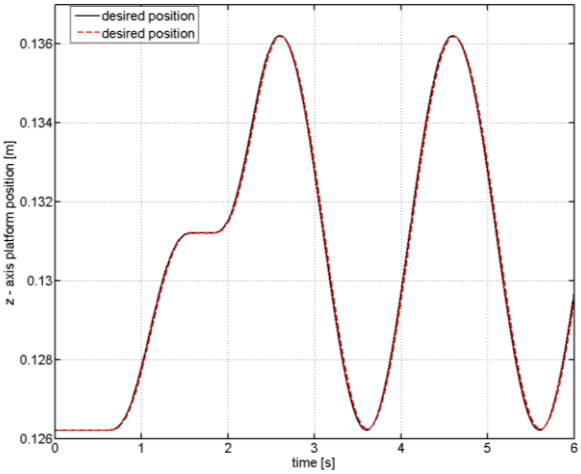

Fig. 9.4 Z – axis position of the platform gravity center (desired and measured)

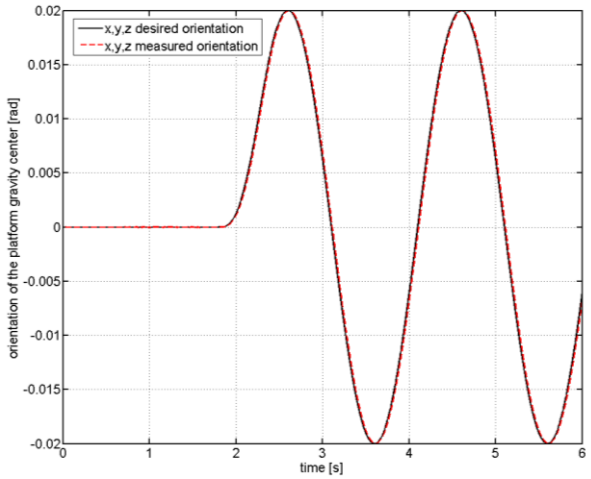

Fig. 9.5 Orientation of the platform gravity center (desired and measured)

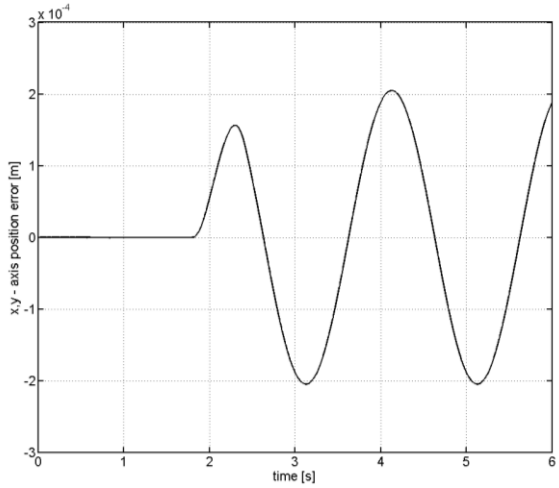

Fig. 9.6 Position error (x, y - axis)

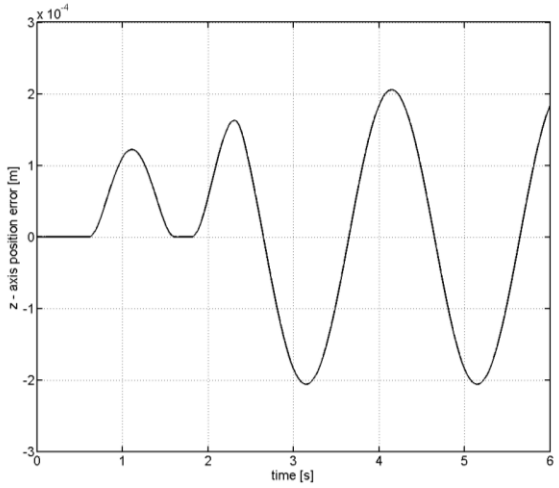

Fig. 9.7 Position error (z - axis)

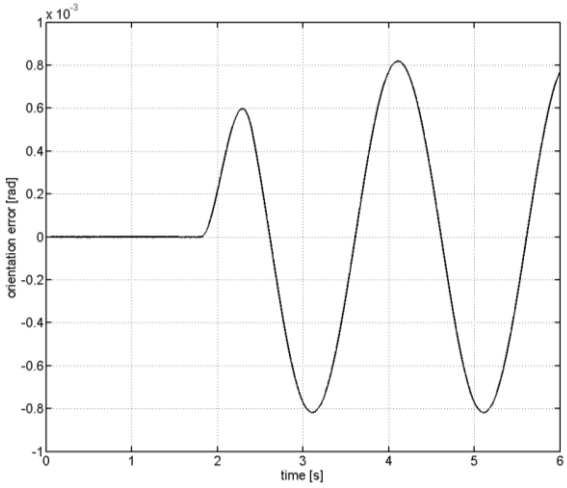

Fig. 9.8 Orientation error (x, y, z - axis)

The position and orientation error is then documented in figures Fig. 9.6, 9.7, 9.8. The maximal positioning error is approximately 0,2mm for movement in each axis. The maximal orientation error is approximately $0{,}8.10^{-3}$ rad for rotation around each axis. There is no special requirement on the device positioning accuracy because of its planned use. Hence the presented accuracy is sufficient.

The following pictures document DC motors torques and voltages, Fig. 9.9 – 9.20. The maximal amplitudes of the torque and voltage are for the given trajectory measured for the link number four which also reaches its maximal extension, Fig. 9.21. The nominal torque for the RE 35 DC motor is 0,0977Nm and its nominal voltage is 42V. The nominal values of torque and voltage were not exceeded during the simulation.

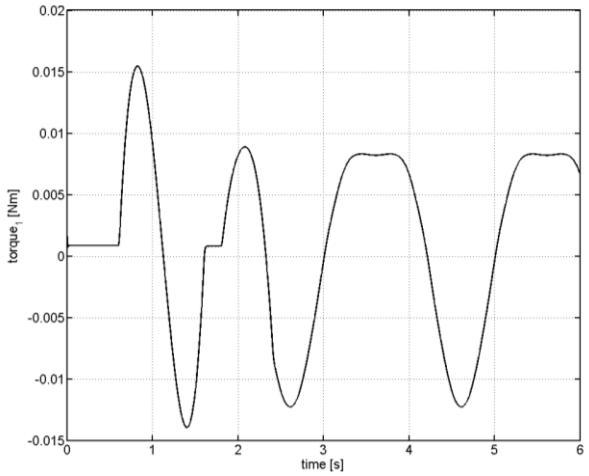

Fig. 9.9 DC motor torque – 1st link

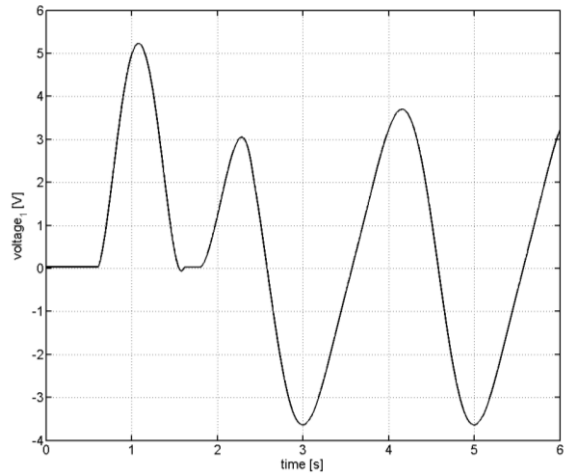

Fig. 9.10 DC motor voltage – 1st link

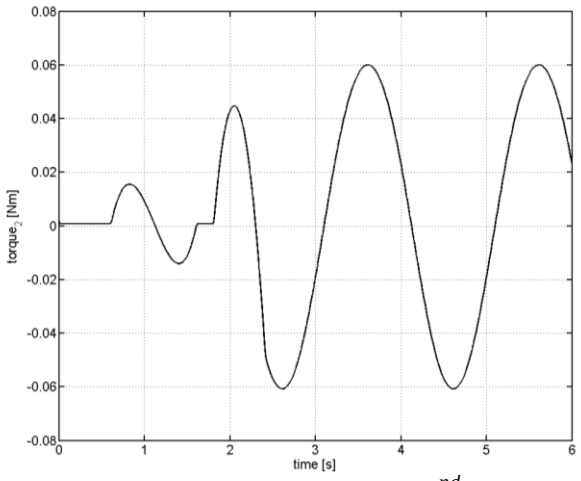

Fig. 9.11 DC motor torque – 2nd link

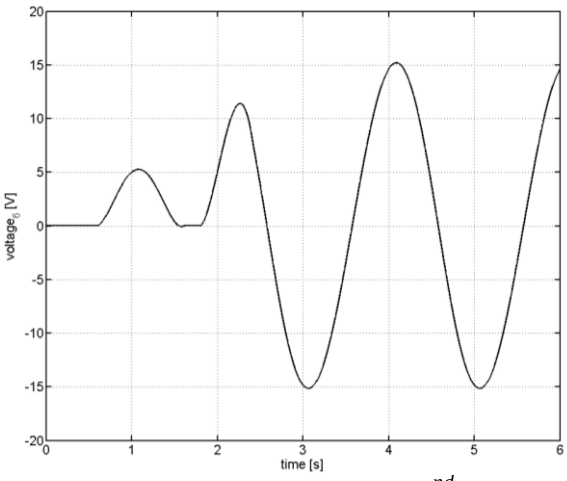

Fig. 9.12 DC motor voltage – 2nd link

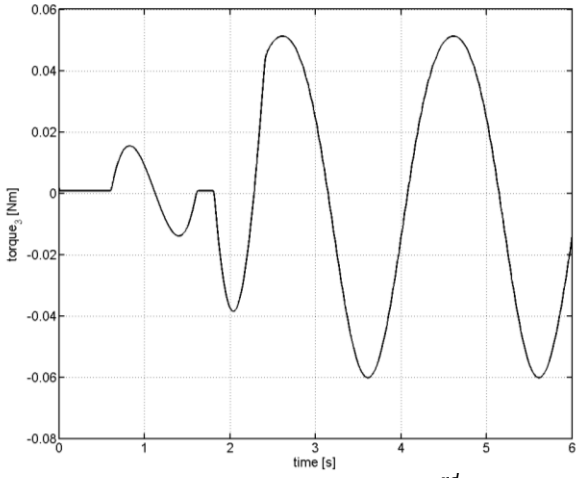

Fig. 9.13 DC motor torque – 3rd link

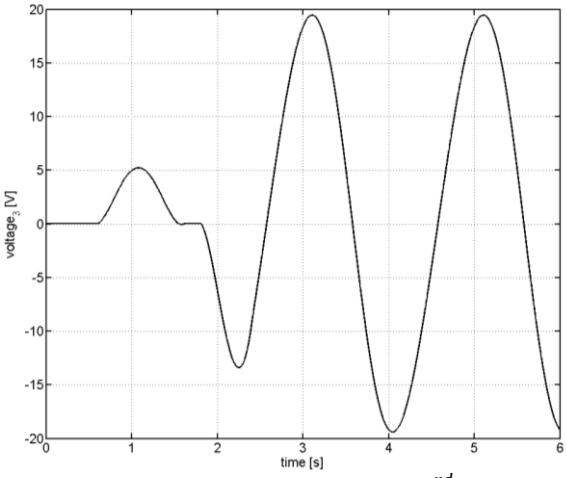

Fig. 9.14 DC motor voltage – 3rd link

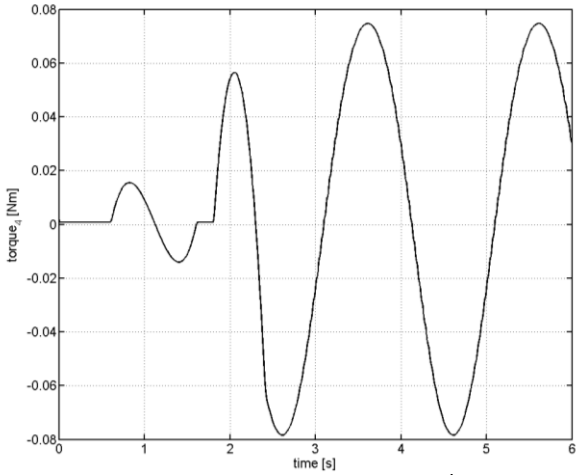

Fig. 9.15 DC motor torque – 4th link

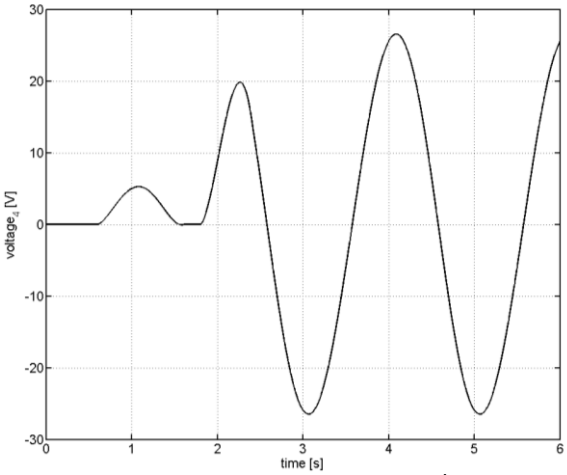

Fig. 9.16 DC motor voltage – 4th link

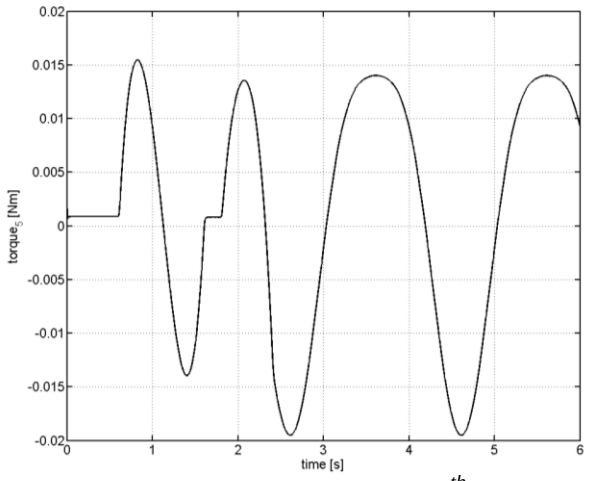

Fig. 9.17 DC motor torque – 5th link

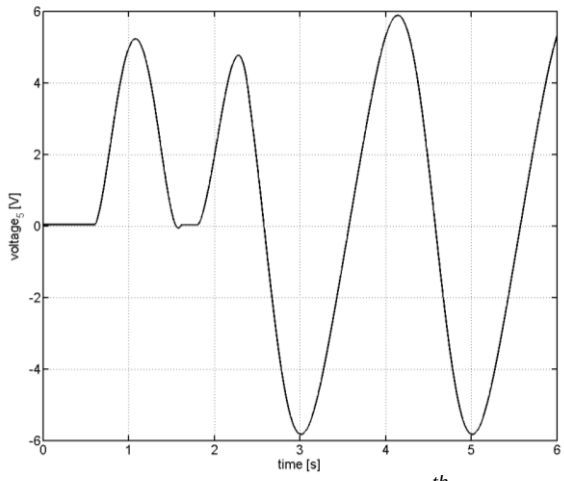

Fig. 9.18 DC motor voltage – 5th link

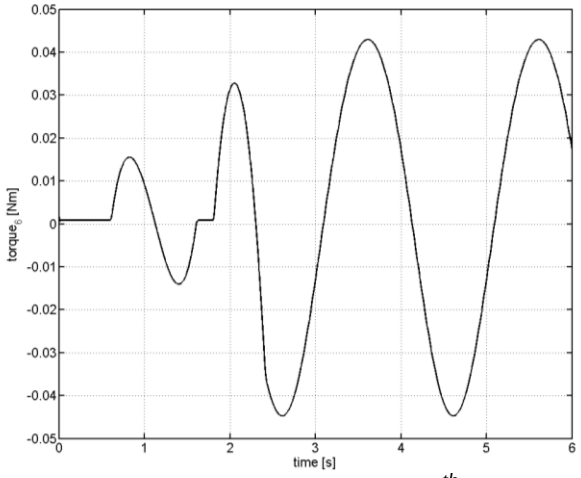

Fig. 9.19 DC motor torque – 6th link

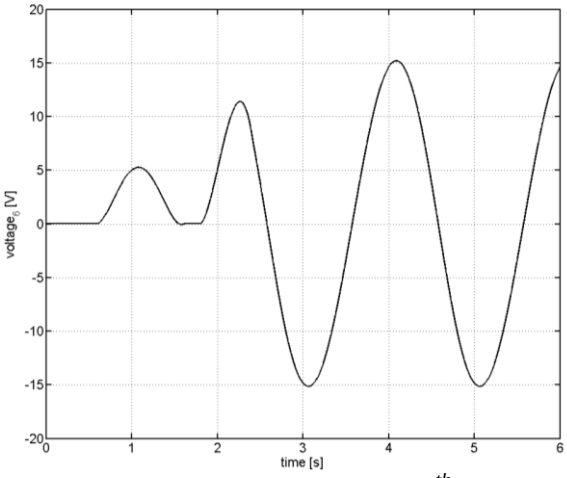

Fig. 9.20 DC motor voltage – 6th link

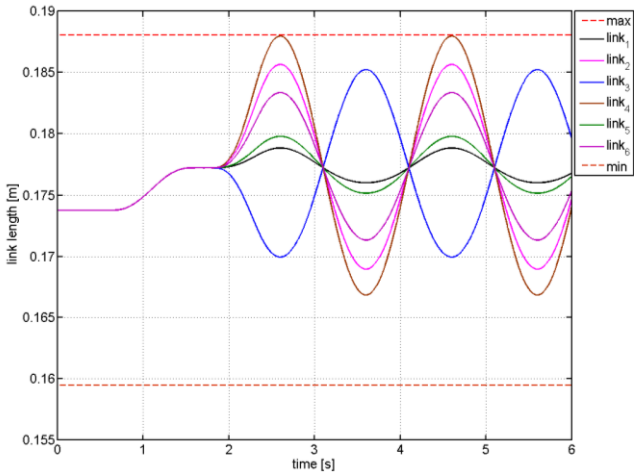

Fig. 9.21 Link extensions

The simulation results proved suitability of the linearized SimMechanics model for the control purposes. The positioning error of the proposed control is acceptable with respect to the assumed application. The model itself is with its twelve states quite simple and usable for a wide spectrum of control design methods.

10.

Uncertain modeling

10.1Model of the DC motor with uncertain parameters

The following DC motor model with uncertain parameters is based on description (7.3) and standard principles of uncertain modeling [33]. The equations may be for $x_1 = i$, $x_2 = \omega$ and by introducing the parametric uncertainty transformed into a form

$$\begin{aligned} x_1' &= \frac{1}{\left(\bar{L}+\delta_L\right)}\left[-\left(\bar{R}+\delta_R\right)x_1 - \left(\bar{K}_b+\delta_{Kb}\right)x_2 + u\right] \\ x_2' &= \frac{1}{\left(\bar{J}+\delta_J\right)}\left[\left(\bar{K}_m+\delta_{Km}\right)x_1 - \left(\bar{K}_f+\delta_{Kf}\right)x_2\right] \end{aligned}, \tag{10.1}$$

where $\bar{L}$, $\bar{R}$, $\bar{K}_b$, $\bar{J}$, $\bar{K}_m$, $\bar{K}_f$ are nominal parameters and δ_L, δ_R, δ_{Kb}, δ_J, δ_{Km}, δ_{Kf} are uncertainties of the nominal parameters. The model with uncertainties is then described by the following scheme, Fig. 10.1.

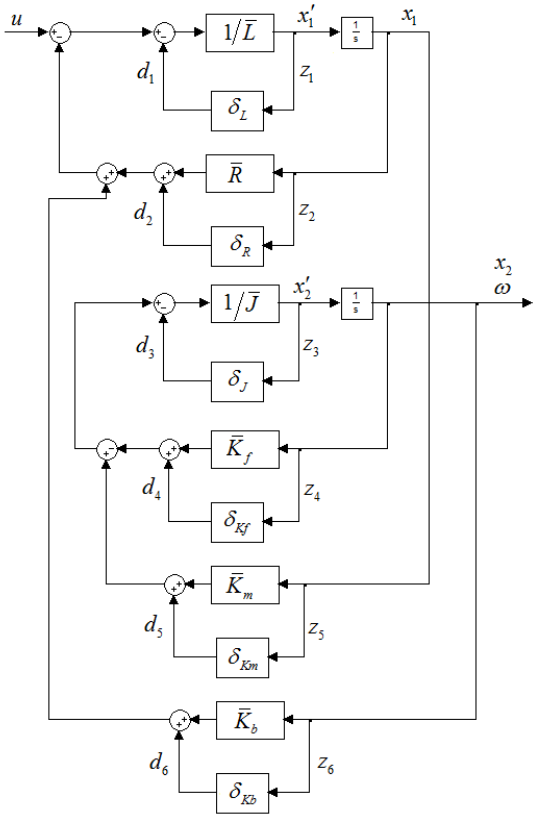

Fig. 10.1 Scheme of the DC motor with uncertain parameters

The uncertain model in matrix form is then obtained according to scheme as

$$\begin{bmatrix} x_1' \\ x_2' \end{bmatrix} = \begin{bmatrix} -\bar{R}/\bar{L} & -\bar{K}_b/\bar{L} \\ \bar{K}_m/\bar{J} & -\bar{K}_f/\bar{J} \end{bmatrix} \begin{bmatrix} x_1 \\ x_2 \end{bmatrix} + \begin{bmatrix} -1 & -1 & 0 & 0 & 0 & -1 \\ 0 & 0 & -1 & -1 & 1 & 0 \end{bmatrix} \begin{bmatrix} d_1 \\ d_2 \\ d_3 \\ d_4 \\ d_5 \\ d_6 \end{bmatrix} + \begin{bmatrix} 1/\bar{L} \\ 0 \end{bmatrix} [u]$$

$$\begin{bmatrix} z_1 \\ z_2 \\ z_3 \\ z_4 \\ z_5 \\ z_6 \end{bmatrix} = \begin{bmatrix} -\bar{R}/\bar{L} & -\bar{K}_b/\bar{L} \\ 1 & 0 \\ \bar{K}_m/J_0 & -\bar{K}_f/\bar{J} \\ 0 & 1 \\ 1 & 0 \\ 0 & 1 \end{bmatrix} \begin{bmatrix} x_1 \\ x_2 \end{bmatrix} + \begin{bmatrix} -1 & -1 & 0 & 0 & 0 & -1 \\ 0 & 0 & 0 & 0 & 0 & 0 \\ 0 & 0 & -1 & -1 & 1 & 0 \\ 0 & 0 & 0 & 0 & 0 & 0 \\ 0 & 0 & 0 & 0 & 0 & 0 \\ 0 & 0 & 0 & 0 & 0 & 0 \end{bmatrix} \begin{bmatrix} d_1 \\ d_2 \\ d_3 \\ d_4 \\ d_5 \\ d_6 \end{bmatrix} + \begin{bmatrix} 1/\bar{L} \\ 0 \\ 0 \\ 0 \\ 0 \\ 0 \end{bmatrix} [u] \qquad (10.2)$$

$$\begin{bmatrix} i \\ \omega \end{bmatrix} = \begin{bmatrix} 1 & 0 \\ 0 & 1 \end{bmatrix} \begin{bmatrix} x_1 \\ x_2 \end{bmatrix}$$

or in a compact form of interconnection matrix **M**

$$\begin{bmatrix} x_1' \\ x_2' \\ z_1 \\ z_2 \\ z_3 \\ z_4 \\ z_5 \\ z_6 \\ \omega \end{bmatrix} = \begin{bmatrix} -\bar{R}/\bar{L} & -\bar{K}_b/\bar{L} & -1 & -1 & 0 & 0 & 0 & -1 & 0 \\ \bar{K}_m/\bar{J} & -\bar{K}_f/\bar{J} & 0 & 0 & -1 & -1 & 1 & 0 & 0 \\ -\bar{R}/\bar{L} & -\bar{K}_b/\bar{L} & -1 & -1 & 0 & 0 & 0 & -1 & 1/\bar{L} \\ 1 & 0 & 0 & 0 & 0 & 0 & 0 & 0 & 0 \\ \bar{K}_m/\bar{J} & -\bar{K}_f/\bar{J} & 0 & 0 & -1 & -1 & 1 & 0 & 0 \\ 0 & 1 & 0 & 0 & 0 & 0 & 0 & 0 & 0 \\ 1 & 0 & 0 & 0 & 0 & 0 & 0 & 0 & 0 \\ 0 & 1 & 0 & 0 & 0 & 0 & 0 & 0 & 0 \\ 0 & 1 & 0 & 0 & 0 & 0 & 0 & 0 & 0 \end{bmatrix} \begin{bmatrix} x_1 \\ x_2 \\ d_1 \\ d_2 \\ d_3 \\ d_4 \\ d_5 \\ d_6 \\ u \end{bmatrix}. \qquad (10.3)$$

At the same time the perturbation matrix **Δ** is defined as

$$\begin{bmatrix} d_1 \\ d_2 \\ d_3 \\ d_4 \\ d_5 \\ d_6 \end{bmatrix} = \begin{bmatrix} \delta_L & 0 & 0 & 0 & 0 & 0 \\ 0 & \delta_R & 0 & 0 & 0 & 0 \\ 0 & 0 & \delta_J & 0 & 0 & 0 \\ 0 & 0 & 0 & \delta_{Kf} & 0 & 0 \\ 0 & 0 & 0 & 0 & \delta_{Km} & 0 \\ 0 & 0 & 0 & 0 & 0 & \delta_{Kb} \end{bmatrix} \begin{bmatrix} z_1 \\ z_2 \\ z_3 \\ z_4 \\ z_5 \\ z_6 \end{bmatrix}. \qquad (10.4)$$

10.1.1 Simulation results

The parameter with the highest possible uncertainty is $\bar{K}_f$ representing the linear approximation of viscous friction. It was proved by a simulation that 35% uncertainty of the parameter covers for the unloaded motor the output difference 1,2% between data obtained from the nominal model and published data by manufacturer (no load speed for the input 42V).

The simulation was performed for the uncertain model with uncertainty 35% in $\bar{K}_f$, i.e. for $\delta_{Kf} = 0{,}000048 \times 0{,}35$.

Fig. 10.2 presents step response of 20 random samples of the uncertain model with marked boundaries of the worst case and the nominal model. Next figure (Fig. 10.3) presents the steady state at input of 42V. The no load speed presented by the manufacturer (788,5 rad/s) is covered by the uncertainty. Graphs also present the worst case corresponding with the most degraded model within the given uncertainty.

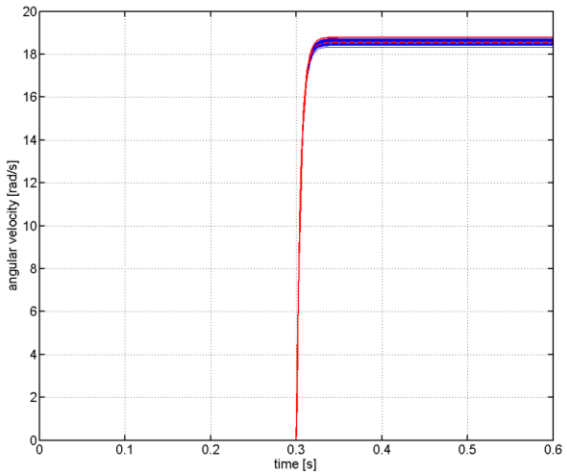

Fig. 10.2 step response of the uncertain system with the worst case boundaries

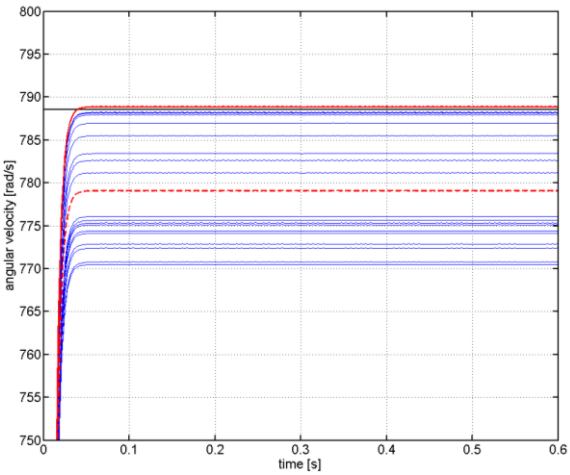

Fig. 10.3 Steady state for the input 42V (full black line – no load speed accodirng to the manufacturer)

(full red line – worst case, dashed red line – nominal model, blue lines samples of the uncertain model)

The worst case satisfies conditions of controllability and observability according to (4.2) and (4.3).

10.2 Stewart platform model with uncertain parameters

The general approach to the parametric uncertainty modeling presented in the previous section is suitable for models where individual parameters are treated as uncertain. The method is strictly concentrated on the given parameters but this might be inconvenient for models of higher orders with large amount of parameters with an uncertainty or for models where the uncertainty in some parameters influences other parameters.

The proposed method works with parametric uncertainty in a more complex way. It is based on knowledge of an uncertain linear model and corresponding linear model with maximally perturbed parameters. The uncertainty is then determined for each parameter of state matrices individually.

The basic idea of uncertainty modeling demonstrated on the Stewart platform model is very simple. The approach is performed for two cases – shifting of operating points and possible modeling inaccuracy of mass and inertia parameters.

There are obtained two linear models by the linearization of the SimMechanics Stewart platform model. The first one is linearized around the operating point defining its initial position and the second one is linearized around the operating point defining the position where the maximal (or minimal) links extensions are reached. The both models are described by state matrices. The uncertainty of such a system is then defined as a difference between parameters of corresponding state matrices of both models. This is the first case of uncertainty modeling which compensates shifting of operating points. The controller based on such a model has constant quality of regulation for the whole workspace between operating points.

The second presented case of the Stewart platform uncertain modeling is describing uncertain modeling of mass and inertia parameters. The principle is same. The uncertainty would be described as a difference between model with nominal parameters and the model with maximal (or minimal) parameters of mass and inertia.

The general principle of the uncertain modeling is then following. The nominal system is described as

$$\begin{aligned}\dot{\mathbf{x}} &= \bar{\mathbf{A}}\mathbf{x} + \bar{\mathbf{B}}\mathbf{u} \\ \mathbf{y} &= \bar{\mathbf{C}}\mathbf{x} + \bar{\mathbf{D}}\mathbf{u}\end{aligned} \tag{10.5}$$

and similarly the model with maximally perturbed parameters

$$\begin{aligned}\dot{\mathbf{x}} &= \mathbf{A}\mathbf{x} + \mathbf{B}\mathbf{u} \\ \mathbf{y} &= \mathbf{C}\mathbf{x} + \mathbf{D}\mathbf{u}\end{aligned}. \tag{10.6}$$

The meaning of equation terms is in case of the Stewart platform state-space model following:

$\mathbf{x}$ represents the vector of twelve states which are established by SimMechanics during the linearization, $\dot{\mathbf{x}}$ represents the vector of the time derivations of the states,

$\mathbf{u} = \begin{bmatrix} M_1 & M_2 & M_3 & M_4 & M_5 & M_6 \end{bmatrix}^T$ is the vector of inputs which are DC motors shaft torques, $\mathbf{y} = \begin{bmatrix} \varphi_1 & \varphi_2 & \varphi_3 & \varphi_4 & \varphi_5 & \varphi_6 & \omega_1 & \omega_2 & \omega_3 & \omega_4 & \omega_5 & \omega_6 \end{bmatrix}^T$ is the vector of outputs which are angular displacement and angular velocity of each one of the ball screw nuts. Matrices $\bar{\mathbf{A}}, \bar{\mathbf{B}}, \bar{\mathbf{C}}, \bar{\mathbf{D}}$ represent state matrices of the nominal system and $\mathbf{A}, \mathbf{B}, \mathbf{C}, \mathbf{D}$ represent the state matrices of the model with perturbed parameters.

State matrices of the system (10.6) may be defined as a sum of particular nominal matrix and a matrix containing the uncertainty. E.g. for A it is

$$\mathbf{A} = \bar{\mathbf{A}} + \mathbf{A}_\Delta, \tag{10.7}$$

thus the uncertainty contribution is $\mathbf{A}_\Delta = \mathbf{A} - \bar{\mathbf{A}}$. Similarly are derived uncertainty contributions for matrices **B**, **C**, **D**.

Applying of the upper linear fractional transformation

$$\mathbf{F}_u\left(\mathbf{M}, \boldsymbol{\Delta}_u\right) = \mathbf{M}_{22} + \mathbf{M}_{21}\boldsymbol{\Delta}_u\left(\mathbf{I} - \mathbf{M}_{11}\boldsymbol{\Delta}_u\right)^{-1}\mathbf{M}_{12} \tag{10.8}$$

and comparing with (10.7) it is obtained $\mathbf{M}_{21}\mathbf{M}_{12} = \mathbf{A}_\Delta$, $\mathbf{M}_{11} = \mathbf{0}$, $\mathbf{M}_{12} = \mathbf{I}$, $\mathbf{M}_{21} = \mathbf{A}_\Delta$ and $\mathbf{M}_{22} = \bar{\mathbf{A}}$. The method is same for other state matrices.

By substituting of the obtained parameters to the interconnection transfer function matrix

$$\mathbf{M} = \begin{bmatrix} \mathbf{M_{11}} & \mathbf{M_{12}} \\ \mathbf{M_{21}} & \mathbf{M_{22}} \end{bmatrix} \tag{10.9}$$

and according to schemes of particular transfer function matrices in Fig. 10.4, it is obtained

$$\begin{bmatrix} \mathbf{y}_{\Delta A} \\ \dot{\mathbf{x}} \end{bmatrix} = \begin{bmatrix} \mathbf{0} & \mathbf{I} \\ \mathbf{A}_\Delta & \bar{\mathbf{A}} \end{bmatrix} \begin{bmatrix} \mathbf{u}_{\Delta A} \\ \mathbf{x} \end{bmatrix}, \quad \begin{bmatrix} \mathbf{y}_{\Delta B} \\ \dot{\mathbf{x}} \end{bmatrix} = \begin{bmatrix} \mathbf{0} & \mathbf{I} \\ \mathbf{B}_\Delta & \bar{\mathbf{B}} \end{bmatrix} \begin{bmatrix} \mathbf{u}_{\Delta B} \\ \mathbf{u} \end{bmatrix} \tag{10.10}$$

and similarly

$$\begin{bmatrix} \mathbf{y}_{\Delta C} \\ \mathbf{y} \end{bmatrix} = \begin{bmatrix} \mathbf{0} & \mathbf{I} \\ \mathbf{C}_\Delta & \bar{\mathbf{C}} \end{bmatrix} \begin{bmatrix} \mathbf{u}_{\Delta C} \\ \mathbf{x} \end{bmatrix}, \quad \begin{bmatrix} \mathbf{y}_{\Delta D} \\ \mathbf{y} \end{bmatrix} = \begin{bmatrix} \mathbf{0} & \mathbf{I} \\ \mathbf{D}_\Delta & \bar{\mathbf{D}} \end{bmatrix} \begin{bmatrix} \mathbf{u}_{\Delta D} \\ \mathbf{u} \end{bmatrix}, \tag{10.11}$$

where $\mathbf{u}_{\Delta A}, \mathbf{u}_{\Delta B}, \mathbf{u}_{\Delta C}, \mathbf{u}_{\Delta D}$ are inputs to the perturbation matrices $\boldsymbol{\Delta}_{\Delta A}, \boldsymbol{\Delta}_{\Delta B}, \boldsymbol{\Delta}_{\Delta C}, \boldsymbol{\Delta}_{\Delta D}$, $\mathbf{y}_{\Delta A}, \mathbf{y}_{\Delta B}, \mathbf{y}_{\Delta C}, \mathbf{y}_{\Delta D}$ are outputs from the perturbation matrices.

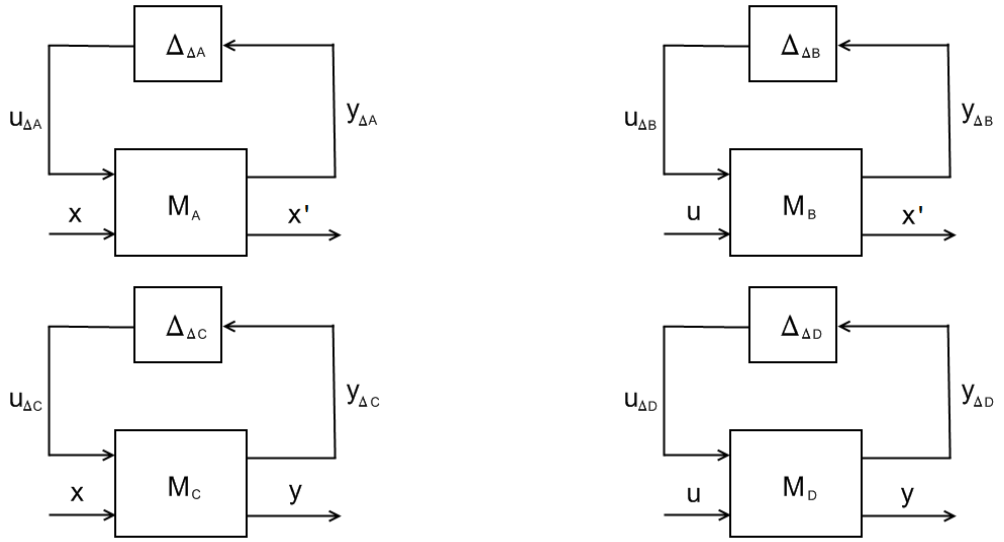

*Fig. 10.4 Schemes of particular transfer function matrices **M** [7]*

It is then valid

$$\dot{\mathbf{x}} = \bar{\mathbf{A}}\mathbf{x} + \mathbf{A}_{\Delta}\mathbf{u}_{\Delta A} + \mathbf{B}_{\Delta}\mathbf{u}_{\Delta B} + \bar{\mathbf{B}}\mathbf{u}$$

$$\mathbf{y}_{\Delta A} = \mathbf{x} \qquad \mathbf{u}_{\Delta A} = \boldsymbol{\Delta}_{\Delta A}\mathbf{y}_{\Delta A}$$

$$\mathbf{y}_{\Delta B} = \mathbf{u} \quad \text{and} \quad \mathbf{u}_{\Delta B} = \boldsymbol{\Delta}_{\Delta B}\mathbf{y}_{\Delta B} \,. \tag{10.12}$$

$$\mathbf{y}_{\Delta C} = \mathbf{x} \qquad \mathbf{u}_{\Delta C} = \boldsymbol{\Delta}_{\Delta C}\mathbf{y}_{\Delta C}$$

$$\mathbf{y}_{\Delta D} = \mathbf{u} \qquad \mathbf{u}_{\Delta D} = \boldsymbol{\Delta}_{\Delta D}\mathbf{y}_{\Delta D}$$

$$\mathbf{y} = \bar{\mathbf{C}}\mathbf{x} + \mathbf{C}_{\Delta}\mathbf{u}_{\Delta C} + \mathbf{D}_{\Delta}\mathbf{u}_{\Delta D} + \bar{\mathbf{D}}\mathbf{u}$$

It is typically $\mathbf{-I} \le \boldsymbol{\Delta}_{\Delta A,B,C,D} \le \mathbf{I}$ for the symmetrical +/- perturbation of the uncertainty around the nominal value.

The matrix representation of the (Stewart platform) uncertain model is then

$$\begin{bmatrix} \dot{\mathbf{x}} \\ \mathbf{y}_{\Delta A} \\ \mathbf{y}_{\Delta B} \\ \mathbf{y}_{\Delta C} \\ \mathbf{y}_{\Delta D} \\ \mathbf{y} \end{bmatrix} = \begin{bmatrix} \bar{\mathbf{A}} & \mathbf{A}_{\Delta} & \mathbf{B}_{\Delta} & \mathbf{0} & \mathbf{0} & \bar{\mathbf{B}} \\ \mathbf{I} & \mathbf{0} & \mathbf{0} & \mathbf{0} & \mathbf{0} & \mathbf{0} \\ \mathbf{0} & \mathbf{0} & \mathbf{0} & \mathbf{0} & \mathbf{0} & \mathbf{I} \\ \mathbf{I} & \mathbf{0} & \mathbf{0} & \mathbf{0} & \mathbf{0} & \mathbf{0} \\ \mathbf{0} & \mathbf{0} & \mathbf{0} & \mathbf{0} & \mathbf{0} & \mathbf{I} \\ \bar{\mathbf{C}} & \mathbf{0} & \mathbf{0} & \mathbf{C}_{\Delta} & \mathbf{D}_{\Delta} & \bar{\mathbf{D}} \end{bmatrix} \begin{bmatrix} \mathbf{x} \\ \mathbf{u}_{\Delta A} \\ \mathbf{u}_{\Delta B} \\ \mathbf{u}_{\Delta C} \\ \mathbf{u}_{\Delta D} \\ \mathbf{u} \end{bmatrix}, \tag{10.13}$$

with the perturbation matrix

$$\begin{bmatrix} \mathbf{u}_{\Delta A} \\ \mathbf{u}_{\Delta B} \\ \mathbf{u}_{\Delta C} \\ \mathbf{u}_{\Delta D} \end{bmatrix} = \begin{bmatrix} \boldsymbol{\Delta}_{\Delta A} & \mathbf{0} & \mathbf{0} & \mathbf{0} \\ \mathbf{0} & \boldsymbol{\Delta}_{\Delta B} & \mathbf{0} & \mathbf{0} \\ \mathbf{0} & \mathbf{0} & \boldsymbol{\Delta}_{\Delta C} & \mathbf{0} \\ \mathbf{0} & \mathbf{0} & \mathbf{0} & \boldsymbol{\Delta}_{\Delta D} \end{bmatrix} \begin{bmatrix} \mathbf{y}_{\Delta A} \\ \mathbf{y}_{\Delta B} \\ \mathbf{y}_{\Delta C} \\ \mathbf{y}_{\Delta D} \end{bmatrix}. \tag{10.14}$$

The ideal representation of the uncertain model for a robust controller design is according to [33] following

$$\mathbf{G} = \begin{bmatrix} \mathbf{A}_v & \mathbf{B}_{v1} & \mathbf{B}_{v2} \\ \mathbf{C}_{v1} & \mathbf{D}_{v11} & \mathbf{D}_{v12} \\ \mathbf{C}_{v2} & \mathbf{D}_{v21} & \mathbf{D}_{v22} \end{bmatrix}. \tag{10.15}$$

The form (10.13) corresponds with (10.15) for

$$\mathbf{A}_v = \bar{\mathbf{A}}, \quad \mathbf{B}_{\mathbf{v1}} = [\mathbf{A}_\Delta \quad \mathbf{B}_\Delta \quad \mathbf{0} \quad \mathbf{0}], \quad \mathbf{B}_{v2} = \bar{\mathbf{B}}, \quad \mathbf{C}_{\mathbf{v1}} = \begin{bmatrix} \mathbf{I} \\ \mathbf{0} \\ \mathbf{I} \\ \mathbf{0} \end{bmatrix}, \quad \mathbf{C}_{v2} = \bar{\mathbf{C}}, \mathbf{D}_{v11} = [\mathbf{0}], \quad \mathbf{D}_{v12} = \begin{bmatrix} \mathbf{0} \\ \mathbf{I} \\ \mathbf{0} \\ \mathbf{I} \end{bmatrix},$$

$$\mathbf{D}_{\mathbf{v21}} = [\mathbf{0} \quad \mathbf{0} \quad \mathbf{C}_\Delta \quad \mathbf{D}_\Delta].$$

The Simulink scheme of the uncertain Stewart platform model is then illustrated in Fig. 10.5. The scheme is identical for both cases of modeled uncertainty. Let's note that the model has added a gravity input for the simulation purposes.

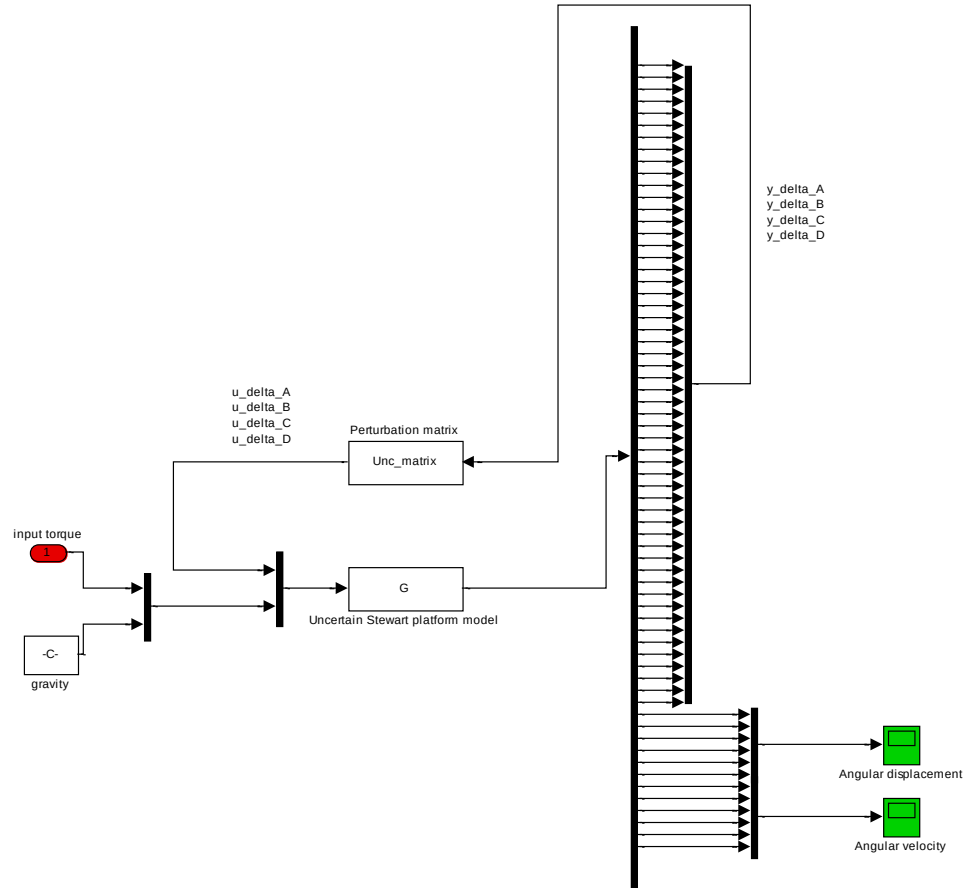

Fig. 10.5 The Simulink scheme of the uncertain Stewart platform model

The advantage of the method is that formulas (10.13), (10.14) describing the uncertain model are applicable on any state-space model of any system. The only necessary inputs are a nominal model and a model with maximally perturbed parameters.

The proposed method was published in [7]. The article also describes a brief experiment with an H-infinity based controller designed according to the uncertain model.

10.3 Simulation of the Stewart platform model with uncertain parameters

10.3.1 Case 1 – Uncertain position of the operating point

The uncertain Stewart platform model is made of the model linearized in its nominal position ([0 0 0,1262m] position of the platform centre of gravity in CSb) and the model linearized in its position with minimal link lengths ([0 0 0,1062m] position of the platform centre of gravity in CSb) which corresponds in this case with the model with maximally perturbed parameters. The input to such an uncertain model was same as the input for comparison of the linear and nonlinear model – input torque represented by a sine wave with amplitude 0,1Nm and frequency 2Hz for all of linear actuators (Fig. 8.1). The following figures document comparison between outputs of the uncertain and the nominal model, Fig. 10.6 – 10.9.

There were done twenty random samples of the uncertain model for $\mathbf{-I} \le \mathbf{\Delta}_{\Delta A,B,C,D} \le \mathbf{I}$. Let's note that maximal difference between outputs of the nominal system and maximal/minimal realization of the uncertain model is approximately ±1,13% of the nominal output value for the given trajectory of the platform. The rest of the outputs of the uncertain model are naturally placed within this range. The worst case (the most degraded model) corresponds with the maximal realization of the uncertainty system in this case, i.e. for $\mathbf{\Delta}_{\Delta A,B,C,D} = \mathbf{I}$.

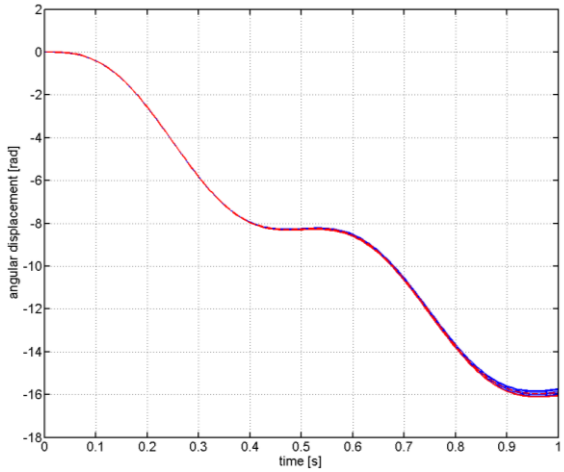

Fig. 10.6 Case 1 – comparison of the outputs of the uncertain model, nominal model and the worst realization – angular displacement

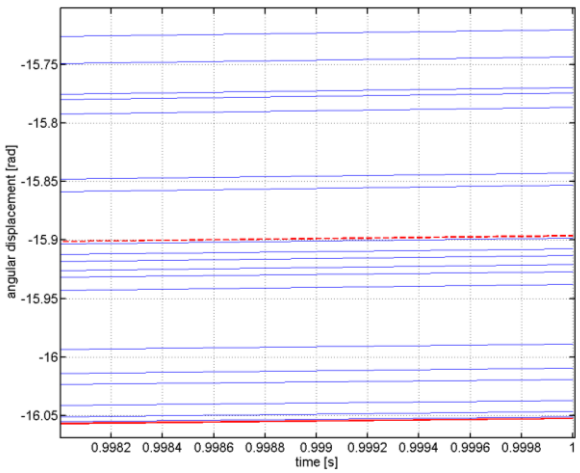

Fig. 10.7 Case 1 – comparison of the outputs of the uncertain model, nominal model and the worst realization – angular displacement – detail

(full red line – the worst case, dashed red line – the nominal model, blue line – uncertain model samples)

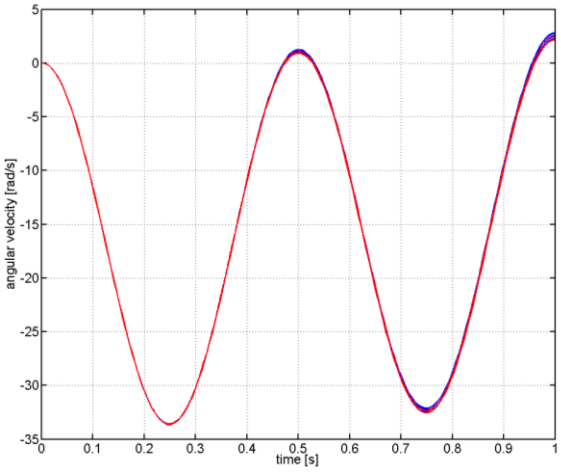

Fig. 10.8 Case 1 – comparison of the outputs of the uncertain model, nominal model and the worst realization – angular velocity

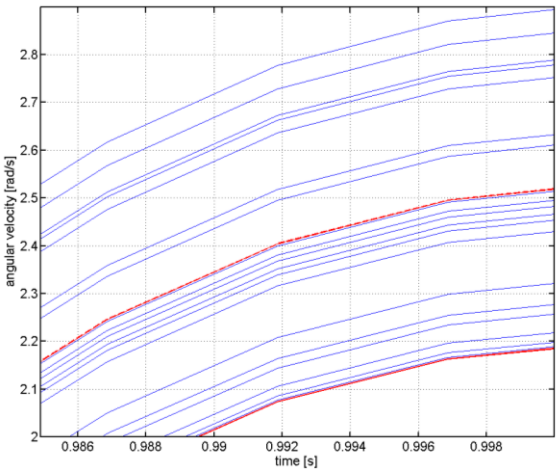

Fig. 10.9 Case 1 – comparison of the outputs of the uncertain model, nominal model and the worst realization – angular velocity – detail

(full red line – the worst case, dashed red line – the nominal model, blue line – uncertain model samples)

10.3.2 Case 2 – Uncertain masses and inertia moments

The second case works with uncertain parameters of mass and inertia of chosen bodies. The uncertain model is created from the model with nominal values of masses and inertia moments and from the model with maximal values of masses and inertia moments. Both models are linearized in its initial position.

The lower part of the link (position 3a in the Fig. 6.2) was modeled as uncertain at first. This part was selected because of its complicated geometry thus quite high possibility of modeling inaccuracy. The uncertainty of both mass and inertia moment was experimentally set to ±2,5% of the nominal value (Case 2a).

There were compared outputs of the nominal and uncertain model (twenty random samples for the uncertainty perturbed from $-\mathbf{I} \le \mathbf{\Delta}_{\Delta A,B,C,D} \le \mathbf{I}$), Fig. 10.10 – 10.13. The maximal difference between outputs of the nominal and uncertain model is approximately ±0,014% of the nominal values.

The worst case corresponds with the minimal realization of the uncertain model, i.e. $\mathbf{\Delta}_{\Delta A,B,C,D} = -\mathbf{I}$ in this case. This is also typical for the following examples.

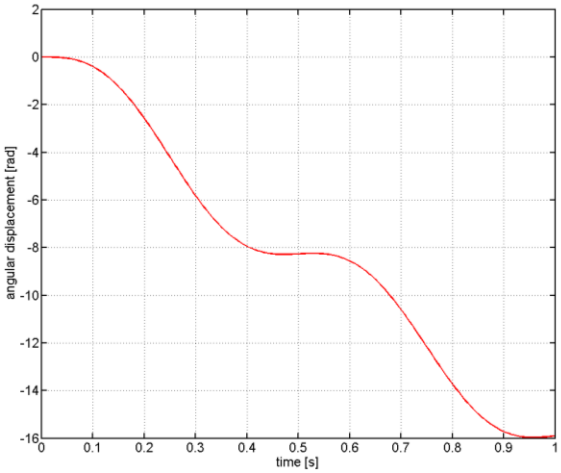

Fig. 10.10 Case 2a – comparison of the outputs of the uncertain model, nominal model and the worst realization – angular displacement

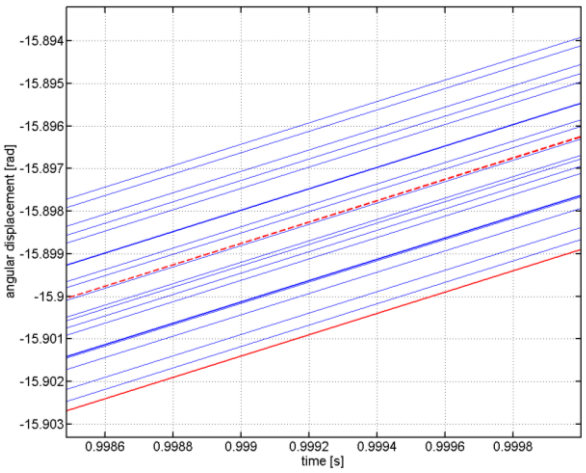

Fig. 10.11 Case 1 – comparison of the outputs of the uncertain model, nominal model and the worst realization – angular displacement – detail

(full red line – the worst case, dashed red line – the nominal model, blue line – uncertain model samples)

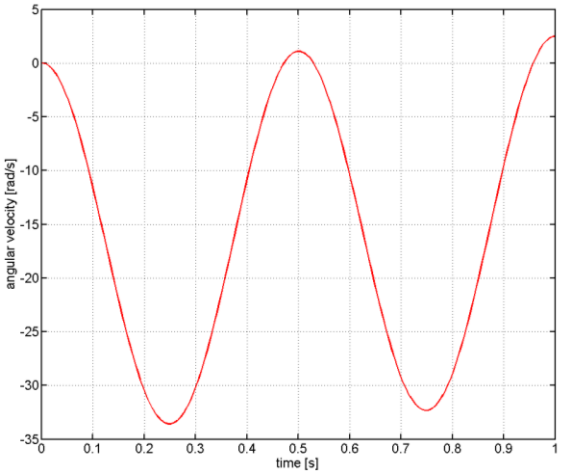

Fig. 10.12 Case 2a – comparison of the outputs of the uncertain model, nominal model and the worst realization – angular velocity

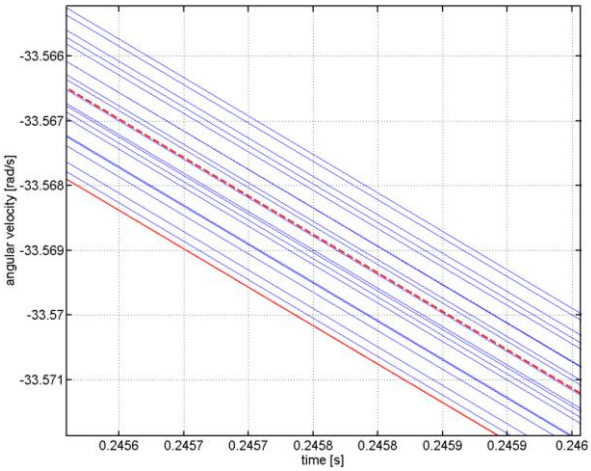

Fig. 10.13 Case 2a – comparison of the outputs of the uncertain model, nominal model and the worst realization – angular velocity – detail

(full red line – the worst case, dashed red line – the nominal model, blue line – uncertain model samples)

The maximal difference in outputs between nominal and uncertain models is even for the uncertainty ±10% of the mass and inertia moment of the lower link body (Case 2b) still quite negligible - ±0,060% of the nominal values, Fig. 10.14 – 10.17.

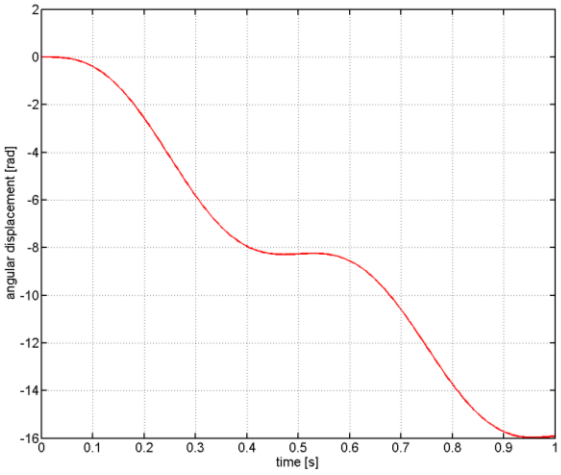

Fig. 10.14 Case 2b – comparison of the outputs of the uncertain model, nominal model and the worst realization – angular displacement

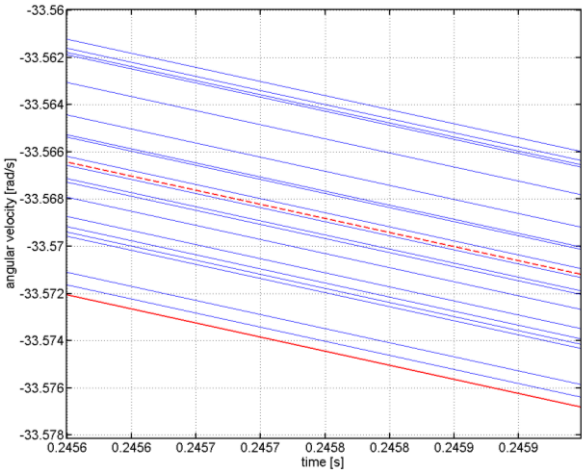

Fig. 10.15 Case 2b – comparison of the outputs of the uncertain model, nominal model and the worst realization – angular displacement - detail

(full red line – the worst case, dashed red line – the nominal model, blue line – uncertain model samples)

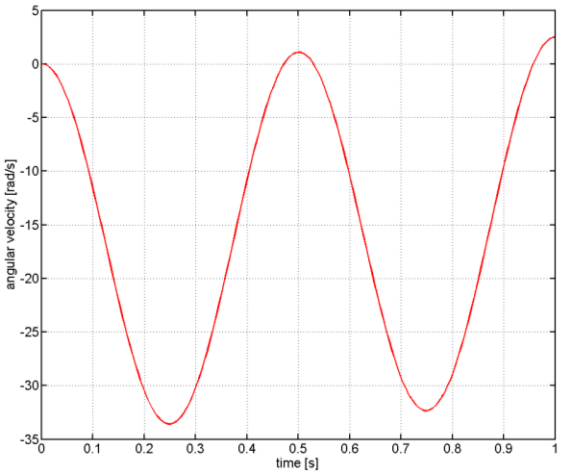

Fig. 10.16 Case 2b – comparison of the outputs of the uncertain model, nominal model and the worst realization – angular velocity

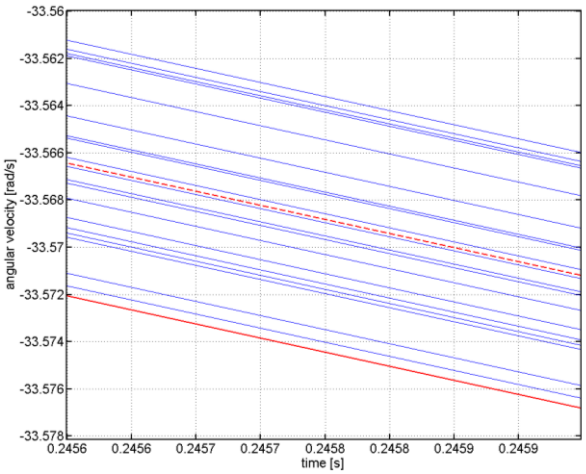

Fig. 10.17 Case 2b – comparison of the outputs of the uncertain model, nominal model and the worst realization – angular velocity – detail

(full red line – the worst case, dashed red line – the nominal model, blue line – uncertain model samples)

The difference in outputs is higher in following example where the uncertainty ±2,5% is set for all masses and inertia moments of all modeled bodies (Case 2c). The maximal difference between the nominal and uncertain outputs is then ±2,54%. This is documented in Fig. 10.18 – 10.21.

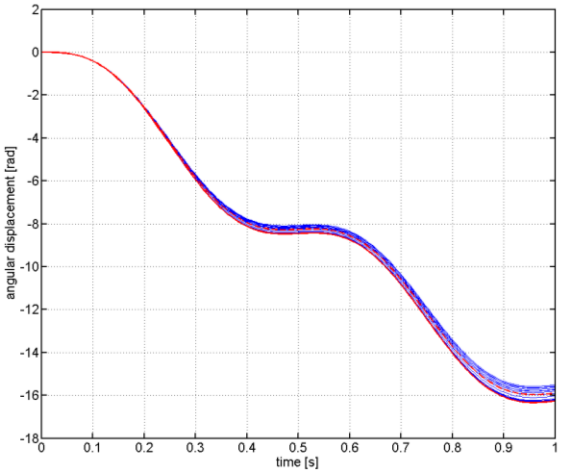

Fig. 10.18 Case 2c – comparison of the outputs of the uncertain model, nominal model and the worst realization – angular displacement

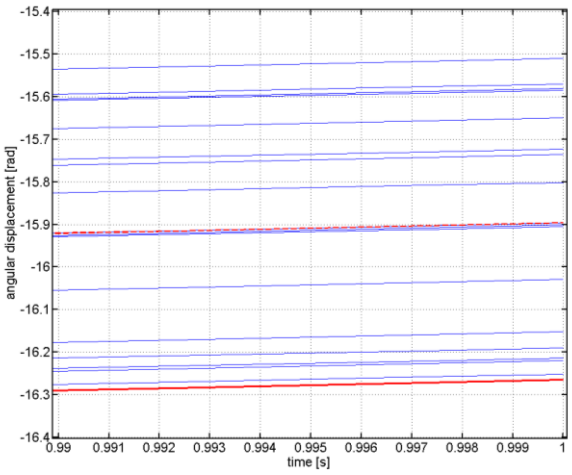

Fig. 10.19 Case 2c – comparison of the outputs of the uncertain model, nominal model and the worst realization – angular displacement - detail

(full red line – the worst case, dashed red line – the nominal model, blue line – uncertain model samples)

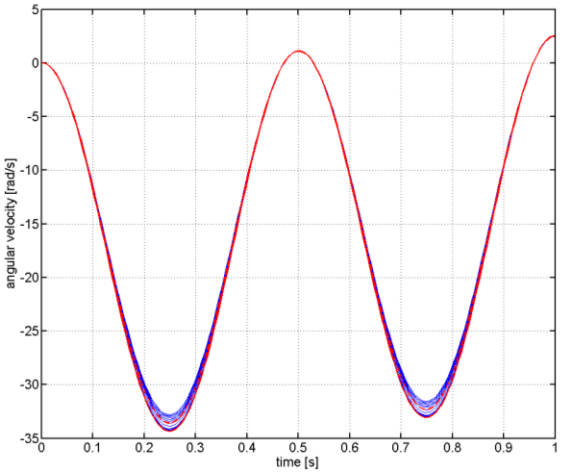

Fig. 10.20 Case 2c – comparison of the outputs of the uncertain model, nominal model and the worst realization – angular velocity

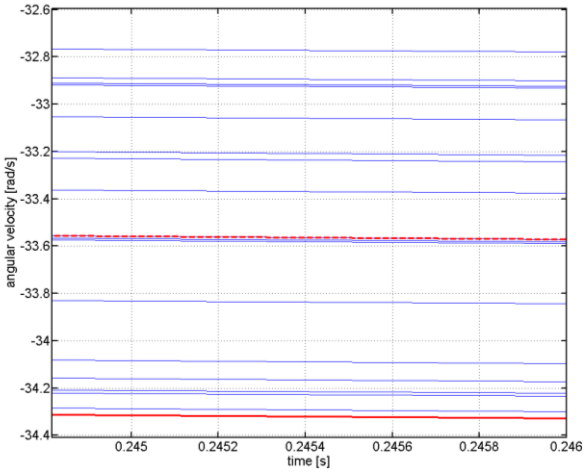

Fig. 10.21 Case 2c – comparison of the outputs of the uncertain model, nominal model and the worst realization – angular velocity – detail

(full red line – the worst case, dashed red line – the nominal model, blue line – uncertain model samples)

11.

The model verification

The following chapter is dealing with verification of the proposed SimMechanics and derived uncertain models. The verification was performed for the single linear actuator with the DC.

The very basic approach to the linear actuator control design will be described because the principle of the verification is then more obvious. Let's note that following approach is nowadays implemented in the real device.

The task of the linear actuator control design was simplified into a task of the DC motor control design according to [1]. The overall length of the link which is desired for the position control of the actuator as well as for the whole Stewart platform control is due to the complicated sensor attachment (to the Stewart platform) measured indirectly.

The angular displacement of the motor shaft is measured directly by an IRC sensor (MR Enc L type). The link length is then obtained by using a formula:

$$L_a = \frac{\varphi_{mot} p}{2\pi k}, \tag{11.1}$$

where L_a is the length of the link, φ_{mot} is the angular displacement of the motor shaft, p is the ball screw-thread and k represents overall gear ratio implemented by planetary gearbox and spur gearing.

The verification itself is based on comparison between measured and simulated values of the angular displacement and the angular velocity of the motor shaft on a single link for the same input voltage. The link is during the experiment part of a test jig which guarantees only linear movement of the attached cart, Fig. 11.1.

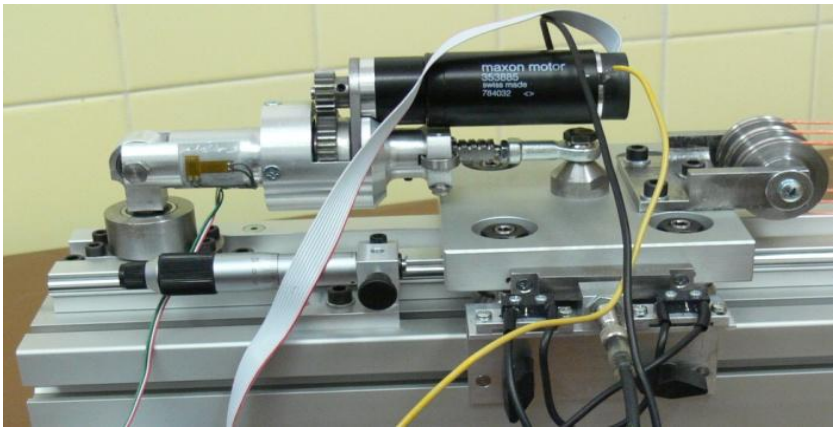

Fig. 11.1 Test jig with the linear actuator

The IRC sensor data acquisition and the motor control are provided via NI LabVIEW interface communicating with a real-time computer complemented by a field - programmable gate arrays (FPGA) card, [1]. The motor driving voltage is approximately ±11,8V during the experiment, Fig. 11.2, 11.3 . The obtained data from IRC sensor are stored in universal form of *.txt file. This is then easily imported into Matlab workspace and used as the data for comparison with simulation results, Fig. 11.4.

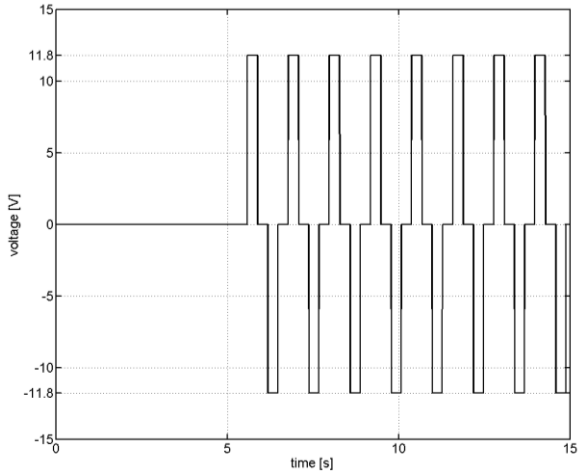

Fig. 11.2 Motor driving voltage

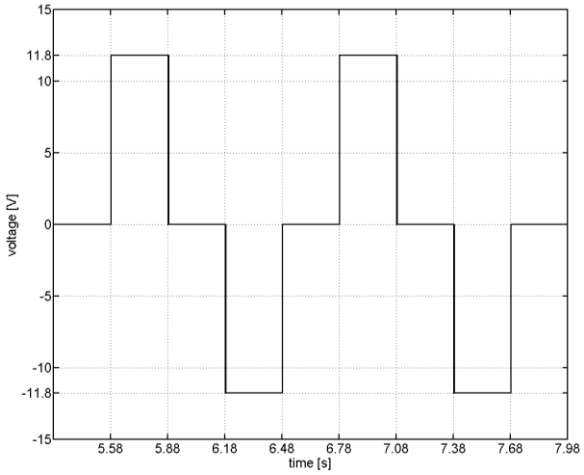

Fig. 11.3 motor driving voltage – detail

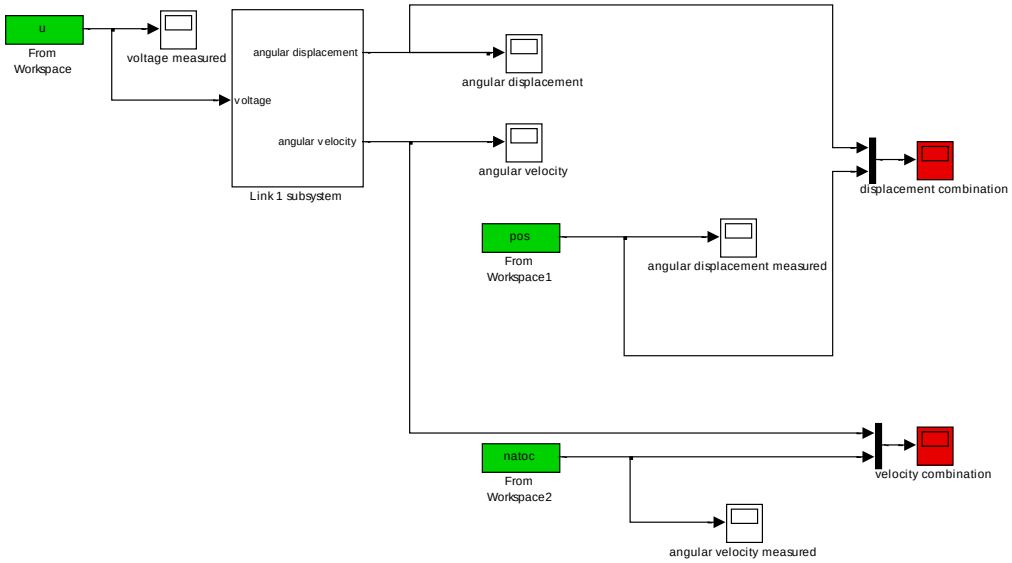

Fig. 11.4 Comparison of measured and simulated data – scheme

The following pictures (Fig 11.5 – 11.8) documents comparison between measured data and data obtained from the simulation. The simulation was performed for the nominal (SimMechanics) model of the link with the nominal (Simulink) model of the DC motor.

The maximal difference between the data obtained from the simulation and from the experiment is 11% in case of the angular displacement and 12,5% in case of the angular velocity for the given input voltage.

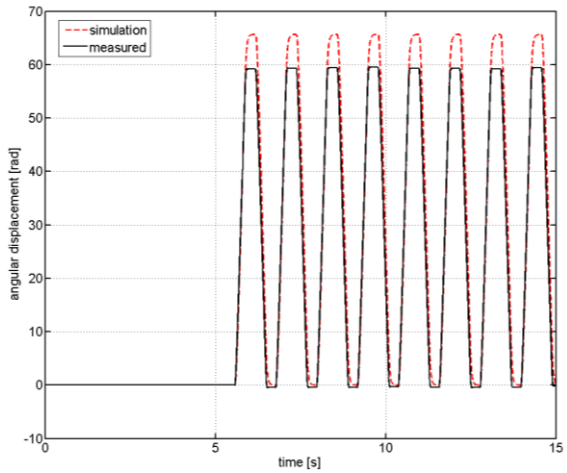

Fig. 11.5 Comparison of measured and simulated data for nominal models (motor and link) – angular displacement

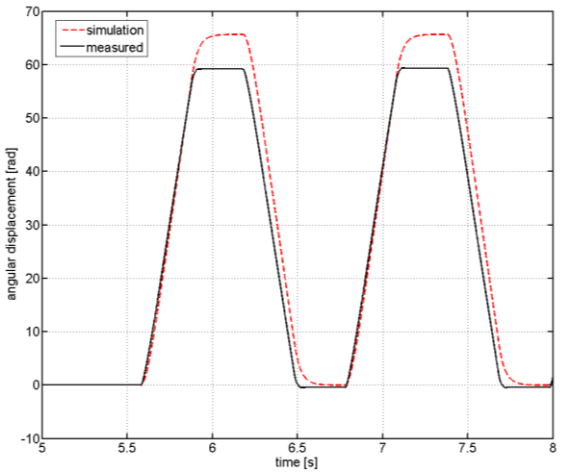

Fig. 11.6 Comparison of measured and simulated data for nominal models (motor and link) – angular displacement (detail)

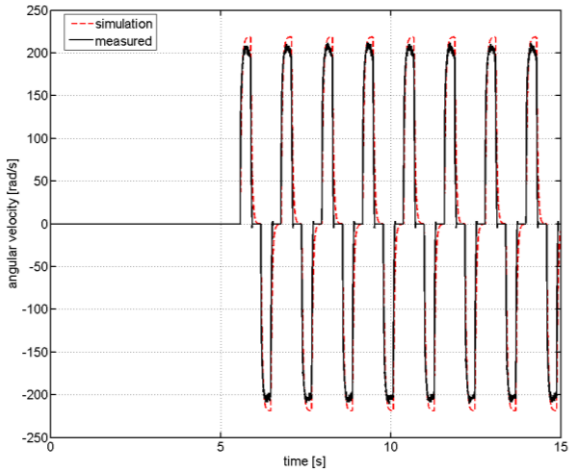

Fig. 11.7 Comparison of measured and simulated data for nominal models (motor and link) – angular velocity

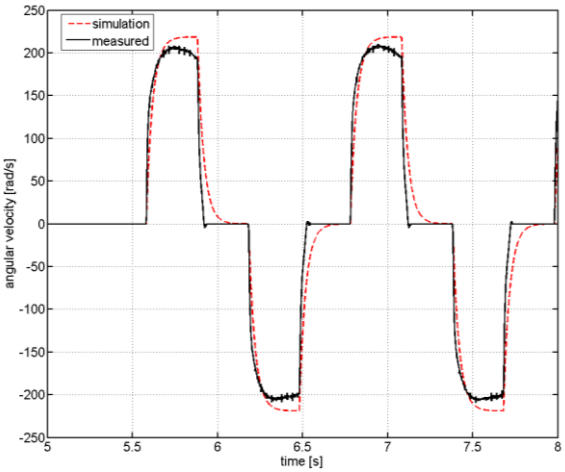

Fig. 11.8 Comparison of measured and simulated data for nominal models (motor and link) – angular velocity (detail)

Such a difference may be caused by nonlinearities in the system, modeling inaccuracy, etc. This may be at least partially compensated by the proposed uncertain model.

11.1 Uncertain model of the DC motor combined with the nominal (SimMechanics) model of the link

The following case combines uncertain model of the DC motor with the nominal SimMechanics model of the link. The uncertainties in the parameters of the DC motor model correspond with the tested case from the previous chapter, i.e. 35% uncertainty in K_f .

The difference between the nominal and the worst case of the uncertain model is for the peak values 9,3% for the angular displacement and 11,2% for the angular velocity, Fig. 11.9 – 11.12.

The result is still not satisfactory although the difference between models is smaller than in the case of nominal models.

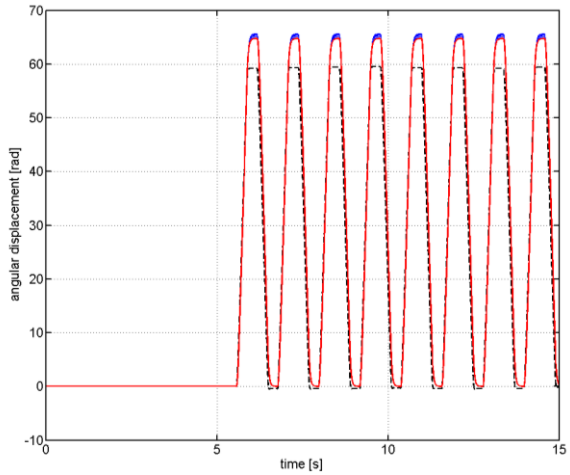

Fig. 11.9 Comparison of measured and simulated data for nominal model of the link and uncertain model of the motor – angular displacement

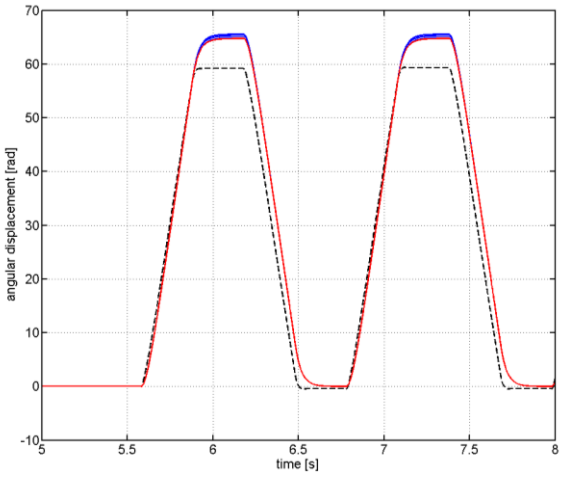

Fig. 11.10 Comparison of measured and simulated data for nominal model of the link and uncertain model of the motor – angular displacement (detail)

(black dashed line – measured data, red full line – the worst case, blue full line – samples of the uncertain model)

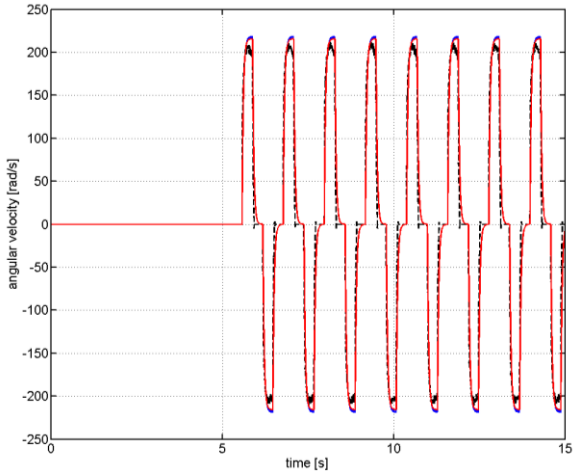

Fig. 11.11 Comparison of measured and simulated data for nominal model of the link and uncertain model of the motor – angular velocity

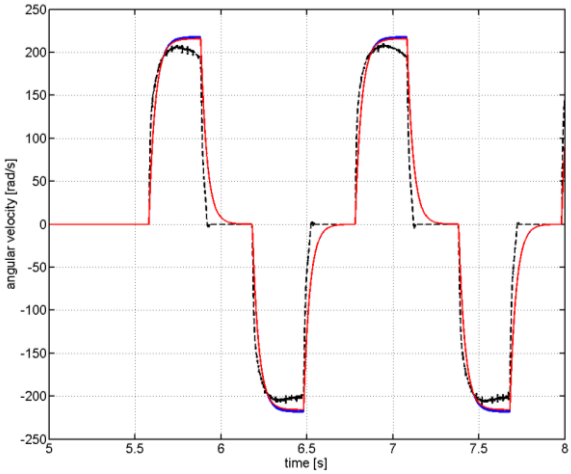

Fig. 11.12 Comparison of measured and simulated data for nominal model of the link and uncertain model of the motor – angular velocity (detail)

(black dashed line – measured data, red full line – the worst case, blue full line – samples of the uncertain model)

11.2 Nominal (Simulink) model of the DC motor combined with the uncertain model of the link

The model combining the nominal model of the DC motor and uncertain model of the link is providing much better results. The uncertain model of the link was experimentally modeled with 10% uncertainty for all body masses and inertia moments.

The maximal difference between the measured data and the worst case of the uncertain model is 1% for the angular displacement and 2,2% for the angular velocity at the peaks, Fig. 11.13 – 11.16.

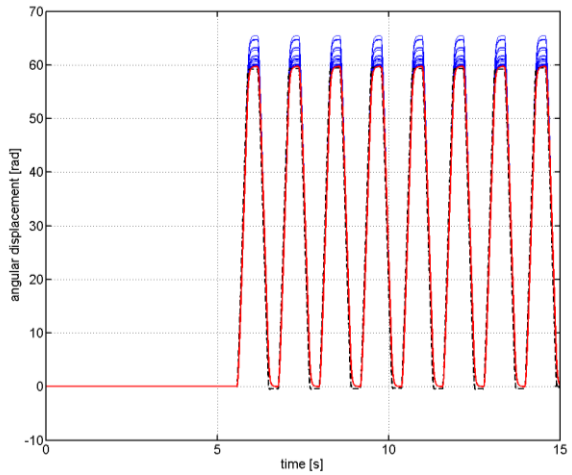

Fig. 11.13 Comparison of measured and simulated data for nominal model of the motor and uncertain model of the link – angular displacement

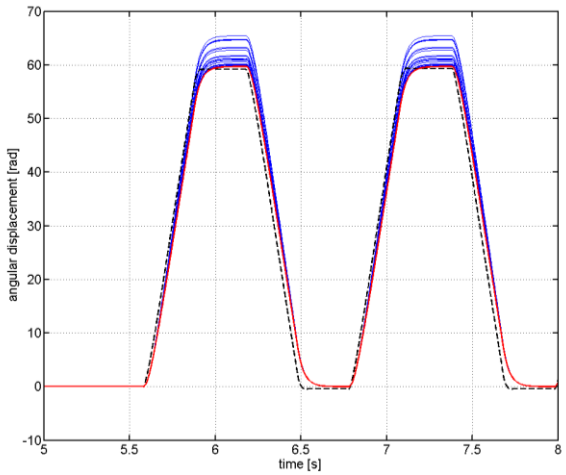

Fig. 11.14 Comparison of measured and simulated data for nominal model of the motor and uncertain model of the link – angular displacement (detail)

(black dashed line – measured data, red full line – the worst case, blue full line – samples of the uncertain model)

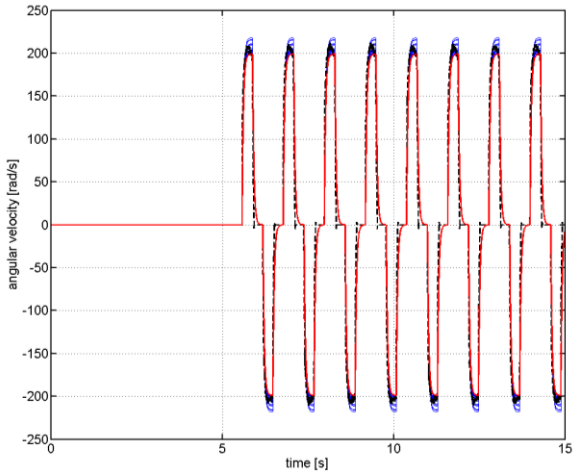

Fig. 11.15 Comparison of measured and simulated data for nominal model of the motor and uncertain model of the link – angular velocity

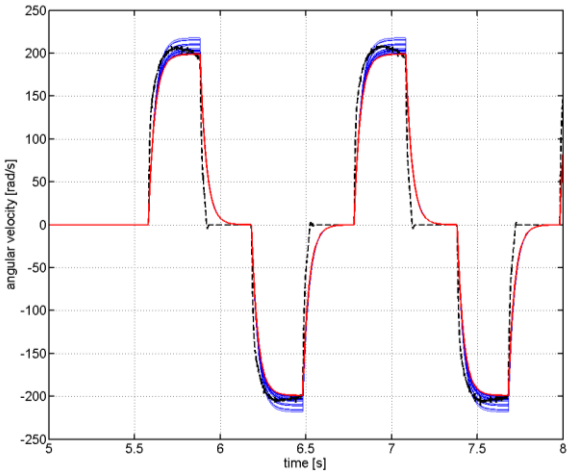

Fig. 11.16 Comparison of measured and simulated data for nominal model of the motor and uncertain model of the link – angular velocity (detail)

(black dashed line – measured data, red full line – the worst case, blue full line – samples of the uncertain model)

11.3 Uncertain model of the DC motor combined with the uncertain model of the link

The best results were obtained for the combination of the uncertain model of the DC motor with the uncertain model of the link. The peak values of the measured data are covered by the uncertainty, Fig. 11.17 – 11.20.

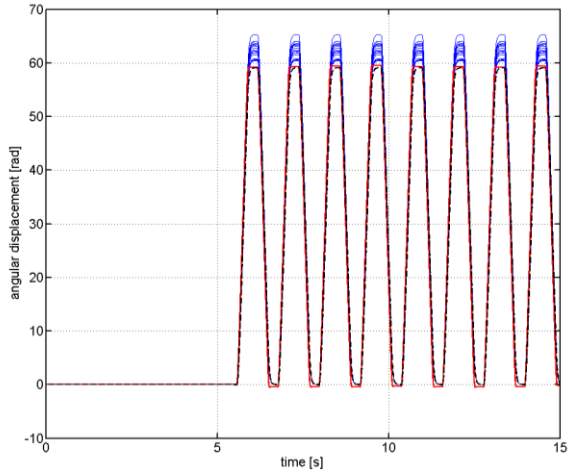

Fig. 11.17 Comparison of measured and simulated data for uncertain model of the motor and uncertain model of the link – angular displacement

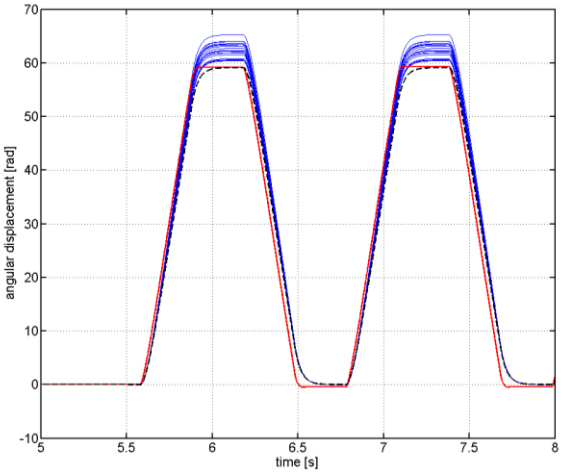

Fig. 11.18 Comparison of measured and simulated data for uncertain model of the motor and uncertain model of the link – angular displacement (detail)

(black dashed line – measured data, red full line – the worst case, blue full line – samples of the uncertain model)

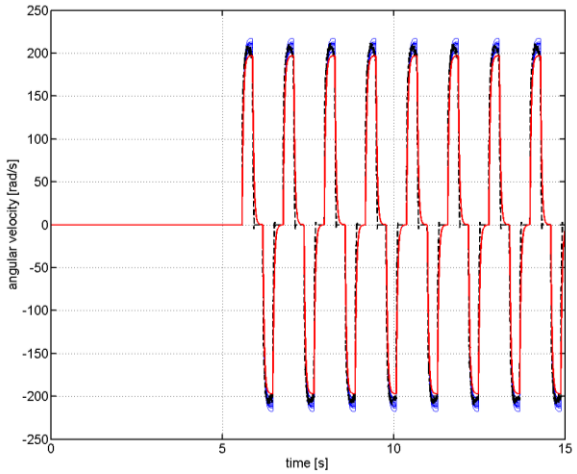

Fig. 11.19 Comparison of measured and simulated data for uncertain model of the motor and uncertain model of the link – angular velocity

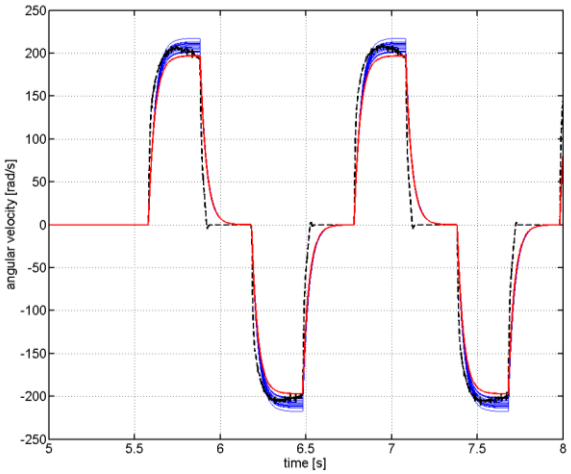

Fig. 11.20 Comparison of measured and simulated data for uncertain model of the motor and uncertain model of the link – angular velocity (detail)

(black dashed line – measured data, red full line – the worst case, blue full line – samples of the uncertain model)

The last presented example is the most suitable for the robust control design of the device. The worst case of the uncertain model is very close to the measured data, thus the robust controller designed according to such a model should be able to stabilize even the real machine.

The model is still keeping its simple structure and computational modesty of the linear model. Let’s note that all worst cases of the previous examples are controllable and observable according to conditions (4.2), (4.3).

12.

Contribution of the thesis

12.1 Theoretical contribution

The main theoretical contribution of the thesis is application of the uncertain modeling theory on modeling of dynamics of a parallel kinematics machine for a robust control design purposes. The sectional contributions may be summarized as follows:

- there was created a SimMechanics model of the specific Stewart platform developed at BUT, the model is suitable for simulations of the machine dynamics,
- consequently there was obtained a linear model of the Stewart platform for a control design purposes,
- there was proposed a method for modeling of a parametric uncertainty for individual parameters of linear state-space models,
- there were created uncertain models of the Stewart platform – one for description of the error caused by shifting of operating points with the workspace of the machine and the second one for description of the modeling inaccuracy of body masses and inertia moments,
- there was verified a single linear actuator with the uncertain model.

12.2 Practical contribution

The practical contributions of the thesis are following:

- proposed control of the Stewart platform based on the linear model
- possibility of application of the uncertain model of the Stewart platform for the robust control design purposes,
- versatility of the proposed method for the uncertain modeling and possibility of its application on other types of parallel kinematic machines or other mechatronic structures.

12.3 Pedagogic contribution

The thesis presents approach to the simulation modeling of a parallel kinematic machine which is applicable to many other mechatronic systems. The selected parts of the approach may be easily included into technical education as very actual topics.

13.

Results

The proposed work presents an approach for building of dynamic models of parallel kinematics machines optimal for a control design purposes. Such an optimal model must satisfy following requirements:

- evaluation in the shortest possible time,
- possibility of the processing of the deviations from the reality,
- (simple) investigation of the system controllability
- (simple) investigation if it is possible to use the model for estimation of selected parameters (especially in cases of parameters which is difficult or impossible to measure)

The approach is based on modeling of the system dynamics and kinematics in Matlab SimMechanics followed by a linearization of the system and introducing of uncertain parameters. The inverse kinematics was also derived by classical analytical approach for the control purposes.

The approach is presented on a Stewart platform which is a parallel manipulator with six degrees of freedom. The obtained linear model from SimMechanics is for its state-space representation with twelve states in case of Stewart platform quite simple thus it is computationally modesty with possible real-time evaluation. The model also satisfied conditions of observability and controllability.

The linear model was consequently used for a controller design which was successfully tested with the original nonlinear SimMechanics model.

The modeling itself introduced some modeling errors which, according to the verification with the assembled linear actuator, caused approximately 11% difference between outputs of the real and simulated system.

The modeling inaccuracies caused by the linearization or inexact definition of the model parameters were compensated by defining of uncertain parameters and describing the system as uncertain. The method is based on definition of structured parametric uncertainty for a nominal linear model. The uncertainty is given by a difference between corresponding parameters of state matrices of the nominal model and a model with maximally perturbed parameters. The method is then treating all of the individual parameters in the state matrices as uncertain. The proposed approach is especially advantageous for large scale models where

defining of a parametric uncertainty individually for all of the system parameters would be very demanding.

The application of the method results into an uncertain model which keeps its state-space structure thus its simplicity and computational modesty. Such a model is suitable for analyzing of the "worst case scenario" and for designing of a robust controller.

The uncertainty modeling was used for designing of uncertain model of a DC motor which is part of the Stewart platform linear actuators. In this case the classical approach [33] was chosen. The uncertainty was defined for the only motor parameter representing the linear approximation of the viscous friction where is large possible source of the modeling inaccuracy.

The proposed approach of the uncertainty modeling was applied in case of the uncertain model of the Stewart platform. The model is of the twelve order, thus it would be uncomfortable to set the uncertainty for the each parameter individually. The proposed method was used for constructing of a model describing the inaccuracy caused by the linearization, i.e. shifting of operating points within the workspace. The second example of the Stewart platform uncertain model describes the inaccuracy in body parameters of masses and inertia moments.

The mentioned 11% difference between outputs of the real and simulated system was then by introducing of the uncertain model almost completely covered by the uncertainties. There was used a model combining the uncertain model of the DC motor with the uncertain model of the Stewart platform linear actuator for this purpose.

The obtained uncertain model is optimal for the robust control because of its ability to describe the model inaccuracies which will be compensated by a robust controller.

The proposed method of uncertain modeling was demonstrated on the Stewart platform parallel manipulator thus its suitability for the modeling of parallel manipulators was proved. The method is very versatile and applicable on any model which is possible to describe in a state-space form. Design of an uncertain model for a robust control design purposes is with obtained formulas (10.13), (10.14) very simple and only necessary inputs are a nominal model and a model with maximally perturbed parameters.

The method reflects actual industry needs leading to increase of a product quality, preciseness, production capacity, dependability, system economy and decrease of the environment damage. The simulation and control of the system significantly influences all of these needs.

Acknowledgement

The presented work was supported from projects MSM0021630518 "Simulation modeling of mechatronic systems" and MŠMT KONTAKT 1P05ME789 "Simulation of mechanical function of selected elements of human body".

References

[1] Andrš, O., Březina, L., Vetiška, J.: Position control implementation of a linear mechanical actuator. *Proceedings of 12th International Conference on Mechatronics Mechatronika 2009*, Trenčín, 2009

[2] Angeles, J., Zanganeh, K.E: The semi-graphical solution of the direct kinematics of general platform manipulators. *Proceedings of ISRAM*, Santa-Fe, 1992

[3] Belda, K., Stejskal, V.: Singular cases of the planar parallel robot. *Proceedings of Engineering mechanics*, Svratka, 2003

[4] Boudreau, R., Turkkan N.: Solving the forward kinematics of parallel manipulators with a genetic algorithm. *Journal of Robotic Systems*, Vol. 13(2) (1996), p. 111-125

[5] Bruzzone, L., Molfino, R., Zoppi, M., Zurlo, G.: The pride prototype: Control layout of a parallel robot for assembly tasks. *Proceedings of International Conference on Modelling, identification and control MIC2003*, Innsbruck, 2003

[6] Březina, L., Andrš, O., Březina, T.: NI LabView – Matlab SimMechanics Stewart platform design. *Applied and computational mechanics*, Vol. 2 (1) (2008), p. 235 -242

[7] Březina, L., Březina, T.: Stewart Platform Model with Uncertain Parameters. *Solid state phenomena*, Vol. 164 (2010), p.177 – 182

[8] Březina, L., Houfek, L., Krejsa, J.: The methodology of parallel mechanisms singular cases analysis. *Proceedings of Computational mechanics, Nečtiny, 2006*

[9] Březina, T., Andrš, O., Houška, P., Březina, L.: Some notes to the design and implementation of the device for cord implants tuning. *Proceedings of Mechatronics 2009*, Luhačovice, 2009

[10] Březina, T. et al.: *Simulation modelling of mechatronic systems II*. BUT, Brno, 2006

[11] Březina, T. et al.: *Simulation modelling of mechatronic systems III*. BUT, Brno, 2007

[12] Březina, T., Březina, L.: The device for implants testing: The control. *Proceedings of Engineering mechanics 2008*, Svratka, 2008

[13] Byun, Y., Cho, H., Kim, W., Baek, S., Chang, H., Ro, K.: Kinematic/Dynamic Analysis, of a 6 DOF Parallel Manipulator with 3-PPSP Serial Subchains and its Implementation. *Proceedings of the IEEE/RSJ*, Canada, 1998

[14] Carvalho, J. C. M., Ceccarelli, M.: A Closed-Form Formulation for the Inverse Dynamics of a Cassino Parallel Manipulator. *Multibody System Dynamics*, Vol. 5(2) (2001), p. 185 – 210

[15] Cheng, H., Yiu, Y., Li, Z.: Dynamics and Control of Redundantly Actuated Parallel Manipulators. *IEEE/ASME Transactions on Mechatronics*, Vol. 8(4) (2003), p. 483 - 491

[16] Choi, H. B., Company, O., Pierot, F., Konno, A., Shibukawa, T.: Design and Control of a Novel 4-DOFs Parallel Robot H4. *Proceedings of IEEE International Conference on Robotics and Automation*, 2003

[17] Codourey, A., Burdet, E.: A Body-oriented Method for Finding a Linear Form of the Dynamic Equation of Fully Parallel Robots. *Robotics and Automation*, Vol. 2 (1997), p. 1612 - 1618

[18] Dasgupta, B., Choudhury, P.: A general strategy based on the Newton-Euler approach for the dynamic formulation of parallel manipulators. *Mechanism and Machine Theory*, Vol. 34(6) (1999), p. 801 - 824

[19] Dasgupta, B., Mruthyunjaya, T. S.: A Newton-Euler formulation for the inverse dynamics of the Stewart platform manipulator. *Mechanism and Machine Theory*, Vol. 33(8) (1998), p. 1135 - 1152

[20] Dasgupta, B., Mruthyunjaya, T.S.: A canonical formulation of the direct position kinematics for a general 6-6 Stewart platform. *Mechanism and Machine Theory*, Vol. 29(6) (1994), p. 819-827

[21] Dasgupta, B., Mruthyunjaya, T. S.: Closed-form dynamic equations of the general Stewart platform through the Newton-Euler approach. *Mechanism and Machine Theory*, Vol. 33(7) (1998), p. 993 - 1012

[22] Davliakos, I., Papadopoulos, E.: Invariant Error Dynamics Controller for a 6-dof Electrohydraulic Stewart Platform. *Proceeding of 6th CISM-IFToMM Symposium on Robot Design, Dynamics, and Control*, Warsaw, 2006

[23] Davliakos, I., Papadopoulos, E: Model-based control of a 6-dof electrohydraulic Stewart–Gough platform. *Mechanism and Machine Theory*, Vol. 43(11) (2008), p. 1485 - 1600

[24] Denkena, B., Grendel, H., Holz, Ch.: Model based feedworward and state control of the parallel kinematics PaLiDA. *Proceedings of the 4th Parallel kinematics seminar*, Chemnitz, 2004

[25] Do, W. Q. D., Yang, D. C. H.: Inverse dynamic analysis and simulation of a platform type robot. *Journal of Robotic Systems*, Vol. 5(3) (1988), p. 209 – 227

[26] Doyle, J.C.: Structured uncertainty in control system design. *Proceedings of the 24 IEEE Conference on Decision and Control*, 1985

[27] Fichter, E.F.: A Stewart platform-based manipulator: general theory and practical construction. The International Journal of Robotics Research, Vol. 5(2) 1986, p. 157 -182

[28] Gallardo, J., Rico, J. M., Frisoli, A., Checcacci, D., Bergamasco, M.: Dynamics of parallel manipulators by means of screw theory. *Mechanism and Machine Theory*, Vol. 38(11) (2003), p. 1113 - 1131

[29] Gosselin, C.: Parallel computational algorithms for the kinematics and dynamics of planar and spatial parallel manipulators. *ASME Journal of Dynamic Systems, Measurement and Control*, Vol. 118(1) (1996), p. 22-28

[30] Gough, V.E., Whitehall, S.G.: Universal tire test machine. *Proceedings of 9th Int. Technical Congress F.I.S.I.T.A.*, London, 1962

[31] Grile, T., McPhee, J.: Inverse dynamic analysis of parallel manipulators with full mobility. *Mechanism and Machine Theory*, Vol. 38(6) (2003), p. 549 - 562

[32] Green, M., Limebeer, D.J.N: *Linear robust control*. Prentice-Hall, 1994

[33] Gu, D.W., Petrov, P.H., Konstantinov, M.M.: *Robust Control Design with Matlab*. Springer, 2005

[34] Haddad, W.M, Leonessa, A., Corrado, J.R., Kapila, V.: State space modeling and robust reduced-order control of combustion instabilities. *Journal of Franklin Institute*, Vol. 336(8) (1999), p. 1283 - 1307

[35] Honegger, M., Codourey, A., Burdet, E.: Adaptive Control of the Hexaglide, a 6 dof Parallel manipulator. *Proceedings of IEEE International Conference on Robotics and Automation*, 1997

[36] Houfek, L., Březina, L.: Singular Cases of Paraller Robot. *Engineering Mechanics*, Vol.12(4) (2005), p.239-244

[37] Inoue, H., Tsusaka, Y., Fukuizumi, T.: Parallel manipulator. *Proceedings of ISRR*, Gouvieux, 1985

[38] Iserman, R.: Modeling and design methodology for mechatronic systems. *Mechatronics*, Vol. 1(1) (1996), p. 19 -28

[39] Jordan, A.J.: Linearization of non-linear state equation. Bulletin of The Polish Academy of Sciences, Vol.54(1) (2006), p. 63 – 73

[40] Kautsky, J., N.K. Nichols: Robust Pole Assignment in Linear State Feedback. *International Journal of Control*,Vol. 41(5) (1985), p. 1129-1155

[41] Krabbes, M., Meissner, Ch.: Dynamic modeling and control of a 6 DOF parallel kinematics. *Proceedings of Modelica 2006*

[42] Lee, S., Song, J., Choi, W., Hong, D.: Position control of a Stewart platform using inverse dynamics control with approximate dynamics. *Mechatronics*, Vol. 13(6) (2003), p. 605 - 619

[43] Lee, T-Y, Shim, J-K: Forward kinematics of the general 6-6 Stewart platform using algebraic elimination. *Mechanism and Machine Theory*, Vol. 36 (2001), p. 1073-1085

[44] Levine, P., McAdam, P., Pearlman, J., Pierse, R.: *Risk management in action: robust monetary rules under structured uncertainty*. European central bank, Frankfurt am Mein, 2008

[45] Li, M., Huang, T., Mei, J., Zhao, X.: Dynamic Formulation and Performance Comparison of the 3-DOF Modules of Two Reconfigurable PKM—the Triceps and the TriVariant. *Journal of Mechanical Design*, Vol. 127 (2005), p. 1129 - 1136

[46] Li, D., Salcudean, S.: Modeling, Simulation, and Control of a Hydraulic Stewart Platform. *Proceedings of International Conference on Robotics and Automation*, Albuquerque, 1997

[47] Li, Q., Wu, F.: Control performance improvement of a parallel robot via the design for control approach. *Mechatronics*, Vol. 14(8) (2004), p. 947 – 964

[48] Liu, K., Fitzgerald J.M., Lewis, F.L.: Kinematic analysis of a Stewart platform manipulator. *IEEE Transactions on Industrial Electronics*, Vol.40(2) (1993), p. 282 - 293

[49] Liu, M., Li, C., Li, Ch.: Dynamics Analysis of the Gough–Stewart Platform Manipulator. *IEEE/ASME Transactions on Mechatronics*, Vol. 16(1) (2000), p. 94 - 98

[50] Merlet, J. P.: *Parallel robots, 2nd Edition*. Kluwer Academic Publishers, Dordrecht, 2005

[51] Merlet, J. P.: Solving the forward kinematics of a Gough-type parallel manipulator with interval anlysis. The International Journal of Robotics Research, Vol. 23(3) (2004), p. 221 - 235

[52] Miller, K.: Dynamics of the New UWA Robot. *Proceedings of Australian Conference on Robotics and Automation*, Sydney, 2001

[53] Morari, M., Zafiriou, E.: *Robust Process Control*. Prentice-Hall, Englewood Cliffs, 1989

[54] Neugebauer, R., Denkena, B., Wegener, K.: Mechatronic systems for machine tools. *Annals of the CIRP*, Vol. 56(2) (2007)

[55] Ogata, K.: *Modern Control Engineering* (3rd ed.). Prentice-Hall, Upper Saddle River, 1997

[56] Pierrot, F., Dauchez, P., Fournier, A.: Fast parallel robots. *Journal of Robotic Systems*, Vol. 8(6) (1991), pp. 829 - 840

[57] Reboulet, C., Berthomieu, T.: Dynamic model of a six degree of freedom parallel manipulator. *Proceedings of ICAR*, Pise, 1991

[58] Safonov, M.G.: Stability margins of diagonally perturbed multivariable feedback systems. *Control theory and applications*, Vol.129(6) (1982), p. 251–256

[59] Sahinkaya, M., Li, Y.: Motion planning and control of parallel mechanisms through inverse dynamics. *Proceedings of IUTAM Symposium on Vibration Control of Nonlinear Mechanisms and Structures*, 2005

[60] Salhi, M.A. et al.: Structured Uncertainty Assessment for Fahud Field through the Application of Experimental Design and Response Surface Methods. *Proceedings of SPE Middle East Oil and Gas Show and Conference*, Kingdom of Bahrain, 2005

[61] Smith, N., Wendlandt, J.: Creating a Stewart platform model using Matlab SimMechanics. *Matlab Digest*, Vol. 10(5) (2002)

[62] Vivas, A., Poignet, P., Pierot, F.: Predictive functional control for a parallel robot. *Proceedings of International Conference on Intelligent Robots and Systems*, 2003

[63] Wang, S., Hikita, H., Kubo., H., Zhao., Y., Huang., Z., Ifukube, T.: Kinematics and dynamics of a 6 degree-of-freedom fully parallel manipulator with elastic joints. *Mechanism and Machine Theory*, Vol. 38(5) (2003), p. 439 - 461

[64] Wang, J., Wu, J., Wang, L., Li, T.: Simplified strategy of the dynamic model of a 6-UPS parallel kinematic machine for real-time control. *Mechanism and Machine Theory*, Vol. 42(9) (2007), p. 1119 - 1140

[65] Wu, F., Zhang, W., Li, Q., Ouyang, P.: Integrated Design and PD Control of High-Speed Closed-loop Mechanisms. *Journal of Dynamic Systems, Measurement, and Control*, Vol. 124(4) (2002), p. 522 – 528

[66] Yang, Z., Wu, J., Mei, J., Gao, J., Huang, T.: Mechatronic Model Based Computed Torque Control of a Parallel Manipulator. *International Journal of Advanced Robotic Systems*, Vol. 5(1) (2008), p. 123 – 128

Appendix A – Parameters of the linear actuator model

A1 – Body parameters of the linear actuator model

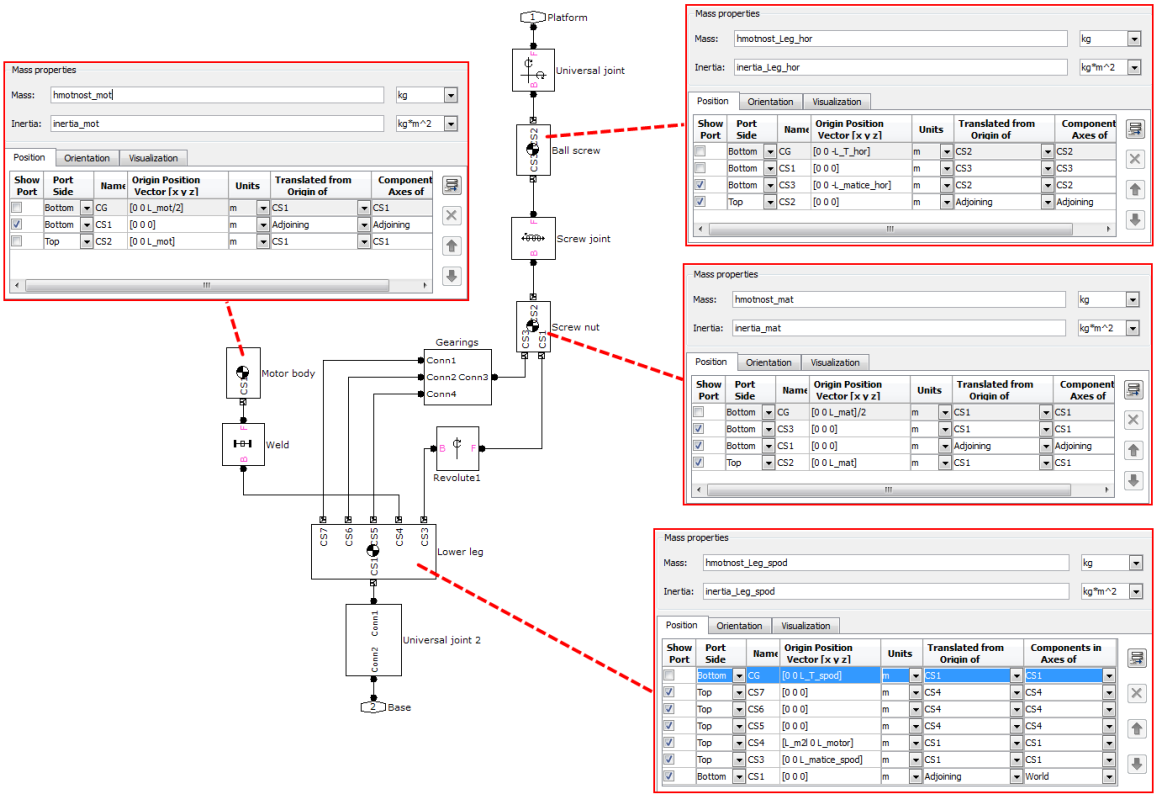

Fig. A1 The body parameters of the linear actuator

Terms of vectors defining position of connection points as well as mass and inertia of particular bodies were exported from the construction design of the device (by P. Houška) created at Inventor.

The lower link (leg)

CS1 [0 0 0] representing the conection point between the base and the lower link. CS1 represents the origin of the local coordinate system of the body. Other CSs are defined with respect to this CS.

CS3 [0 0 L_matice_spod] representing the connection point between the lower link and the screw nut. L_matice_spod = 0,08412m.

CS4 [L_m2l 0 L_motor] represents the connection point between the lower link and the motor body. L_m2l = 0,03m; L_motor = 0,1041m.

CS5, CS6, CS7 represent connection points for particular parts of the gearbox. Their position vectors are identical with CS4.

CG [0 0 L_T_spod] represents the body center of gravity. L_T_spod = 0.06309m.

The body mass hmotnost_leg_spod = 0,435kg and its inertia inertia_Leg_spod = [0.000507492 0 0; 0 0.000499276 0; 0 0 0.000131934] kg.m^2.

The screw nut

CS1 [0 0 0] representing the connection point between the screw nut and the lower link. CS1 represents the origin of the local coordinate system of the body. Other CSs are defined with respect to this CS.

CS2 [0 0 L_mat] represents the connection point between the screw nut and the ball screw. L_mat = 0,008m.

CS3 [0 0 0] represents the onnection point between the screw nut and the gearbox.

CG [0 0 L_mat]/2 represents the center of gravity of the screw nut.

The body mass hmotnost_mat = 0,125kg and its inertia inertia_mat = [0.000019318 0 0; 0 0.000019312 0; 0 0 0.000022071] kg.m^2.

The ball screw

CS2 [0 0 0] representing the connection point between the ball screw and the screw nut. CS2 represents the origin of the local coordinate system of the body. Other CSs are defined with respect to this CS.

CS3 [0 0 -L_matice_hor] represents the connection point between the ball screw and the screw nut. L_matice_hor = 0,1095m.

CG [0 0 –L_T_hor] represents the centre of gravity of the ball screw. L_T_hor = 0,07414m.

The body mass hmotnost_leg_hor = 0,112kg and its inertia inertia_leg_hor = [0.000193005 0 0; 0 0.000192973 0; 0 0 0.000001996] kg.m^2.

The motor body

CS1 [0 0 0] representing the connection point between the lower link and the motor body. CS1 represents the origin of the local coordinate system of the body. Other CSs are defined with respect to this CS.

CS2 [0 0 L_mot] represents no connection point. L_mot = 0,1087m.

CG [0 0 L_mot/2] represents the motor center of gravity.

The body mass hmotnost_mot = 0,34kg and its inertia inertia_mat = [0.000373333 0 0; 0 0.000373325 0; 0 0 0.000064002] kg.m^2.

The position vectors are defined in local coordinate systems defined according to (7.2).

A2 – Joint parameters of the linear actuator model

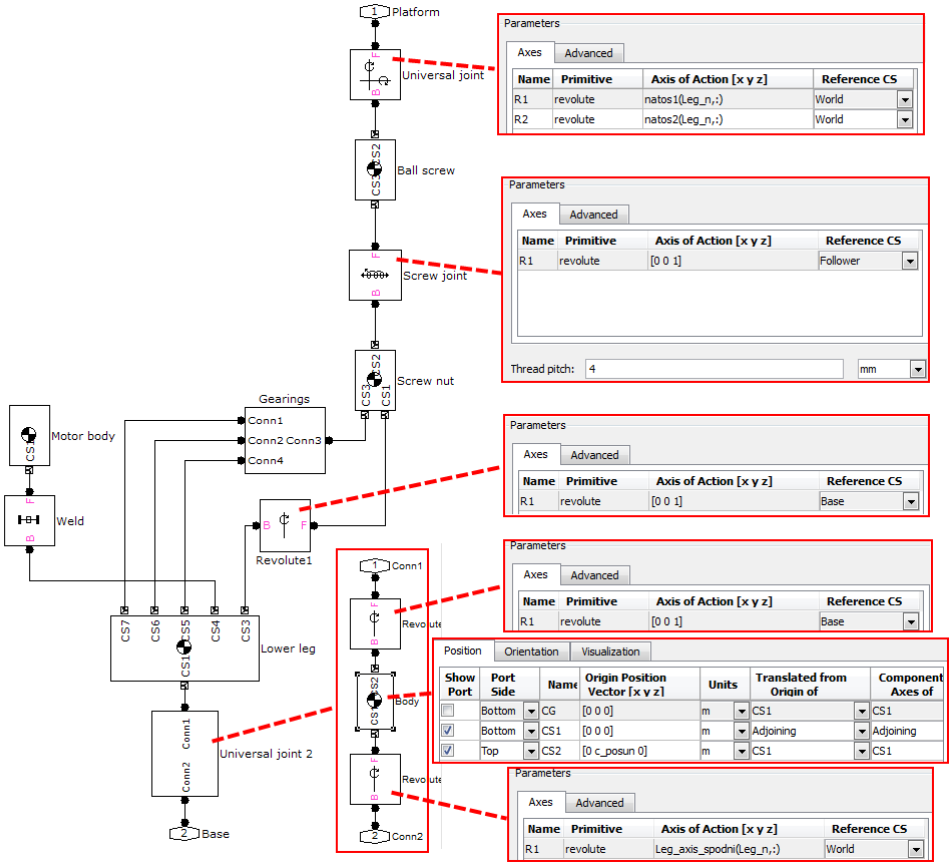

Fig. A2 The joints parameters of the linear actuator

Universal joint

natos1(Leg_n,:) corresponds with unit vector $\hat{\mathbf{I}}_i$ according to (7.2).

natos2(Leg_n,:) corresponds with unit vector $\hat{\mathbf{J}}_i$ according to (7.2).

Universal joint 2

c_posun = 10mm

Leg_axis_spodni(Leg_n,:) corresponds with the vector (6.5) $\mathbf{x}_i^* = \mathbf{b}_i - \mathbf{m}_i$

Screw joint and revolute

The rotation around an axis defined by unit vector $\hat{\mathbf{K}}_i$ according to (7.2).

Gearbox

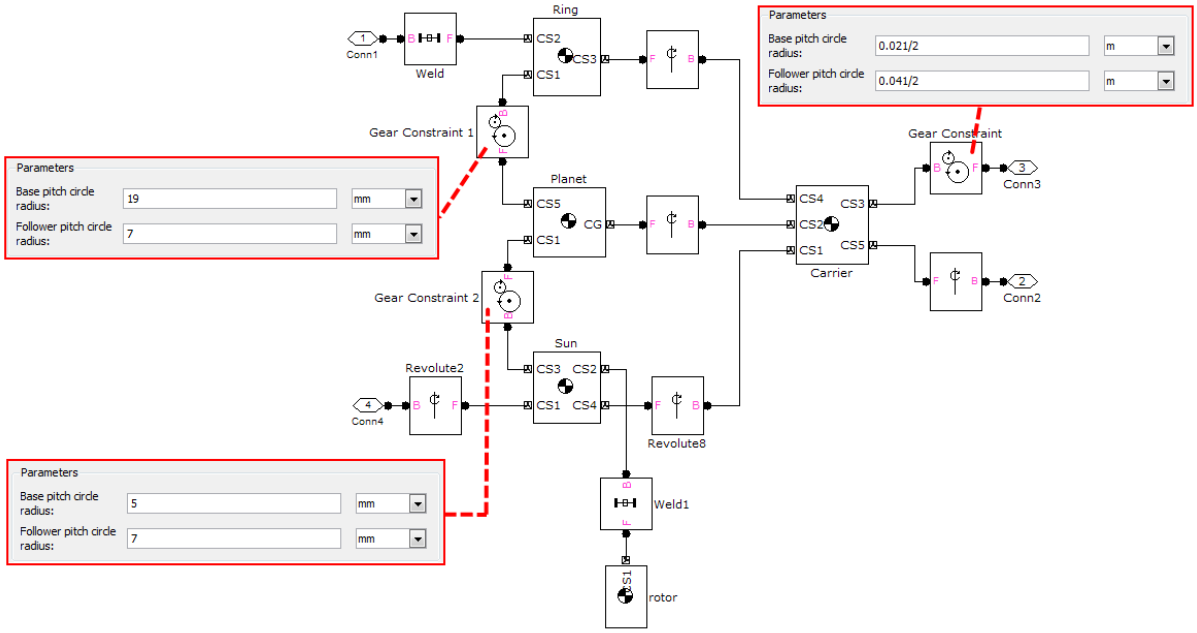

Fig. B3 Gear constraint blocks settings

Appendix B - Body parameters of the Stewart platform model

P_points_SSB_trans(i,:) defines the platform transformed points $\mathbf{p}_{T_i}$ for $i = 1,...,6$. Their coordinates transformed to the global coordinate system are for the platform initial position following:

	X [mm]	Y [mm]	Z [mm]
$\mathbf{p}_{T_1}$	174,2	75,8	126,2
$\mathbf{p}_{T_2}$	152,8	113	126,2
$\mathbf{p}_{T_3}$	-152,8	113	126,2
$\mathbf{p}_{T_4}$	-174,2	75,8	126,2
$\mathbf{p}_{T_5}$	-21,4	-188,8	126,2
$\mathbf{p}_{T_6}$	21,4	-188,8	126,2

B_points_SSB_trans(i,:) defines the base points $\mathbf{b}_i$ for $i = 1,...,6$. Their coordinates are in the global coordinate systems following:

	X [mm]	Y [mm]	Z [mm]
$\mathbf{b}_1$	165,3	-57,4	0
$\mathbf{b}_2$	32,9	171,9	0
$\mathbf{b}_3$	-32,9	171,9	0
$\mathbf{b}_4$	-165,3	-57,4	0
$\mathbf{b}_5$	-132,4	-114,5	0
$\mathbf{b}_6$	132,4	114,5	0

Auxiliary points $\mathbf{m}_i$

	X [mm]	Y [mm]	Z [mm]
$\mathbf{m}_1$	160	-73,5	16,9
$\mathbf{m}_2$	163,3	175,4	16,9
$\mathbf{m}_3$	-163,3	175,4	16,9
$\mathbf{m}_4$	-160	-73,5	16,9
$\mathbf{m}_5$	-143,7	-101,8	16,9
$\mathbf{m}_6$	143,7	-101,8	16,9

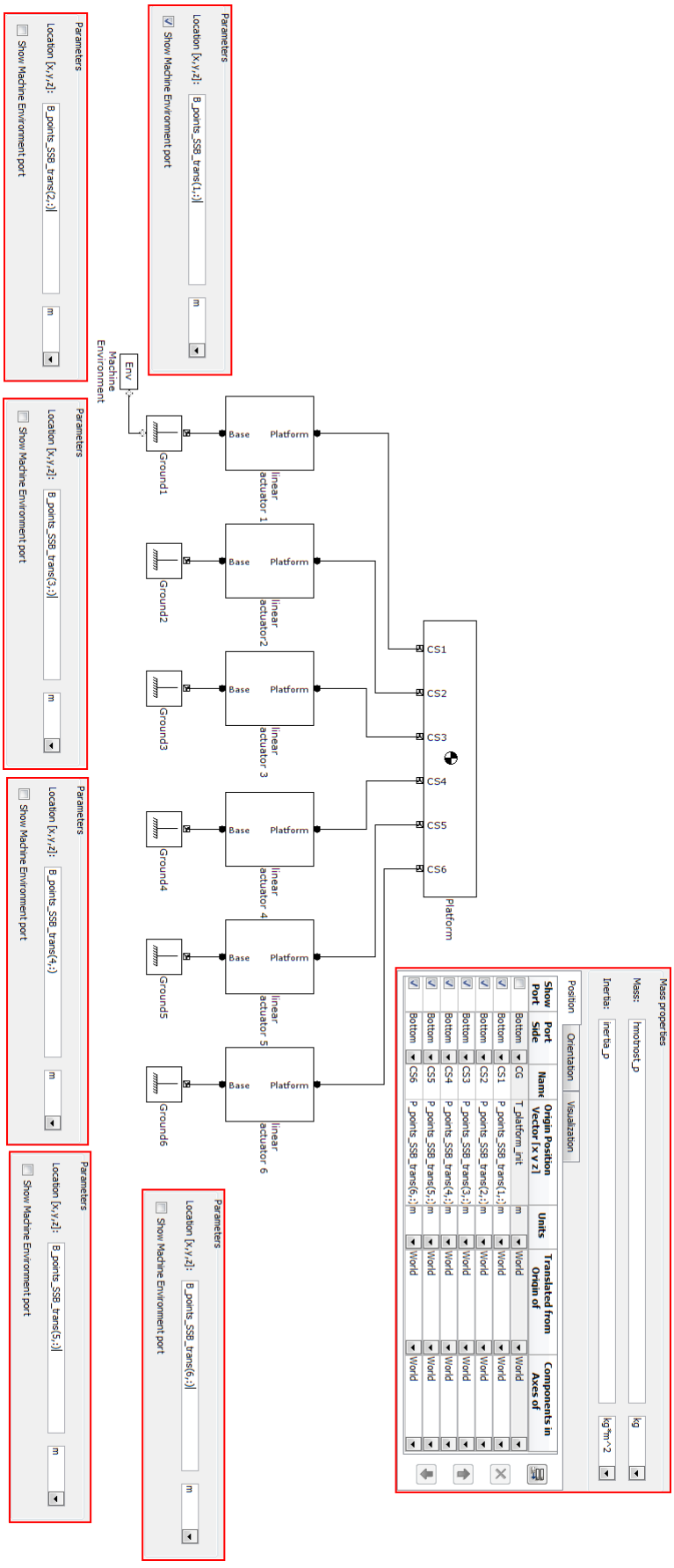

Fig. B1 Base and platform points of the Stewart platform model

Appendix C – Maxon RE 35 datasheet

RE 35 ∅35 mm, Graphite Brushes, 90 Watt

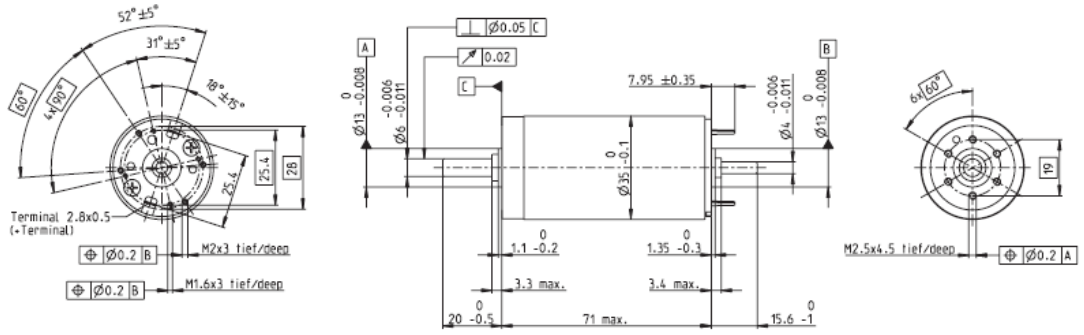

M 1:2

Stock program
Standard program
Special program (on request)

	Order Number												
according to dimensional drawing	273752	323890	273753	273754	273755	273756	273757	273758	273759	273760	273761	273762	273763
shaft length 15.6 shortened to 4 mm	285785	323891	285786	285787	285788	285789	285790	285791	285792	285793	285794	285795	285796
Motor Data													
Values at nominal voltage													
1 Nominal voltage	V	15.0	24.0	30.0	42.0	48.0	48.0	48.0	48.0	48.0	48.0	48.0	48.0
2 No load speed	rpm	7070	7670	7220	7530	7270	6650	5960	4740	3810	3140	2570	2100	1620
3 No load current	mA	245	168	123	92.7	77.3	68.7	59.7	44.7	34.2	27.1	21.6	17.2	12.9
4 Nominal speed	rpm	6270	6910	6420	6770	6490	5860	5150	3920	2970	2280	1710	1220	732
5 Nominal torque (max. continuous torque)	mNm	73.2	93.3	92.4	97.7	96.5	98.2	98.8	102	105	105	105	104	104
6 Nominal current (max. continuous current)	A	4.00	3.36	2.50	1.95	1.63	1.51	1.36	1.12	0.915	0.752	0.621	0.503	0.391
7 Stall torque	mNm	874	1160	949	1070	967	878	766	613	493	394	320	253	194
8 Starting current	A	45.0	39.7	24.4	20.3	15.5	12.9	10.1	6.43	4.16	2.74	1.83	1.18	0.704
9 Max. efficiency	%	81	84	84	86	85	85	84	83	82	80	79	77	74
Characteristics													
10 Terminal resistance	Ω	0.334	0.605	1.23	2.07	3.09	3.72	4.75	7.46	11.5	17.5	26.2	40.5	68.2
11 Terminal inductance	mH	0.085	0.191	0.340	0.620	0.870	1.04	1.29	2.04	3.16	4.65	6.89	10.3	17.1
12 Torque constant	mNm / A	19.4	29.2	38.9	52.5	62.2	68	75.8	95.2	119	144	175	214	276
13 Speed constant	rpm / V	491	328	246	182	154	140	126	100	80.5	66.4	54.6	44.7	34.6
14 Speed / torque gradient	rpm / mNm	8.43	6.79	7.76	7.16	7.62	7.67	7.89	7.85	7.84	8.08	8.19	8.46	8.55
15 Mechanical time constant	ms	5.97	5.60	5.50	5.40	5.38	5.38	5.39	5.38	5.37	5.38	5.39	5.39	5.41
16 Rotor inertia	gcm²	67.6	78.7	67.6	72.0	67.4	67.0	65.2	65.4	65.5	63.6	62.8	60.8	60.4

Specifications

Thermal data

17	Thermal resistance housing-ambient	6.2 K / W
18	Thermal resistance winding-housing	2.0 K / W
19	Thermal time constant winding	30 s
20	Thermal time constant motor	1050 s
21	Ambient temperature	-30 ... +100°C
22	Max. permissible winding temperature	+155°C

Mechanical data (ball bearings)

23	Max. permissible speed	12000 rpm
24	Axial play	0.05 - 0.15 mm
25	Radial play	0.025 mm
26	Max. axial load (dynamic)	5.6 N
27	Max. force for press fits (static)	110 N
	(static, shaft supported)	1200 N
28	Max. radial loading, 5 mm from flange	28 N

Other specifications

29	Number of pole pairs	1
30	Number of commutator segments	13
31	Weight of motor	340 g

Values listed in the table are nominal.
Explanation of the figures on page 49.

Option
Hollow shaft as special design
Preloaded ball bearings

Operating Range

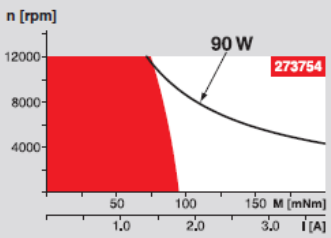

Comments

Continuous operation
In observation of above listed thermal resistance (lines 17 and 18) the maximum permissible winding temperature will be reached during continuous operation at 25°C ambient.
= Thermal limit.

Short term operation
The motor may be briefly overloaded (recurring).

Assigned power rating

maxon Modular System

Overview on page 16 - 21

Planetary Gearhead
Ø32 mm
0.75 - 6.0 Nm
Page 230 / 232 / 233

Planetary Gearhead
Ø32 mm
4.0 - 8.0 Nm
Page 235

Planetary Gearhead
Ø42 mm
3 - 15 Nm
Page 238

Spindle Drive
Ø32 mm
Page 249 / 250 / 251

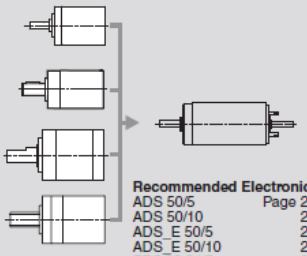

Encoder MR
256 - 1024 Imp.,
3 channels
Page 263

Encoder HED_ 5540
500 Imp.,
3 channels
Page 266 / 268

DC-Tacho DCT
Ø22 mm
0.52 V
Page 276

Brake AB 28
24 VDC
0.4 Nm
Page 318

Recommended Electronics:

ADS 50/5	Page 282
ADS 50/10	283
ADS_E 50/5	283
ADS_E 50/10	283
EPOS2 24/5	305
EPOS2 50/5	305
EPOS2P 24/5	308
Notes	**18**